



**Calhoun: The NPS Institutional Archive**  
**DSpace Repository**

---

Theses and Dissertations

1. Thesis and Dissertation Collection, all items

---

1984-06

## Observations of the California Countercurrent

Harrod, Robert L.

Monterey, California. Naval Postgraduate School

---

<http://hdl.handle.net/10945/19477>

---

This publication is a work of the U.S. Government as defined in Title 17, United States Code, Section 101. Copyright protection is not available for this work in the United States.

*Downloaded from NPS Archive: Calhoun*



Calhoun is the Naval Postgraduate School's public access digital repository for research materials and institutional publications created by the NPS community. Calhoun is named for Professor of Mathematics Guy K. Calhoun, NPS's first appointed -- and published -- scholarly author.

**Dudley Knox Library / Naval Postgraduate School**  
**411 Dyer Road / 1 University Circle**  
**Monterey, California USA 93943**

<http://www.nps.edu/library>







DUDLEY KNOX LIBRARY  
NAVAL POSTGRADUATE SCHOOL  
MONTEREY, CALIFORNIA 93943









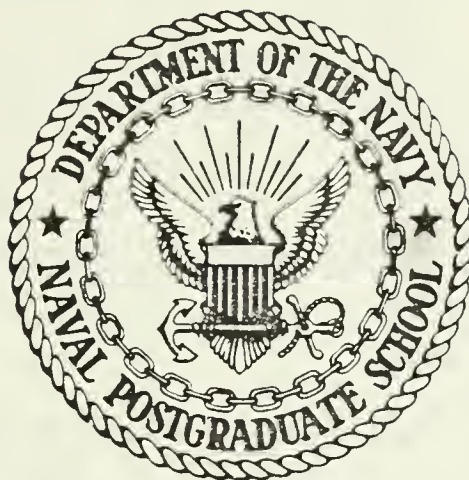






# NAVAL POSTGRADUATE SCHOOL

Monterey, California



## THESIS

OBSERVATIONS OF THE  
CALIFORNIA COUNTERCURRENT

by

Robert L. Harrod

June 1984

Thesis Advisors:

J. B. Wickham  
S. P. Tucker

Approved for public release; distribution unlimited.

T222093



SECURITY CLASSIFICATION OF THIS PAGE (When Data Entered)

REPORT DOCUMENTATION PAGE		READ INSTRUCTIONS BEFORE COMPLETING FORM
1. REPORT NUMBER	2. GOVT ACCESSION NO	3. RECIPIENT'S CATALOG NUMBER
4. TITLE (and Subtitle)  Observations of the California Countercurrent		5. TYPE OF REPORT & PERIOD COVERED Master's Thesis June 1984
		6. PERFORMING ORG. REPORT NUMBER
7. AUTHOR(s)  Robert L. Harrod		8. CONTRACT OR GRANT NUMBER(s)
9. PERFORMING ORGANIZATION NAME AND ADDRESS Naval Postgraduate School Monterey, California 93943		10. PROGRAM ELEMENT PROJECT TASK AREA & WORK UNIT NUMBERS
11. CONTROLLING OFFICE NAME AND ADDRESS Naval Postgraduate School Monterey, California 93943		12. REPORT DATE June 1984
		13. NUMBER OF PAGES 147
14. MONITORING AGENCY NAME & ADDRESS (if different from Controlling Office)		15. SECURITY CLASS. (of this report)  UNCLASSIFIED
		15a. DECLASSIFICATION DOWNGRADING SCHEDULE
16. DISTRIBUTION STATEMENT (of this Report)  Approved for public release; distribution unlimited.		
17. DISTRIBUTION STATEMENT (of the abstract entered in Block 20, if different from Report)		
18. SUPPLEMENTARY NOTES		
19. KEY WORDS (Continue on reverse side if necessary and identify by block number)  California Countercurrent, California Undercurrent, Davidson Current, California Current, Eastern boundary currents, metered currents.		
20. ABSTRACT (Continue on reverse side if necessary and identify by block number)  Results from moored current meters, 150-350 m, are described for a region over the continental slope off Cape San Martin from January 1979 to April 1980.  Current vector time series were constructed from the data and compared to the local coastal upwelling index. Progressive vector diagrams were also constructed, and spectrum analysis was performed for alongshore		

and cross-slope currents.

The California Countercurrent was found to be present in the study area during the entire period. Seasonally, the countercurrent was substantially stronger during the spring. Frequent current reversals and oscillations occurred between equatorward and poleward flow, less often at the nearshore station. Preferred low frequency energy peaks were found at periods of about 10 days. The intensity of the countercurrent increased with increasing coastal upwelling index, and the cross-slope flow also appeared to be related to the local coastal upwelling index.



Approved for public release; distribution unlimited.

Observations of the  
California Countercurrent

by

Robert L. Harrod  
Lieutenant Commander, United States Navy  
B.S., Oregon State University, 1975

Submitted in partial fulfillment of the  
requirements for the degree of

MASTER OF SCIENCE IN METEOROLOGY AND OCEANOGRAPHY

from the

NAVAL POSTGRADUATE SCHOOL  
June 1984

Results from moored current meters, 150 - 350 m, are discussed for a region over the continental slope off Cape San Martin, California from January 1979 to April 1980.

Current vector time series were constructed from the data and compared to a local upwelling index. Progressive vector diagrams of the data were also constructed, and spectrum analysis was performed for alongshore and cross-slope currents.

The California Countercurrent was found to be present in the study area during the entire period. Seasonally, the countercurrent was substantially stronger during the spring. Frequent current reversals and oscillations occurred between equatorward and poleward flow, less often at the nearshore station. Preferred low frequency energy peaks were found at periods of about 10 days. The intensity of the countercurrent increased with increasing coastal upwelling index, and the cross-slope flow also appeared to be related to the local coastal upwelling index.

# TABLE OF CONTENTS

DUDLEY KNOX LIBRARY  
NAVAL POSTGRADUATE SCHOOL  
MONTEREY, CALIFORNIA 93943

I.	INTRODUCTION AND BACKGROUND -----	12
II.	DIRECT CURRENT OBSERVATIONS -----	20
	A. DATA COLLECTION -----	20
	B. DATA PROCESSING -----	21
III.	STUDY OBJECTIVES -----	24
IV.	DESCRIPTION AND ORGANIZATION OF GRAPHICS -----	25
V.	ANALYSIS -----	28
	A. RELATION BETWEEN CURRENT AND LOCAL WIND FORCING -----	28
	1. Analysis at Station 2 -----	29
	2. Analysis at Station 7 -----	31
	3. Comparison of Stations 2 and 7 -----	32
	B. SPECTRUM ANALYSIS -----	34
	C. INFERENCES FROM PROGRESSIVE VECTOR DIAGRAMS -----	36
	D. CROSS-SLOPE CURRENT -----	41
	E. TIME SERIES -----	41
VI.	CONCLUSIONS -----	43
	APPENDIX A: TIME SERIES PLOTS -----	52
	APPENDIX B: SPECTRUM ANALYSES OF ALONGSHORE FLOW AND ON/OFFSHORE FLOW -----	75
	APPENDIX C: PROGRESSIVE VECTOR DIAGRAMS -----	91
	APPENDIX D: COMPUTER PROGRAM LISTINGS -----	107
	LIST OF REFERENCES -----	143
	INITIAL DISTRIBUTION LIST -----	146

## LIST OF TABLES

TABLES	PAGE
I. Comparison of high energy peaks-----	37
II. Comparison of mean current and temperature-----	38

# LIST OF FIGURES

FIGURES	PAGE
1. The study area-----	45
2. Chronology of current meter deployment-----	46
3. Vertical section showing representative locations of current meters off Cape San Martin, California-----	47
4. Current meter array-----	48
5. Mean onshore currents-----	49
6. Mean temperatures at Station 2-----	50
7. Mean temperatures at Station 7-----	51
8. Point Sur Upwelling Index and stickplots of hourly current vectors for the current meters at Station 7 deployed on 5 January 1979-----	52
9. U component, V component, and temperature plots versus time for the current meter at 152 m depth at Station 7 deployed on 5 January 1979-----	53
10. U component, V component, and temperature plots versus time for the current meter at 223 m depth at Station 7 deployed on 5 January 1979-----	54
11. Point Sur Upwelling Index and stickplots of hourly current vectors for the current meters at Station 2 deployed on 23 April 1979-----	55
12. U component, V component, and temperature plots versus time for the current meter at 169 m depth at Station 2 deployed on 23 April 1979-----	56
13. U component, V component, and temperature plots versus time for the current meter at 241 m depth at Station 2 deployed on 23 April 1979-----	57
14. Point Sur Upwelling Index and stickplots of hourly current vectors for the current meters at Station 7 deployed on 7 July 1979-----	58
15. U component, V component, and temperature plots versus time for the current meter at 158 m depth at Station 7 deployed on 7 July 1979-----	59



16.	U component, V component, and temperature plots versus time for the current meter at 231 m depth at Station 7 deployed on 7 July 1979-----	60
17.	U component, V component, and temperature plots versus time for the current meter at 356 m depth at Station 7 deployed on 7 July 1979-----	61
18.	Point Sur Upwelling Index and stickplots of hourly current vectors for the current meters at Station 2 deployed on 21 July 1979-----	62
19.	U component, V component, and temperature plots versus time for the current meter at 165 m depth at Station 2 deployed on 21 July 1979-----	63
20.	U component, V component, and temperature plots versus time for the current meter at 237 m depth at Station 2 deployed on 21 July 1979-----	64
21.	Point Sur Upwelling Index and stickplots of hourly current vectors for the current meters at Station 7 deployed on 7 October 1979-----	65
22.	U component, V component, and temperature plots versus time for the current meter at 127 m depth at Station 7 deployed on 7 October 1979-----	66
23.	U component, V component, and temperature plots versus time for the current meter at 200 m depth at Station 7 deployed on 7 October 1979-----	67
24.	Point Sur Upwelling Index and stickplots of hourly current vectors for the current meters at Station 2 deployed on 24 November 1979-----	68
25.	U component, V component, and temperature plots versus time for the current meter at 194 m depth depth at Station 2' deployed on 24 November 1979--	69
26.	U component, V component, and temperature plots versus time for the current meter at 266 m depth at Station 2 deployed on 24 November 1979-----	70
27.	Point Sur Upwelling Index and stickplots of hourly current vectors for the current meters at Station 7 deployed on 3 March 1980-----	71
28.	U component, V component, and temperature plots versus time for the current meter at 113 m depth depth at Station 7 deployed on 3 March 1980-----	72

29.	U component, V component, and temperature plots versus time for the current meters at 186 m depth at Station 7 deployed on 3 March 1980-----	73
30.	U component, V component, and temperature plots versus time for the current meter at 311 m depth at Station 7 deployed on 3 March 1980-----	74
31.	Energy density spectrum of current meter at 152 m depth at Station 7 deployed on 5 January 1979-----	75
32.	Energy density spectrum of current meter at 223 m depth at Station 7 deployed on 5 January 1979-----	76
33.	Energy density spectrum of current meter at 169 m depth at Station 2 deployed on 23 April 1979-----	77
34.	Energy density spectrum of current meter at 241 m depth at Station 2 deployed on 23 April 1979-----	78
35.	Energy density spectrum of current meter at 158 m depth at Station 7 deployed on 7 July 1979-----	79
36.	Energy density spectrum of current meter at 231 m depth at Station 7 deployed on 7 July 1979-----	80
37.	Energy density spectrum of current meter at 356 m depth at Station 7 deployed on 7 July 1979-----	81
38.	Energy density spectrum of current meter at 165 m depth at Station 2 deployed on 21 July 1979-----	82
39.	Energy density spectrum of current meter at 237 m depth at Station 2 deployed on 21 July 1979-----	83
40.	Energy density spectrum of current meter at 127 m depth at Station 7 deployed on 7 October 1979-----	84
41.	Energy density spectrum of current meter at 200 m depth at Station 7 deployed on 7 October 1979-----	85
42.	Energy density spectrum of current meter at 194 m depth at Station 2 deployed on 24 November 1979---	86
43.	Energy density spectrum of current meter at 266 m depth at Station 2 deployed on 24 November 1979---	87
44.	Energy density spectrum of current meter at 113 m depth at Station 7 deployed on 3 March 1980-----	88

45.	Energy density spectrum of current meter at 186 m depth at Station 7 deployed on 3 March 1980-----	89
46.	Energy density spectrum of current meter at 311 m depth at Station 7 deployed on 3 March 1980-----	90
47.	Progressive vector diagram for the current meter at 127 m depth at Station 7 from 9 January to 28 February 1979-----	91
48.	Progressive vector diagram for the current meter at 223 m depth at Station 7 from 9 January to 26 February 1979-----	92
49.	Progressive vector diagram for the current meter at 169 m depth at Station 2 from 24 April to 13 June 1979-----	93
50.	Progressive vector diagram for the current meter at 241 m depth at Station 2 from 24 April to 12 June 1979-----	94
51.	Progressive vector diagram for the current meter at 158 m depth at Station 7 from 9 July to 30 August 1979-----	95
52.	Progressive vector diagram for the current meter at 231 m depth at Station 7 from 9 July to 29 August 1979-----	96
53.	Progressive vector diagram for the current meter at 356 m depth at Station 7 from 9 July to 30 August 1979-----	97
54.	Progressive vector diagram for the current meter at 165 m depth at Station 2 from 23 July to 11 September 1979-----	98
55.	Progressive vector diagram for the current meter at 237 m depth at Station 2 from 23 July to 13 September 1979-----	99
56.	Progressive vector diagram for the current meter at 127 m depth at Station 7 from 9 October to 29 November 1979-----	100
57.	Progressive vector diagram for the current meter at 200 m depth at Station 7 from 9 October to 29 November 1979-----	101

58.	Progressive vector diagram for the current meter at 169 m depth at Station 2 from 27 November 1979 to 16 January 1980-----	102
59.	Progressive vector diagram for the current meter at 266 m depth at Station 2 from 27 November 1979 to 18 January 1980-----	103
60.	Progressive vector diagram for the current meter at 311 m depth at Station 7 from 4 March to 15 April 1980-----	104
61.	Progressive vector diagram for the current meter at 186 m depth at Station 7 from 4 March to 12 April 1980-----	105
62.	Progressive vector diagram for the current meter at 311 m depth at Station 7 from 4 March to 10 April 1980-----	106





## I. INTRODUCTION AND BACKGROUND

Eastern boundary currents are the subject of scientific investigation for a variety of reasons, particularly the impact of these currents on the fishing industry. Ryther (1969) concluded certain fishing grounds such as those off Peru, California, northwest and southwest Africa, Somalia, and the Arabian coast are so fertile, that they supply over half of the worlds fish harvest, yet constitute less than one percent of the oceans. These fishing grounds are invariably located close to shore, and their great fertility is due to frequent replenishment of near-surface nutrients from a few hundred meters deep in the open ocean offshore. The primary process for this is coastal upwelling, which in the Western Hemisphere is associated most markedly with the eastern boundary currents off North and South America. The economic need to understand these currents is made evident by the devastation of the coastal regions of Ecuador and Peru in 1982-1983 by the sudden influx of warm water termed El Niño. The socioeconomic effects included; flooding, landslides, destruction of transportation facilities, huge agricultural losses, disturbance of coastal fisheries, and loss of life (Halpern et al., 1983). This warm water influx takes place from

time-to-time, and recovery from a severe occurrence may take several years (Smith 1983).

Off the North American west coast, the eastern boundary flow regime is known as the California Current System. A comprehensive summary of the present knowledge of this system is given by Hickey (1978). The California Current System includes the southward flowing California Current, and a number of manifestations of a counter-flow: the California Undercurrent, the Davidson Current, and the Southern California Countercurrent. This system is part of the general circulation of the North Pacific Ocean which is dominated by an oceanwide, clockwise circulation known as the North Pacific Gyre. The eastern limb of the gyre is the California Current System, which extends along the North American continent from southern Canada to Mexico. The system includes both poleward and equatorward flows which vary on many time-scales. There are, for example, inter-annual variations such as El Niño, seasonal variations, and large variations with periods associated with weather systems. The California Current is a slow and broad equatorward surface flow, branching from the North Pacific Current, and marked by cold subarctic water type. The waters of the various countercurrents may be characterized by their admixture with water of equatorial origin which has relatively high levels of temperature, salinity and phosphate, and relatively low dissolved

oxygen. During the winter months a surface current with poleward flow occurs in nearshore regions off the west coast of the United States. This current, inshore of the California Current, is known as the Davidson Current and is ordinarily found north of Point Conception. The Davidson Current may be a surface manifestation of the California Undercurrent. The Southern California Countercurrent is the name applied to the poleward flow from San Diego to Point Conception; during winter months, this nearshore flow is sometimes continuous with the Davidson Current.

The study of eastern boundary currents is of both theoretical and practical interest. Dynamical models with features of observed eastern boundary currents have been developed since the turn of the century. Ekman (1905) described the effects of a steady wind blowing on an ocean, and stated the concepts now known as the Ekman spiral and the Ekman transport. Sverdrup, Johnson, and Fleming (1941) provided some understanding of the dynamics of the upwelling process. Munk (1950) computed the mass transports in a wind-driven ocean from the curl of the estimated wind stress.

Recent models include the two-dimensional and three-dimensional upwelling models, and sea breeze produced upwelling models reviewed by O'Brien (1977). These models considered the influences of horizontal boundaries, bottom topography, and the variability of wind stress on the

ocean. The first numerical model of coastal upwelling was constructed by O'Brien and Hurlburt (1972); this two-layer model successfully predicted the observed equatorward jet but failed to produce a poleward undercurrent. Sugimotohara (1974) used a model with a straight coast and a bottom topography which did not vary in a coastwise direction. His model succeeded in developing a poleward flow in the lower layer. A later review of models is given by Allen (1980). These models permit inferences, such as the effects of shelf width and coastal winds, to be made about shelf-flow motions which have time scales like those of the atmospheric weather systems which drive them. Irregularities of the coastline and bottom topography force three-dimensional motions. However, there has been little theoretical work in this area until recently. An important conclusion from the models is that the currents arise from and are maintained by both local and remote atmospheric forcing. Significantly improved models of coastal upwelling include more realistic wind stress and finer resolution of bottom topography, especially the shelf break and steep bottom slopes.

Complementing models are field experiments which provide the basis for their motivation and verification. Two recent comparisons of models to field observations are Hickey (1980) and Janowitz (1980). Hickey used the two-dimensional, baroclinic, time-dependent model of

Hamilton (1978) and found it to be effective for time periods as long as fifteen days in predicting the displacement of isopycnals off the Oregon coast.

Janowitz's comparison of a model of time-dependent quasi-geostrophic upwelling to moored meter data concluded tentatively that the model may have some validity, but further comparisons and verification should be undertaken.

Early observational studies of the California Current System emphasized relatively large-scale motions. Sverdrup and Fleming (1941) utilized T-S relationships to define the origins of water of two sorts (in northern hemispheric eastern boundary flows): northern water with increasing salinity as temperature decreases with depth and southern water with relatively constant salinity as temperature decreases. That the warmer water was a northward-flowing current was also demonstrated by Sverdrup and Fleming (1941) utilizing geostrophy; later, Reid, et al. (1958) showed that geo-strophic shear of the flow at the 200-dbar surface with respect to the 500 and the 1000-dbar surfaces indicates a northward flowing undercurrent. During the fifties and early sixties most Lagrangian current measurements were limited to drift bottle estimates of surface currents. One important exception was the tracking (for a few days) of deep drogues by Reid (1962), which also indicated a northward-flowing undercurrent off the central California coast. It is in the last decade that moored



current meters have provided a means to examine details of the flow over long time-periods. Moored current meters can be positioned to give direct measurements of the currents over extended periods (approximately two months for the Aanderaa meter, if a ten-minute sampling interval is used). Moored meters provide an excellent means for detailed local studies to elucidate better the properties, relationships, and interactions of the several portions of the California Current System. Studies of the California Current System during the 1960's using moored meters were primarily of the coastal waters off Oregon and Washington. While few current measurements have been made in the California Current and reliable wind stations are sparse, continuing studies off Washington and Oregon by Hickey (1979, 1980) and Huyer et al. (1979) show a significant relationship between local wind forcing and currents. Hickey stated that the seasonal variation of the nearshore region of strong flow appears to be related to the seasonal variation of the alongshore component of wind stress at the coast. Huyer et al. show that the transition from the predominantly northward surface currents of the winter oceanographic regime to the predominantly southward surface currents of the spring oceanographic regime over the Oregon continental shelf occurs within a period of several days during a strong southward wind event. Recent work for waters off the central region of the California

coast includes descriptive studies by Wickham (1975), Coddington (1979) and Dreves (1980). Wickham (1975) made salinity-temperature-depth (STD) sections, and parachute drogue observations off Monterey Bay. Wickham found the California Countercurrent to be present 15 km off the coast in August 1972 and in August 1973. Coddington (1979) compared direct current measurements from an array moored off Cape San Martin to indirect measurements from geostrophy. Coddington found the California Countercurrent to be present during the study period from November 1978 to February 1979. Dreves (1980) studied the relationship between local sea level gradient and alongshore flow for the same study period as Coddington. Dreves found that current and sea level gradient energy distributions were in close agreement, showing high energy concentration at the low frequency end of the spectrum.

The region of the central California coast off Cape San Martin (Figure 1) was chosen for study for several reasons: there is relatively little ship traffic or fishing and, consequently, less risk of current meter damage or loss; the bottom topography is relatively devoid of complications, consisting of an extremely narrow shelf, sharp shelf break, and depth contours approximately parallel to the coast; additionally, the close proximity of the study area to Monterey was a logistical convenience.

The current meter data used by Coddington and Dreves,

some six sets of current meter observations spanning six months from 25 July 1978 until 22 January 1979, have been augmented as part of the continuous monitoring of the countercurrent off Cape San Martin. An observational data base of direct current measurements of more than one year's duration now exists.

The objective of this study is to provide a preliminary analysis of current meter data for the period January 1979 to April 1980.

## II. DIRECT CURRENT OBSERVATIONS

### A. DATA COLLECTION

The data for this study were collected using Aanderaa Model RCM-4 recording current meters, which are self-recording and intended to be anchored in the ocean below the wind wave zone; they record current speed and direction and water temperature.

The meters were deployed off Cape San Martin, California, from August 1978 until July 1980 (see Figure 2). The station locations are shown in Figure 3. The present study covers the period from January 1979 to May 1980. Coddington (1979) and Dreves (1980) have discussed data collected during the period from April 1978 to January 1979. Deployment of the arrays was accomplished with the Naval Postgraduate School's research vessel ACANIA. Each mooring of several meters was launched by being strung out behind the ship, the uppermost meter and flotation devices first and the anchor last. The array's descent was slowed by a small drogue about two meters in diameter attached to the anchor. An array of three meters was used at Station 2 ( $35^{\circ} 52.16'N$ ,  $121^{\circ} 33.76'W$ ) and four meters at Station 7 ( $35^{\circ} 51.4'N$ ,  $121^{\circ} 46.54'W$ ). They were arranged approximately as depicted in Figure 4. The anchor consisted of

one or two railroad wheels attached to an AMF-Sealink Model 242 acoustic release. Benthos 17-inch glass spheres in plastic hard hats (55 pounds net buoyancy each) were used to provide wire tension, with two spheres directly above each current meter and six above the release. The entire array was moored below the region of strong surface wave action and was recovered by acoustically activating the release. Upon recovery the meters were returned to the laboratory for maintenance prior to subsequent redeployment.

#### B. DATA PROCESSING

The data were recorded on three-inch reels of 1/4-inch audio tape (Scotch Brand number 295) at ten-minute sampling intervals. Conversion of the data from the tapes recorded by the RCM-4 meters into a computer-acceptable format was accomplished with a Hewlett-Packard 9845 computer and an Aanderaa tape translator. The 1/4-inch tape was played back on a Wollensach audio deck and an oscilloscope was used to give a visual confirmation that data were present and of appropriate amplitude. The data were then translated from long and short to high and low voltage pulses and recorded on IBM-compatible 9-track tape on a Kennedy 9-track tape recorder. The Hewlett-Packard 9845 computer was also used to plot and print portions of the data.

Five different programs were used with the Naval Postgraduate School's IBM 360 computer in processing the data. They are listed in Appendix D. The initial program reads in the raw data from the 9-track magnetic tape, allows an initial look at the data if desired, and stores the data in mass storage for quicker, more efficient utilization. The second program applies temperature, speed, and direction calibrations to the data for each current meter. The third program reads in the calibrated output from program two, identifies missing records, and uses established cut-off parameters to suppress noise. Temperatures greater than  $12^{\circ}\text{C}$ , and less than  $5^{\circ}\text{C}$  are discarded, along with current speeds in excess of  $100\text{ cm-s}^{-1}$ . Discarded and missing records are filled in by the following process: upon encountering a faulty value, searching continues until a value is found that meets the acceptance criteria. Linear interpolation is used to obtain fill-in values. Initial looks at the data revealed only minimal gaps in the records. Program three, by means of a binomial, converts the data record from ten-minute values to hourly values and then produces four plots. Currents are presented in the form of stickplots, and three other plots display U and V components of the current (respectively, eastward and northward for positive values), and temperature as functions of time. The fourth program reads in the output of program two, fills in missing and



faulty records, and then performs a spectrum analysis of the data. Its output consists of two plots of frequency versus power density for onshore and alongshore components of current. The fifth program uses the hourly records produced in program three to construct progressive vector plots. Two of the current meters used in the study were very noisy and gave unrealistically high indications of the speed. These noisy data are not shown here.

### III. STUDY OBJECTIVES

The objective of this study is to provide a preliminary analysis of the current meter data. Questions to be considered are:

1. Do the data reveal seasonal variations of the flow?
2. Do the data reveal differences or similarities in the flow between Stations 2 and 7?
3. Are there indications of mesoscale events?
4. Are such mesoscale events coherent with respect to depth and/or position?
5. Is there a generalization about variation with depth that can be made?
6. How do the currents appear to be related to Bakun's coastal upwelling index (Bakun, 1980)?

#### IV. DESCRIPTION AND ORGANIZATION OF GRAPHICS

To highlight the salient features of the variations, and to examine them in the framework of Section III the data are presented in several ways. There are seven different graphical representations in Appendixes A, B, and C. These plots are:

1. Time series of Bakun's coastal upwelling index (Bakun, 1980).
2. Time series of current vectors.
3. Time series of eastward components of the current vectors.
4. Time series of northward components of the current vectors.
5. Time series of temperature.
6. Spectrum analyses of alongshore flow and on/offshore flow.
7. Progressive vector diagrams.

The plots are organized chronologically according to deployment date of the meters, beginning 5 January 1979 and ending in March 1980.

In Appendix A there are sets of time series. For example, Figure 8 and those like it contain time series of Bakun's coastal upwelling index (UI), and current series

(stickplots), in this case for the meters deployed on 5 January 1979 at Station 7, permitting visual comparison of one aspect of local forcing and the associated motions. The coastal upwelling indices are indicative of onshore-offshore Ekman transport, as estimated from wind stress at the position in the vicinity of Point Sur indicated in Figure 1. The procedure for calculating upwelling indices is presented in detail by Bakun (1973). The stickplots are graphical depictions of current speed and current direction. Time-scales are indicated along the top and bottom of Figure 5, and the units of measurement for the ordinates are shown on the left side of the figure. Pertinent information on the figures of this type include: station number, date of deployment, meter serial number, and depth of meter deployment.

Another type is represented by Figures 6 and 7. They depict U, V, and T for the two current meter records represented in Figure 8, where U (positive) is the eastward component of the current vector, V (positive) is the northward component of the current vector, and T is the temperature. Again, time scales and pertinent station information are given in the figure. The time series of these variables are complementary to the progressive vector diagrams found in Appendix C since they accentuate higher frequency events such as inertial and tidal oscillations.

The figures in Appendix B contain spectrum analyses of

alongshore flow and on/offshore flow for each current meter. The abscissa (frequency) and the ordinate (power density function) are clearly labeled, and each figure also lists station number, meter serial number, meter deployment depth, and date of deployment. The spectrum analyses indicate regions of high energy in the frequency domain and suggest forces at work.

Appendix C contains the progressive vector diagrams (PVD). The vertical and horizontal scales are equal (kilometers), and true North is indicated. Crosses are positioned at 3-day intervals, and the letter "F" indicates the final plotted position. In addition to station number, meter number, meter depth, and period of computation, the mean speed and mean direction for the entire period are indicated. The PVD's depict well the low frequency variations, so-called "events", such as eddies.

Appendix D contains the listings of the computer programs used to process and plot the current meter data.

## V. ANALYSIS

### A. RELATION BETWEEN CURRENT AND LOCAL WIND FORCING

The coastal mountains of California tend to deflect the low level winds so that they blow equatorward parallel to the coast. Consequently, the average Ekman transport is offshore (Stewart 1967). In the simple Ekman model, the offshore flow lies generally above the level at which our current meters are moored. But there are strong vertical motions (up-and-downwelling) and other intense mesoscale exchange mechanisms in the area of study which negate the application of the simple Ekman model to observed cross-slope flow and suggest the possibility of a deeper "virtual" Ekman layer extending well into the pycnocline.

In this section qualitative relations between current and local wind forcing are examined through use of the time series of stickplots and upwelling index and also by referring to Figure 5. These relations will first be examined separately at each mooring station, and then for the time period July - August 1979, when current meters were deployed at both Station 2 and Station 7. Finally, seasonal and geographical variations will be considered.



## 1. Analysis at Station 2

The corresponding UI and current velocity for Station 2, the inshore station, are shown in Figure 11 for the period from 23 April to mid-June. There are event-scale (ca. one week) changes in current direction and speed that appear to be coherent with depth. The upwelling index is positive all during the months of May and June with nearly periodic episodes of great intensity. It is reasonable that there be upwelling in this period of strong positive upwelling index ( $\overline{UI}=+138$ ). The mean cross slope flow ( $\overline{U}'$ ) for this period (Table II) is small and positive, which indicates that the meters are below the Ekman layer. The poleward alongshore flow shown by the stickplots indicates the presence of a countercurrent at 169 and 241 m. Strong equatorward winds (positive UI) seem to correlate well with strong poleward flow of the countercurrent during this time period, especially at the level nearest the surface. Also, very large drops in the index are associated with a slightly lagging decrease in the poleward current speed, and increased variability in current direction during intervals centered on 21 May, 1 June, and 9 June (Figure 11).

Continuing at Station 2 in the period 21 July - 12 September 1979 (Figure 18), there is also an overall tendency for poleward flow associated with positive upwelling index especially at the level nearest the surface. The mean cross-slope flow (Table II) for this

period of strong upwelling index ( $\overline{UI}=+125$ ) is negative; if an extended Ekman layer is postulated, this cross-slope flow can be interpreted as lying within a layer which includes both meters. The magnitude of UI declines during the latter part of this period. On a shorter time-scale (about 9 days) the rise and fall of the upwelling index is accompanied throughout the record, beginning about 10 August, by poleward currents during periods of high upwelling index, and equatorward or diminished poleward currents during periods of reduced upwelling index. Thus, decreases in the upwelling index clearly relate to decreases in, or disappearance of, the counter current on these time scales (ca. 9 days), especially at the greater depth, 237 m.

In the following period, 24 November 1979 through 18 January 1980, as shown in Figure 24, the upwelling index is further reduced ( $\overline{UI}=-20$ ), becoming dominantly negative after mid December. The meter at 194 m (Figure 24) is suspect due to lack of direction changes. This could be the result of a stuck vane, or a malfunction in the sensor. The alongshore current at depth 266 m alternates between poleward and equatorward flows with durations between three and ten days. There is a marked change in currents after 23 December; they become weak and variable following a strong surge in the downwelling index at that time.

## 2. Anaylsis at Station 7

First consider the winter period January - February 1979, illustrated in Figure 8. The mean flow at both levels (152 m and 223 m) is predominantly poleward; but there are important event-scale variations. There are also alternating periods of positive and negative upwelling index during this period. The significant current variations and the upwelling index changes do not seem correlated. For example, from 5 to 10 January 1979 the currents at both depths were toward the southwest and during the next 15 to 17 days rotated clockwise. While the upwelling index varied erratically about zero, a similar rotation of the currents and unrelated variation of the upwelling index continued until about mid-February, when predominantly poleward flow again resumed, and the currents flowed in this direction for the remainder of the record, approximately twelve days. A fair conclusion for this period, when wind forcing is inconsistent and weak, is that there is no simple relation between the local upwelling index and the observed behavior of the currents on time scales of tens of days, and that some other mechanism than local forcing is involved.

During July and August 1979 (Figure 14), the index is positive and the flow at Station 7, is also predominatly poleward at 158, 231, and 356 m, especially in July. Large events involving reversals in the currents can be seen on

about 7 August and 24 August at all three observed levels. These events appear to occur at all depths almost simultaneously, which suggests that they are not directly related to the local wind.

During October and November 1979 (Figure 21) there is again a period of generally weak upwelling index when that index has no obvious relation to the currents. These currents were equatorward from 12 until to 30 October, followed by a reversal to become poleward from 1 through 21 November while the upwelling index again varied erratically near zero.

During the period 3 March through 12 April 1980 (Figure 27) poleward and equatorward flow alternate until about mid-March, while the upwelling index remains low. Following a rise in the upwelling index at that time (mid-March) and its persistence at high levels for nearly three weeks, predominantly poleward flow begins and persists for the remainder of the recorded period, some three weeks.

The meter at 113 m (Figure 27) is suspect due to lack of direction changes and small magnitude, and its data will be ignored.

### 3. Comparision of Stations 2 and 7

Current meter arrays were deployed at both Stations 2 and 7 during the period from 21 July to the end of August, providing an opportunity for examining horizontal

variations. As mentioned above, the currents at Station 2 (depicted in Figure 18) appear to respond with little or no lag to local forcing for this entire period. The response of the currents to local winds is not so clear at Station 7 (Figure 14). The currents at Station 7 may respond differently to local winds than currents at Station 2 because of the increased distance from the controlling boundary (coast). It is also possible that the response of the currents at Station 7 to local forcing may be masked by other influences. Certainly, there is no longer a nearly in-phase response of the current (note, for example, that on 27 August flow at Station 2 is predominantly poleward while flow at Station 7 is predominantly equatorward). If flow at Station 7 is being driven by local winds, the response must lag the wind.

Seasonally, the countercurrent was strongest during the spring months of 1979 at Station 2 (Figure 11). Geographically, the major discernable difference is the closer correlation between the current and the local forcing at Station 2 (inshore) than at Station 7 (offshore).

In summary, there are four important conclusions to the analysis of the currents and their relation to the upwelling index:

1. The entire record from January 1979 to April 1980 indicates currents are predominantly poleward at both stations, especially while Bakun's coastal upwelling index is high and positive.



2. Throughout the period, many events with time scales of tens of days occur at all recorded depths.

3. Current response to local forcing is more apparent at Station 2.

4. The countercurrent runs most strongly during the periods of high upwelling index at the nearshore station (Station 2).

#### B. SPECTRUM ANALYSIS

The current meter data are subjected to spectrum analysis in order to identify regions of high energy in the frequency domain, and consequently suggest forces at work in the study area.

The information from spectrum analysis, in this case via a program using Fast Fourier Transform (FFT), depends upon the record length and the sampling interval. The parameters used in the spectrum analysis program are:

Record length	= $T_R = 1024$ h
Sampling interval	= $\Delta t = 1$ h
No. of points per record	= $N = 1024$
Resolution	= $\Delta f = .0098$ h <sup>-1</sup>
Nyquist frequency	= $f_N = .5$ h <sup>-1</sup>
No. of frequencies resolved	= $M = f_N / \Delta f = 512$
No. of degrees of freedom	= $N/M = 2$

The records available are typically about 50 days (1200 h) long; the maximum resolution attainable by FFT is, therefore, obtained from data sets of length 1024 hours.



For a fixed record length, however, high resolution is paid for at the expense of stability. The resolution with no averaging of spectral estimates over frequency is  $\Delta f = 1024^{-1} \text{ h}^{-1}$ ; and for single spectra (with no ensemble averaging) the estimates of variance have only two degrees of freedom (and are thus uncertain indicators of the variance distribution).

For time series defined at equal time-intervals  $\Delta t$ , the highest frequency component discernable is given by  $N_f = (2\Delta t)^{-1}$ , the "Nyquist frequency". The variance of frequencies higher than this are attributed, spuriously, to lower frequencies. Such misread ("aliased") variance is thought to be of minor concern in the data sets of this study except for those few (discarded) with high frequency instrumental noise. Among forces known to be at work in the ocean which are likely to contribute to energetic currents are tidal and (possibly) inertial forces. Some of the most important components are the semi-diurnal tide-producing forces (Sverdrup, et al., 1942):

Name	Symbol	Period(h)	Frequency( $\text{h}^{-1}$ )
Principal lunar	$M_2$	12.42	.0805
Principal solar	$S_2$	12.00	.0833
Luni-solar	$K_2$	11.97	.0835

The inertial frequency and period, calculated with the average latitude ( $35.8^\circ$ ) of Station 2 and Station 7, are  $f(i) = .0487 \text{ h}^{-1}$ , and  $T(i) = 20.5 \text{ h}$ .

The spectral estimates consistently indicate energetic components at tidal and inertial frequencies as well as at periods of approximately 10 days. The dominant tidal components present are the semi-diurnal, with the most significant peaks appearing to be the luni-solar. In Table I are shown the approximate values of the low frequency, inertial, and semi-diurnal tidal peaks for both alongshore, and onshore/offshore motion. These values in Table I are taken from the spectrum analysis plots to show what, if any, relation there is between high energy and depth, season, and proximity of the shore. In general the spectra indicate greater energy for tidal, inertial, and low frequencies at the upper meters. It appears that motions at these frequencies are also more energetic in winter than in summer. Finally, tidal and low frequency energy are greater near shore, while energy in the inertial frequency is greater offshore.

#### C. INFERENCES FROM PROGRESSIVE VECTOR DIAGRAMS

The PVD's are helpful in observing low frequency variations and the mean currents which are summarized in Table II. As a meander, eddy, or wave in the countercurrent moves through a stations position the boundary between the poleward flow and equatorward flow moves about, with the current meters alternating between either side of that boundary. Such an occurrence is reflected in the PVD's as a current reversal.

TABLE I

COMPARISON OF HIGH ENERGY PEAKS (1000 CM. SQ. HOUR)

STATION	START DATE	DEPTH	LOW FREQ. (10 DAY)			INERTIAL		S.D. TIDAL	
			ALONG SHORE	ON/OFF SHORE		ALONG SHORE	ON/OFF SHORE	ALONG SHORE	ON/OFF SHORE
2	23 APR 79	169 241	5.3 4.0	0.5 SMALL		1.0 1.0	0.5 0.5	8.0 11.0	6.5 5.0
2	21 JUL 79	165 237	17.0 8.0	0.5 0.5		1.0 SMALL	0.3 0.2	3.0 3.0	1.7 1.2
2	24 NOV 79	194* 266	0.3 45.0	0.5 1.0		SMALL 2.0	SMALL 1.0	SMALL 11.0	0.1 17.0
7	5 JAN 79	152 223	6.8 1.5	7.0 5.4		1.8 0.6	2.3 0.5	1.8 1.4	2.0 0.8
7	7 JUL 79	158 231 356	2.6 2.0 0.8	17.0 5.1 1.0		0.2 0.4 0.9	SMALL SMALL 0.7	1.6 1.3 0.5	2.0 1.8 0.6
7	7 OCT 79	127 200	1.0 1.3	1.6 1.1		4.5 2.0	3.4 2.3	3.7 3.0	3.8 2.6
7	3 MAR 80	113* 186 311	0.2 1.8 0.9	0.1 1.1 0.2		0.1 1.4 1.8	0.1 1.5 1.8	0.3 2.6 5.0	0.1 2.0 1.2

S.D. = Semi-Diurnal

\* = Meter is suspect

TABLE II

## COMPARISON OF MEAN CURRENT AND TEMPERATURE

STATION	TIME PERIOD	DEPTH	$\bar{\theta}$ (azim. °T)	$\bar{V}$ (cm/sec)	T (° cent.)	$\bar{V}'$ (cm/sec)	$\bar{U}'$ (cm/sec)
2	23 APR 79	169	341.2	16.0	8.5	+16.0	+ 0.34
	thru 16 JUN 79	241	340.4	11.1	8.0	+11.1	+ 0.08
2	21 JUL 79	165	325.1	6.1	9.0	+ 5.89	- 1.57
	thru 13 SEP 79	237	314.3	1.5	8.5	+ 1.35	- 0.65
2	24 NOV 79	194*	279.8	6.2	9.0	+ 3.08	- 5.38
	thru 18 JAN 80	266	003.1	2.7	8.0	+ 2.48	+ 1.06
7	9 JAN 79	152	354.8	4.6	9.4	+ 4.58	+ 0.39
	thru 28 FEB 79	223	16.6	4.3	8.6	+ 3.84	+ 1.93
7	9 JUL 79	158	312.2	4.5	8.7	+ 3.56	- 2.76
	thru 30 AUG 79	231	330.6	5.8	8.3	+ 5.47	- 1.93
		356	338.6	2.8	7.4	+ 2.74	- 0.55
7	9 OCT 79	127	68.1	5.1	9.3	+ 1.05	+ 4.99
	thru 29 NOV 79	200	70.6	4.1	8.4	+ 0.67	+ 4.05
7	4 MAR 80	113*	310.5	4.4	9.0	+ 3.40	- 2.80
	thru 15 APR 80	186	328.7	3.4	8.0	+ 3.17	- 1.24
		311	8.2	2.7	7.0	+ 2.56	+ 0.84

 $\bar{U}'$  = Mean cross-slope current $\bar{V}'$  = Mean alongshore current

\* = Meter is suspect

Two interesting features readily seen in the progressive vector diagrams Figures 47 through 62, are current reversals of long duration, and the mean current for the duration of the mooring. The mean current direction ( $\theta$ ), given as azimuth, speed ( $V$ ),  $\text{cm-s}^{-1}$ , and temperature ( $T$ ), degrees Celsius, for each current meter for the entire study period are shown in Table II; and they are also shown on the individual plots. Also shown in Table II are the mean onshore and alongshore current components respectively. The alongshore direction in this case is defined as  $340^\circ$  T for Station 2, and  $350^\circ$  T for Station 7, which represent the azimuths of the mean contours at those sites.

For both Stations 2 and 7 over the entire period, the seasonal and depth variations will be considered. The mean alongshore current is always poleward at all observed levels (from 127 m to 356 m) and at both stations. Mean alongshore current speeds were greater nearshore at Station 2, than offshore at Station 7. Mean alongshore current speed at the upper levels appears to vary only slightly seasonally at both stations, approximately 4 to 6  $\text{cm-s}^{-1}$ , with the exception of the upper meter at Station 2, 23 April to mid-June, i.e., the counter current appears weak at observed depths, except in late spring.

The PVD's indicate predominantly unidirectional flow at the near-surface levels of Station 2, while at the deeper,



lower meters there were often current reversals and oscillations possibly associated with meanders, waves, and eddies. Current reversals occurred in greater numbers and were present at all depths at Station 7 which may possibly be due to Station 7 being near a boundary between north and south currents. The semidiurnal components of the currents are at times apparent in the PVD's as for example in Figures 49 and 57.

Shorter term variations are also indicated by the PVD's, in particular reversals. No apparent current reversals are present at the upper meter of Station 2, 24 April to mid-June (Figure 49), and only two minor reversals can be seen near the end of the record for the lower meter (Figure 50). At the same station from 23 July to mid-September, two current reversals of short duration are evident at the upper layer (Figure 54); and more than half a dozen current reversals of from three to twelve days in duration can be seen for the current at greater depth (Figure 55). Current reversals are not present at the upper level of Station 2 (Figure 58), 27 November 1979 to mid-January 1980, but several current reversals of approximately three to nine days duration can be seen at depth (Figure 59).

A single current reversal is present at both meters of Station 7 (Figures 47 and 48), 9 January to the end of February 1979. At the same station, 9 July to the end of



August 1979, three current reversals are apparent at the upper two meters (Figures 51 and 52), and two reversals can be seen in the lower meter (Figure 53). These reversals all appear to be of a relatively long duration, 15 to 20 d. Two current reversals are present at both meters of Station 7 (Figures 56 and 57), 9 October to 29 November 1979. For the period 4 March to 15 April 1980 at the same station, no reversals are seen in the upper meter (Figure 60), but several oscillations and reversals are seen in the two lower meters (Figures 61 and 62).

#### D. CROSS-SLOPE CURRENT

The mean cross-slope currents from Table II are plotted against time in Figure 5. The dominant feature of these currents is an annual variation with onshore flow in winter months and offshore in spring and summer. This annual variation correlates with the strong upwelling occurring in the spring and summer, and the weak upwelling index in the winter.

Qualitatively, the relation between the upwelling index and the cross-slope current means is consistent with a thick layer influenced by a modified surface Ekman regime.

#### E. TIME SERIES

The time series plots of U (positive-east) and V (positive-north) components were primarily used as an aid in interpreting the stickplot data. They are also useful for their resolution of high frequency variations. The

semidiurnal components of the currents are evident as well as the larger scale current oscillations indicated in the stickplots.

The temperature versus time plots also indicate the semidiurnal components and large-scale oscillations found in the stickplots. Approximate mean temperatures for the current meters at Station 2 and 7 throughout the record are shown in Table II. The temperature decreased with depth at all stations. The mean temperatures at Station 2 at all depths (Figure 6) become increasingly warmer during the period from April 1979 to January 1980, while the mean temperatures at Station 7 at all depths (Figure 7) become increasingly cooler. This is consistent with existing wind stresses, which would tend to uplift the isotherms at the nearshore station (Station 2) in the spring (strong upwelling index) and depress them in winter (weak upwelling index). The cooling continues at Station 7 at all depths from December 1979 until April 1980, and no simple explanation is apparent.

#### IV. CONCLUSIONS

A northward flowing current was found for the entire period of this study. It was strongest at the upper levels, roughly between 100 and 200 m. Seasonally, this countercurrent was strong during spring and substantially weaker during winter. The speed and direction of the countercurrent at any given time may differ markedly from the average flow. There were events on scales of tens of days which appeared to be qualitatively coherent between stations and also between depths at a given station. Frequent current reversals and oscillations occurred, consistent with the weak, poorly defined, broad flows associated with eastern boundary currents.

Bakun's coastal upwelling index is an indicator of possible wind-driven coastal upwelling. The coastal upwelling index is, in the mean, consistent with the observations of a deep cross-slope flow (Ekman layer), a large upwelling index corresponding to thickening of the Ekman layer. The countercurrent is present during the entire study, and the low frequency alongshore current is never equatorward.

Relatively high-energy peaks at semidiurnal tidal frequencies and inertial frequencies occurred in the

majority of the current records. Additionally, low frequency energy peaks were found at periods of about 10 d.

At Station 2, (nearshore), the alongshore component of these three frequencies tends to be greater than the on/offshore component, and generally speaking, the low frequency energy peak ( $T = 10$  d) is dominant. At Station 7 (offshore), the on/offshore component of these three frequencies is noticeably greater, but there is no obvious pattern to the energy distribution.

The countercurrent was present at the study site, but it was not possible to unequivocally identify and correlate local forcing with the countercurrent. The vertical migration of the frontal boundary between equatorward and poleward flow was observed at both stations, but less often at the nearshore Station 2 than at Station 7. Hydrographic data from the study area for this time period were not examined at all, and deserve future consideration. Correlation of currents and wind or upwelling index, comparison of observed currents with predictions of various models, and the relation of metered currents to those inferred from hydrographic data are recommended for future studies.

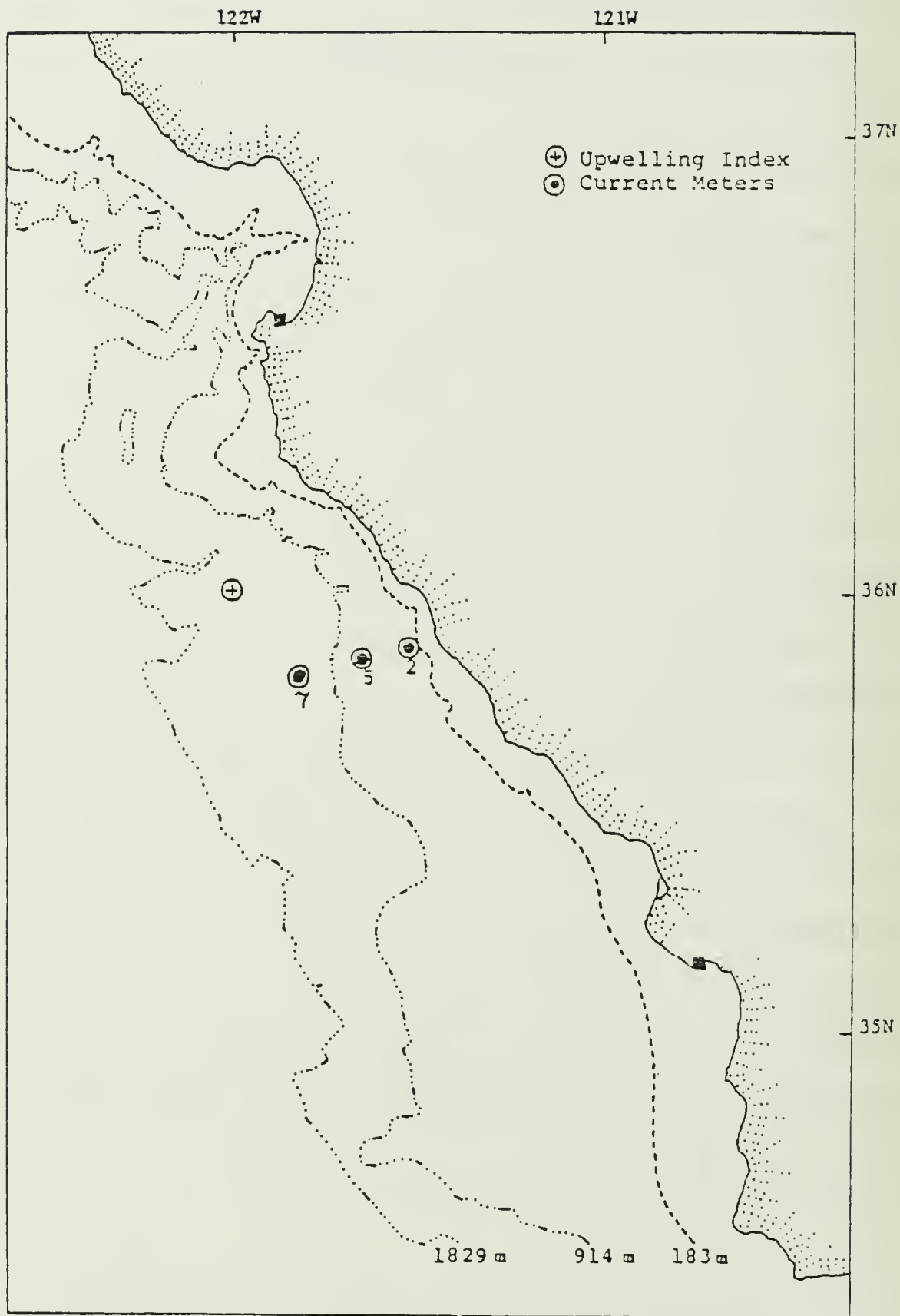


Figure 1. The study area.

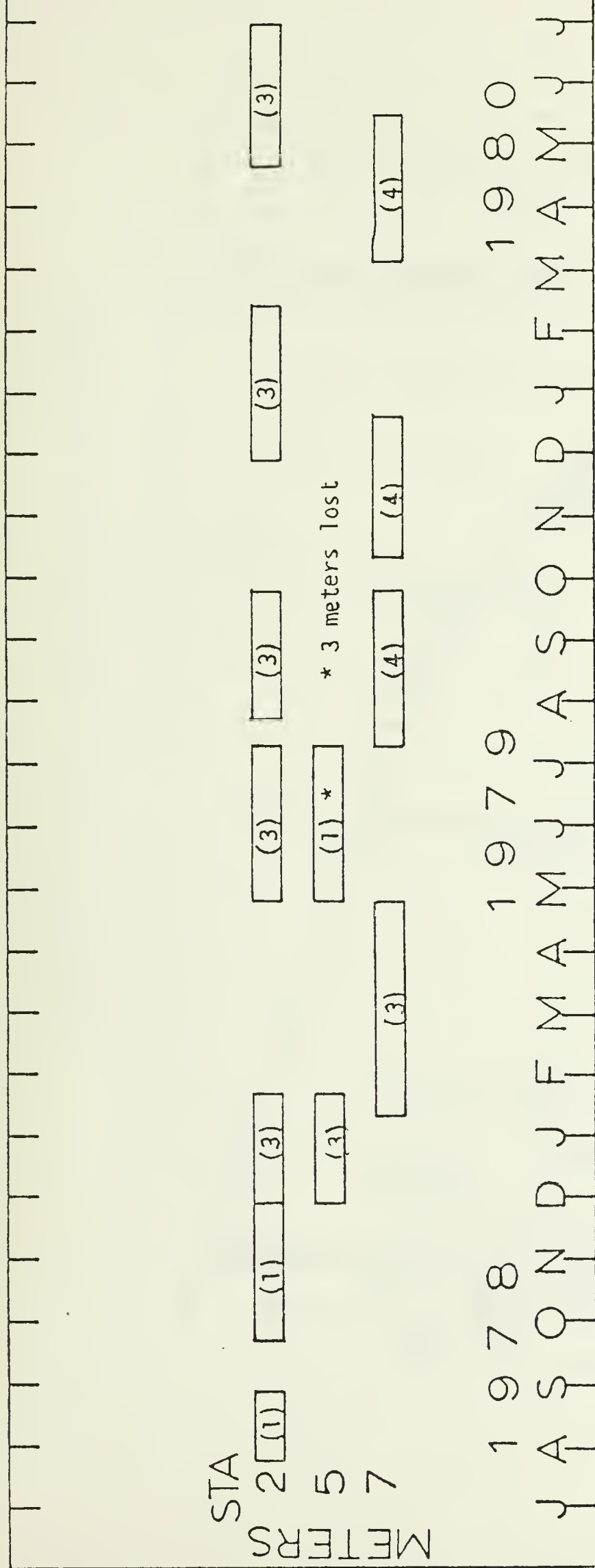


Figure 2. Chronology of current meter deployment.



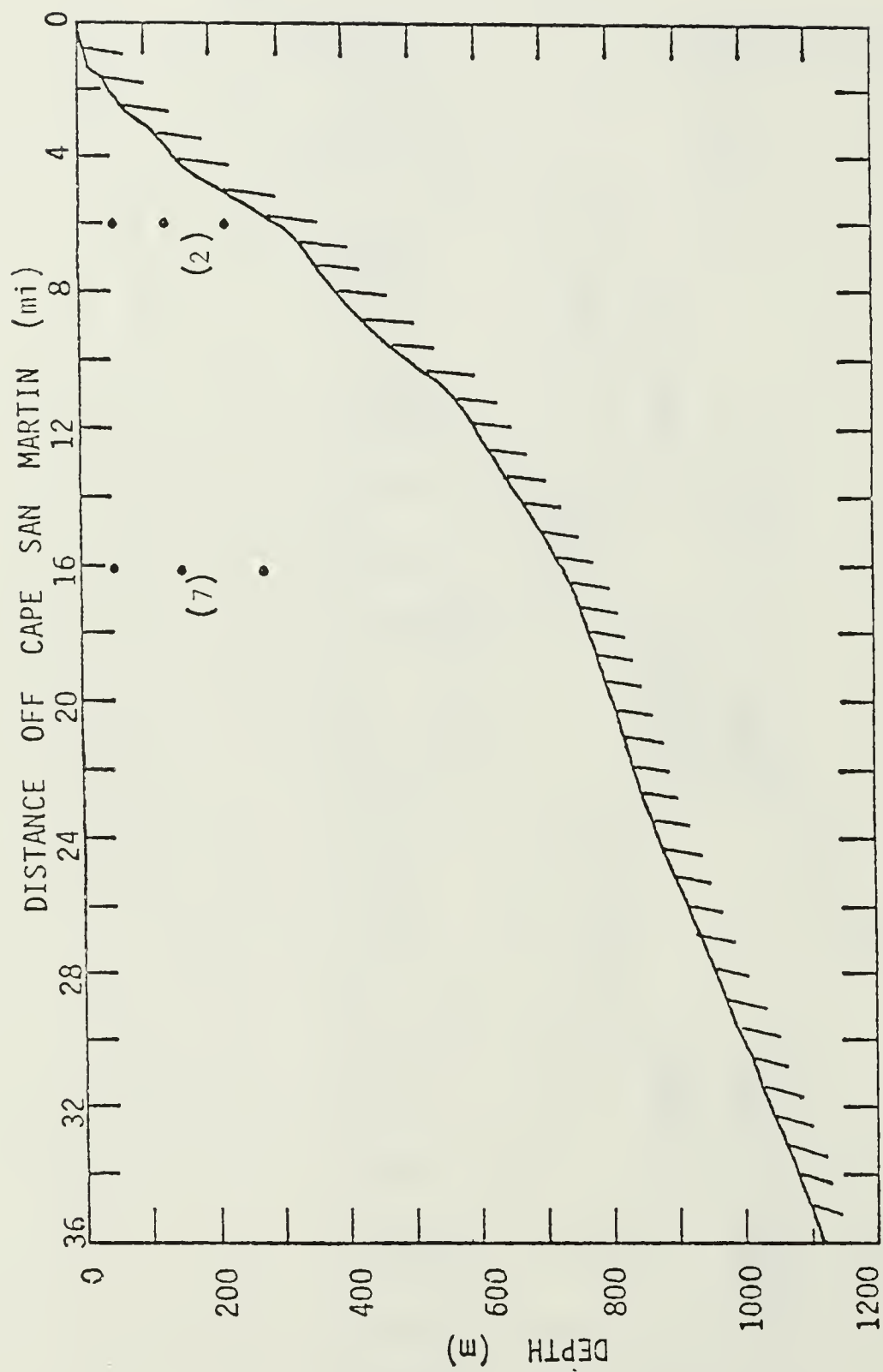


Figure 3. Vertical section showing representative locations of current meters off Cape San Martin, California.

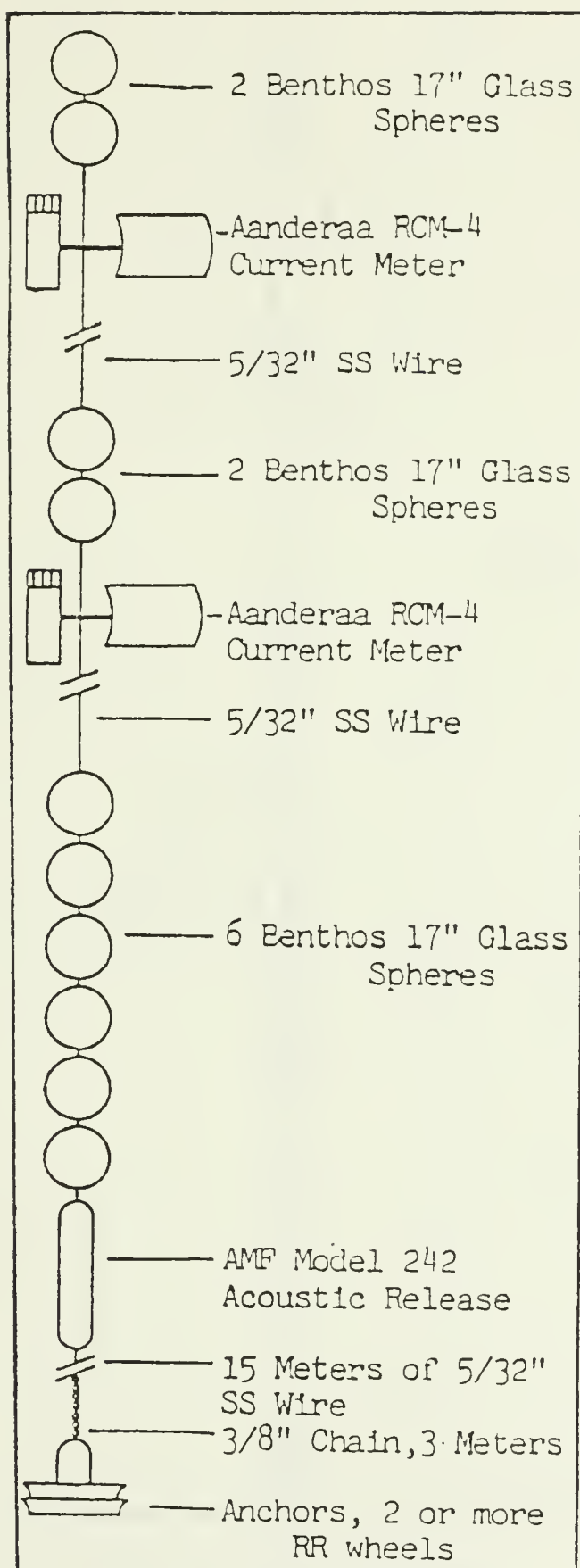


Figure 4. Current meter array.

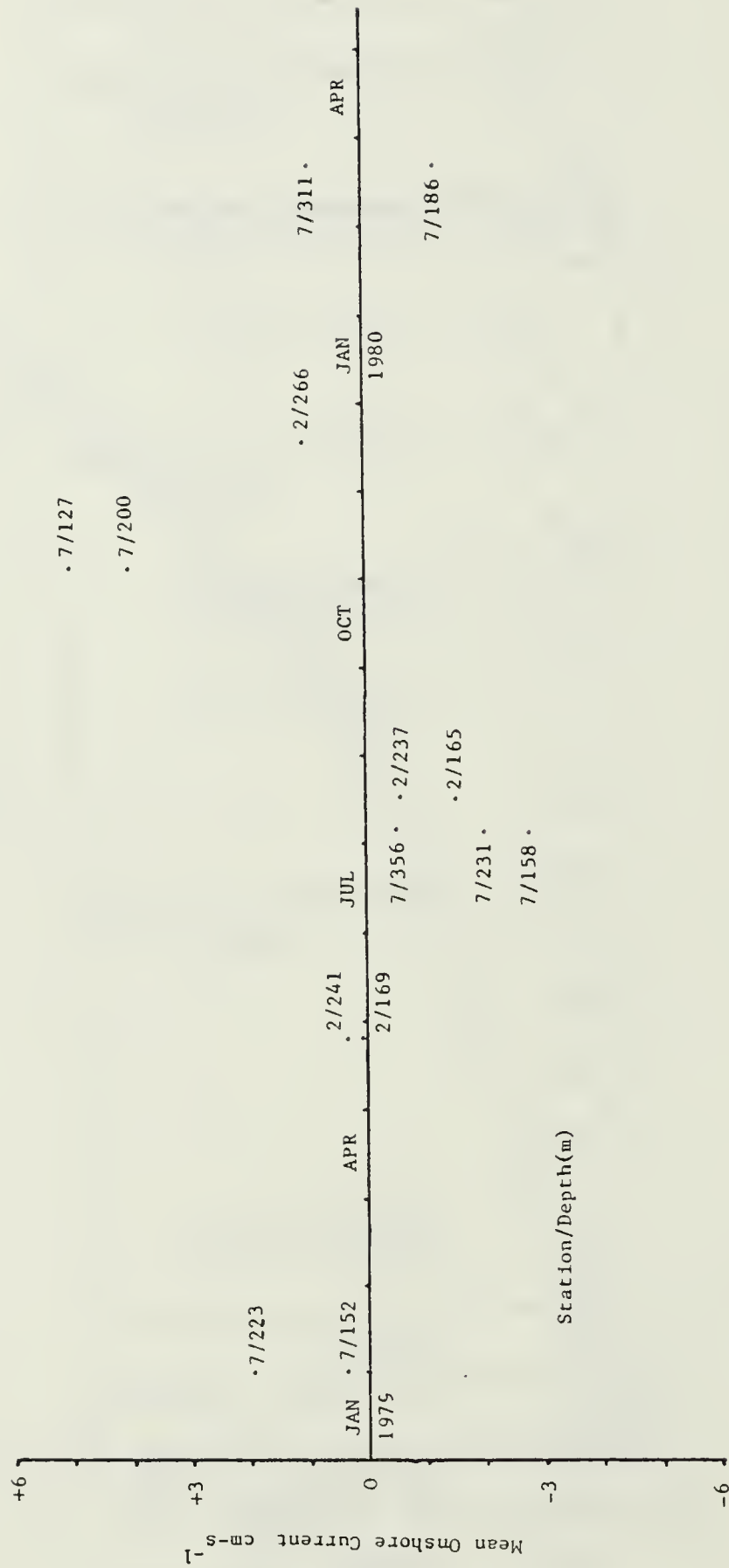


Figure 5. Mean onshore currents.

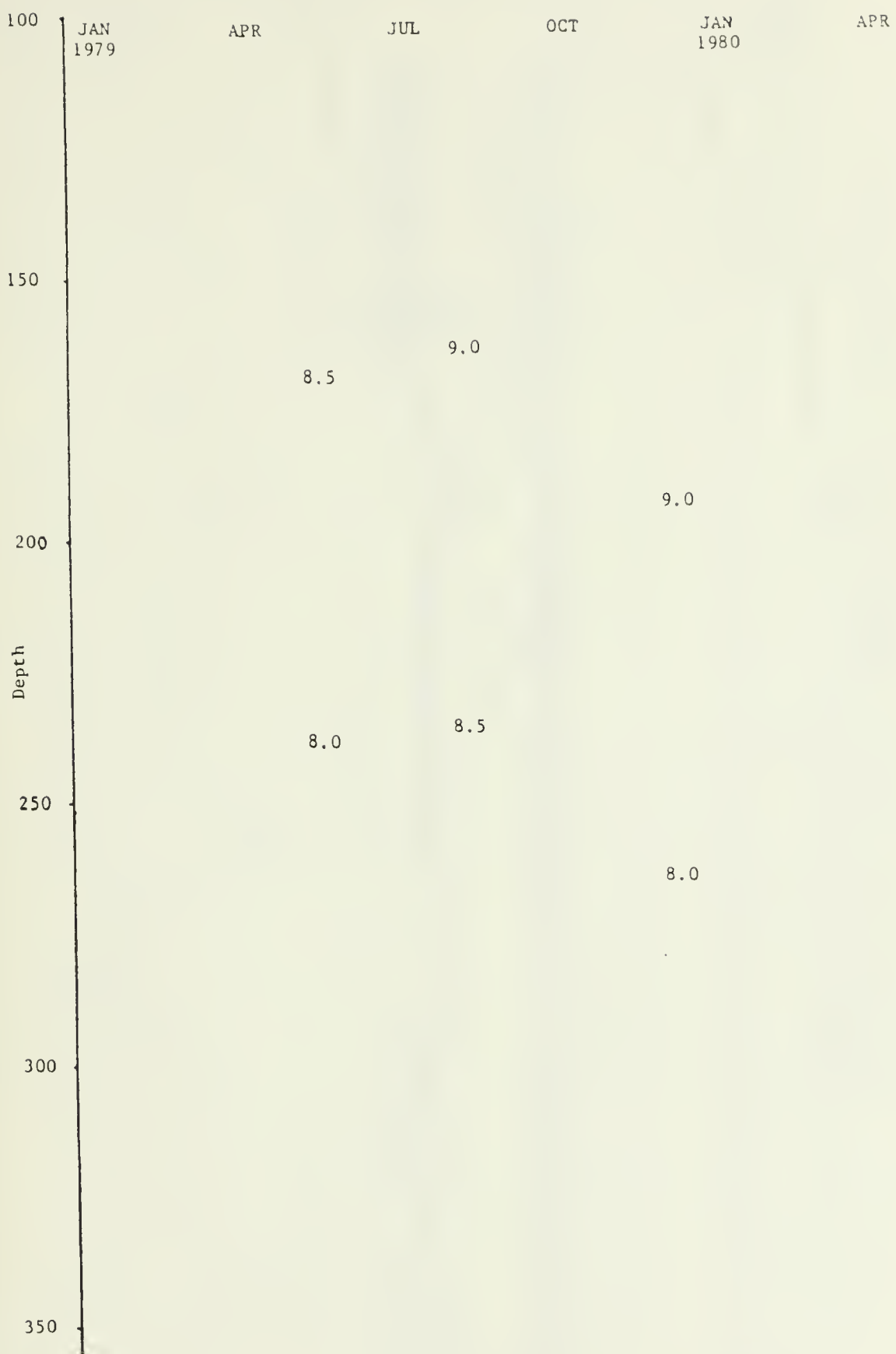


Figure 6. Mean temperatures at Station 2.

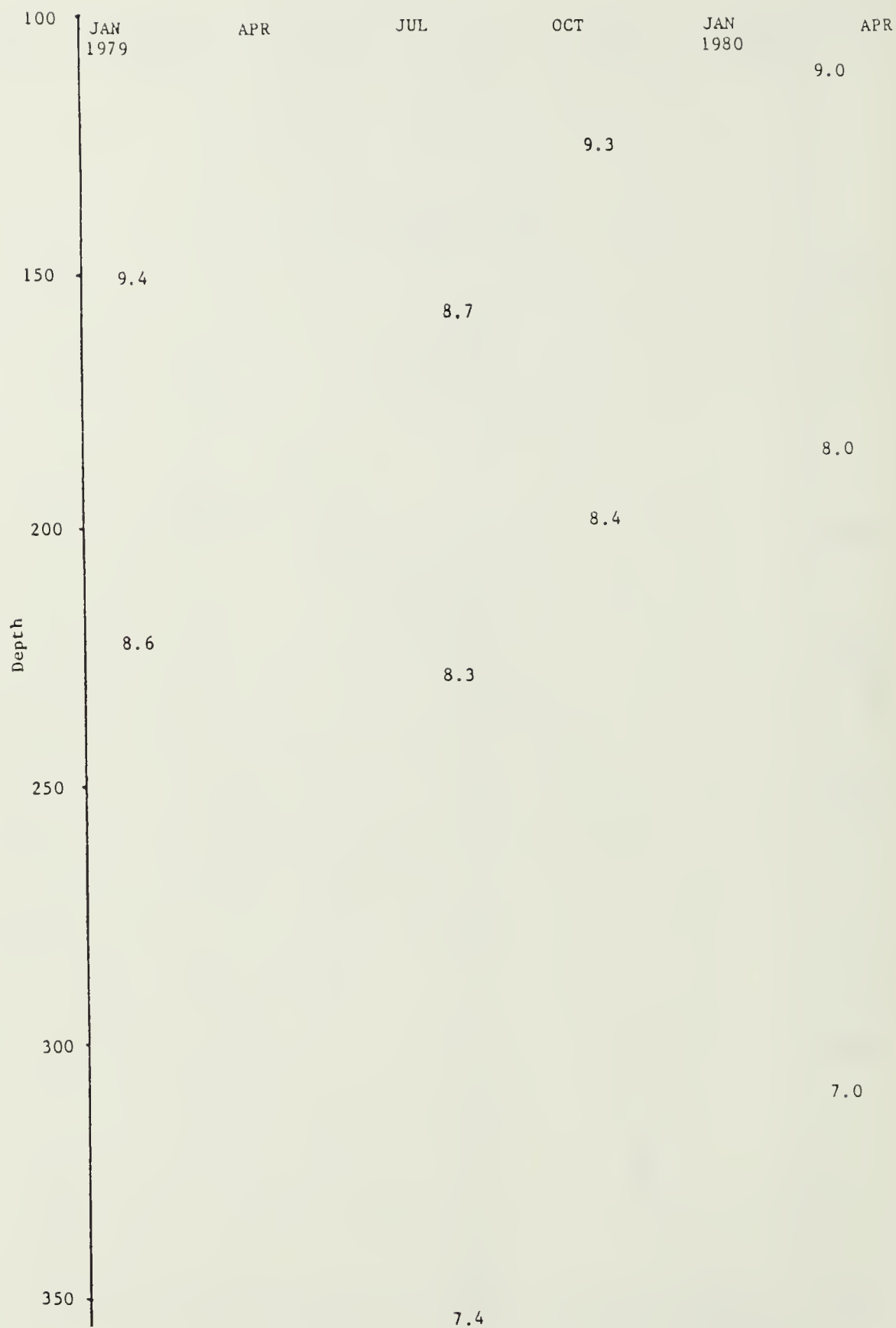


Figure 7. Mean temperatures at Station 7.

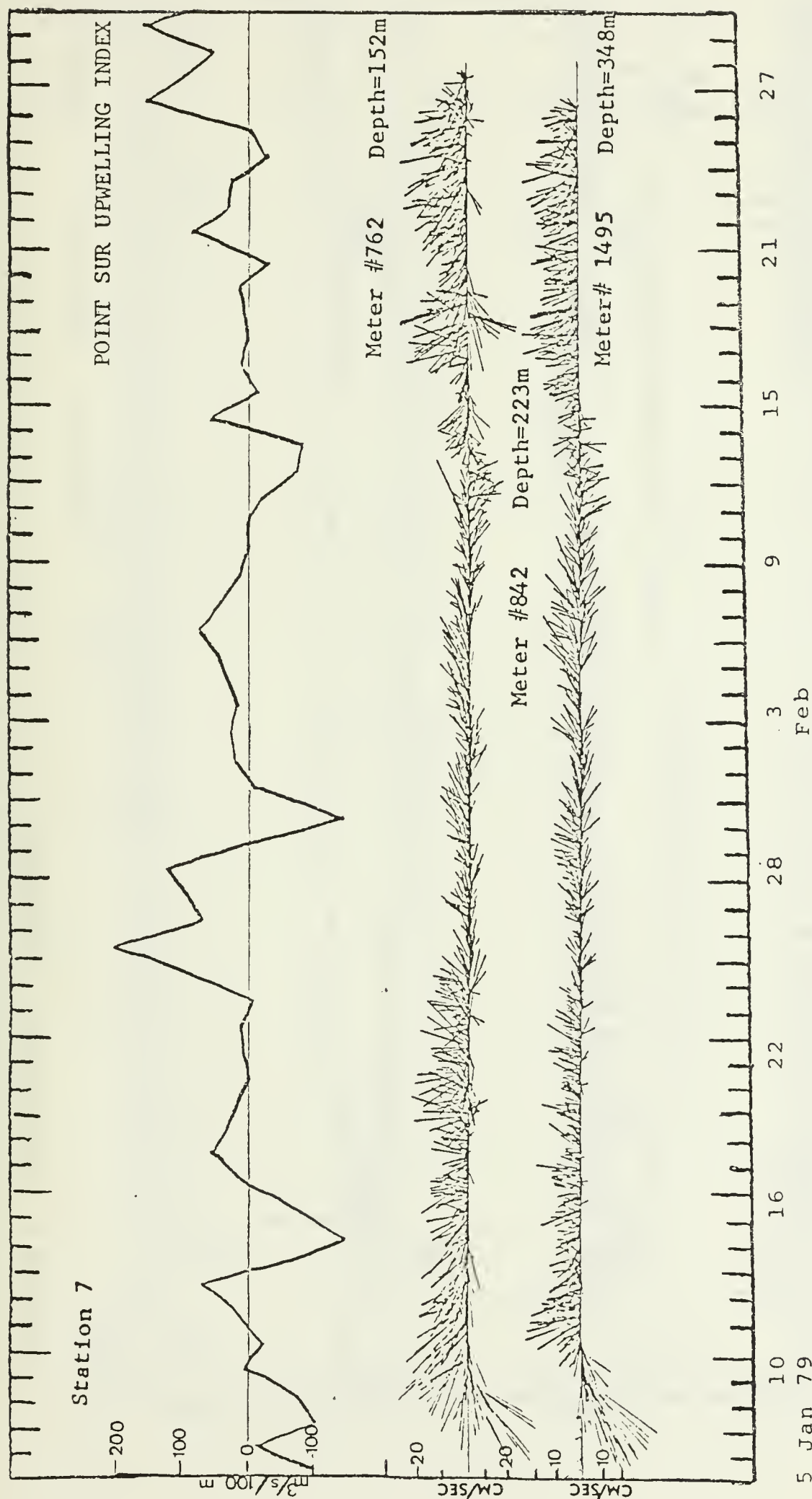


Figure 8. Point Sur Upwelling Index and stickplots of hourly current vectors for the current meters at Station 7 deployed on 5 January 1979.



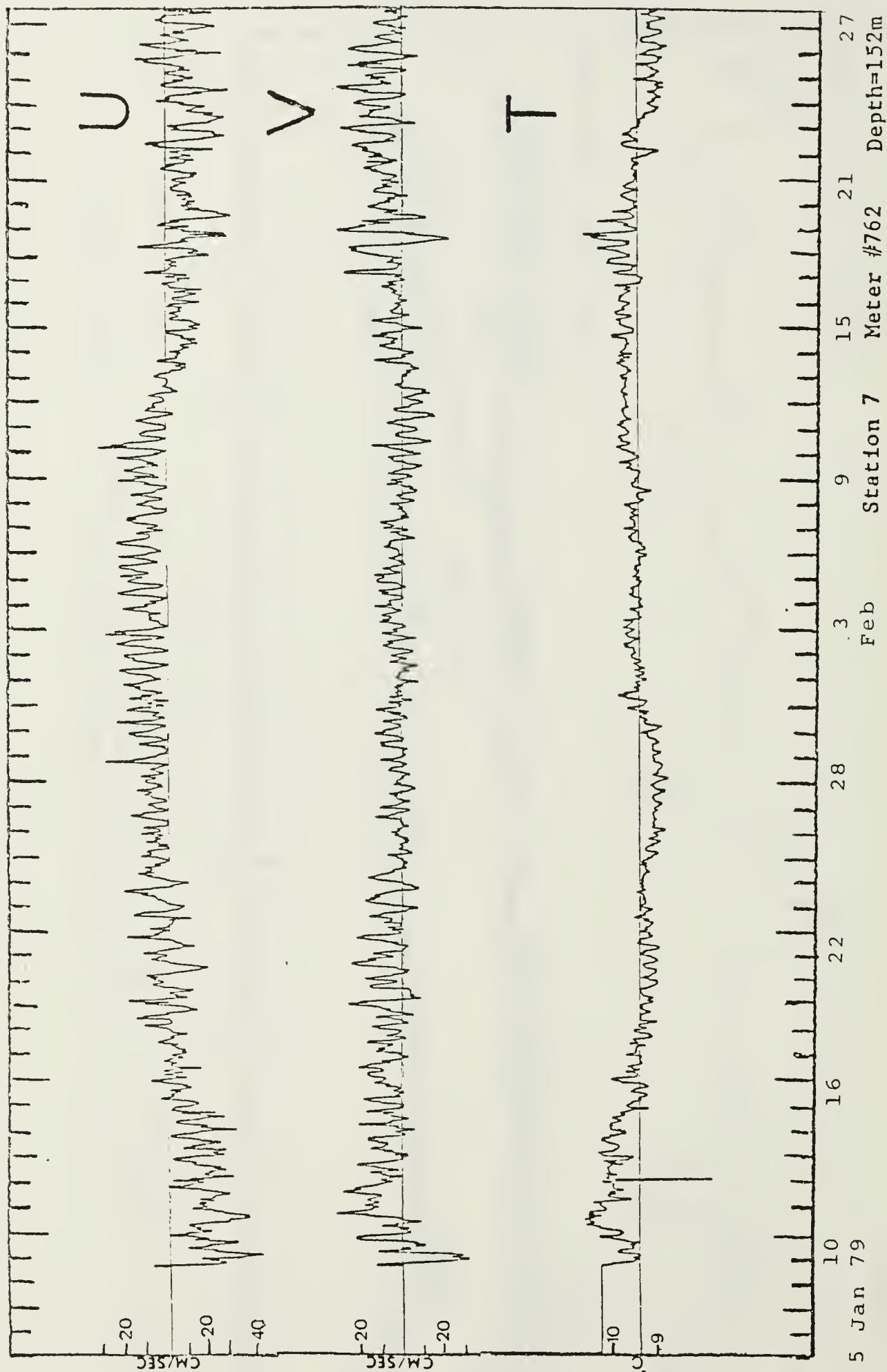


Figure 9. U component, V component, and temperature plots versus time for the current meter at 152 m depth at Station 7 deployed on 5 January 1979.

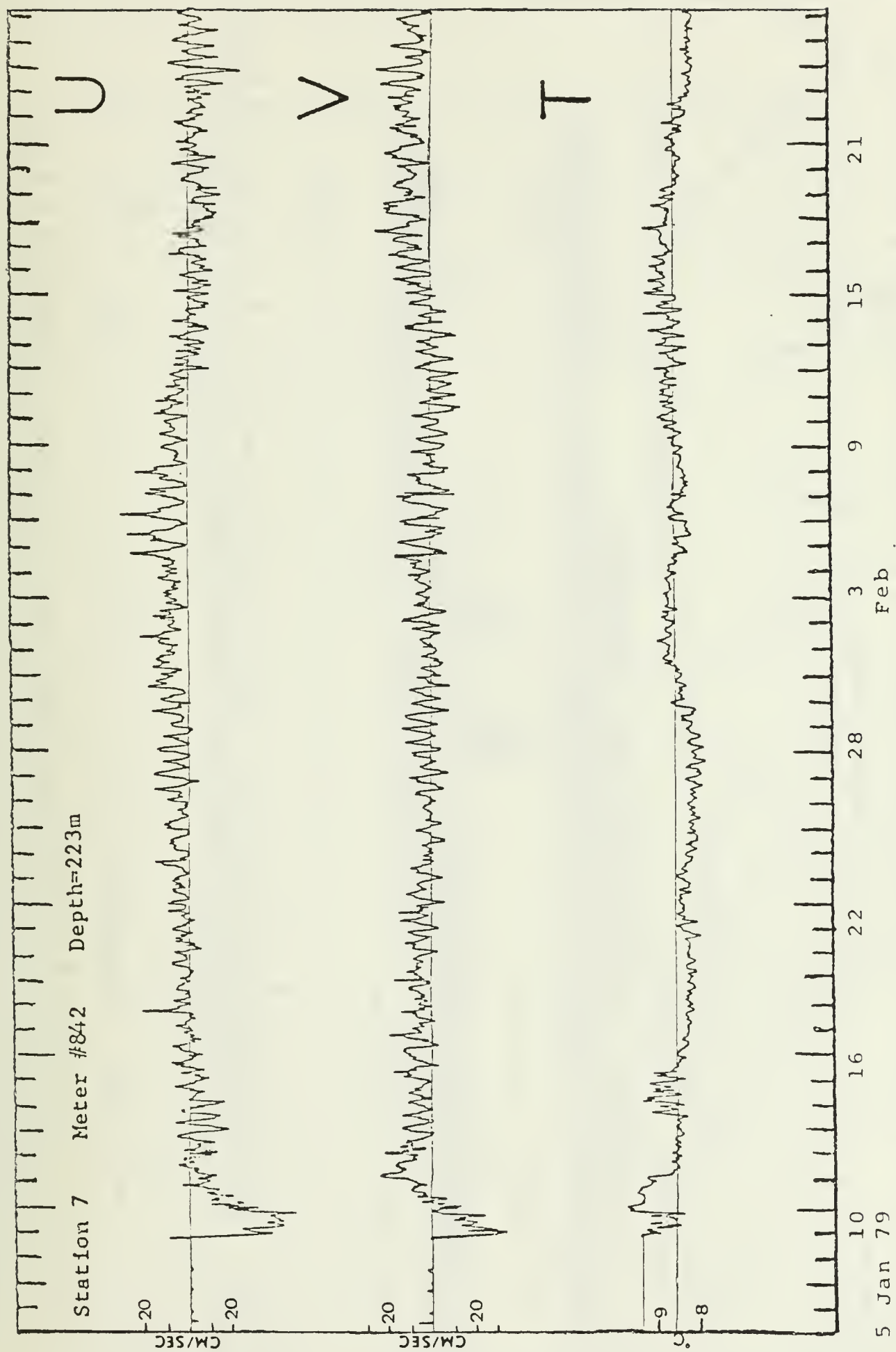


Figure 10. U component, V component, and temperature plots versus time for the current meter at 223 m depth at Station 7 deployed on 23 April 1979.

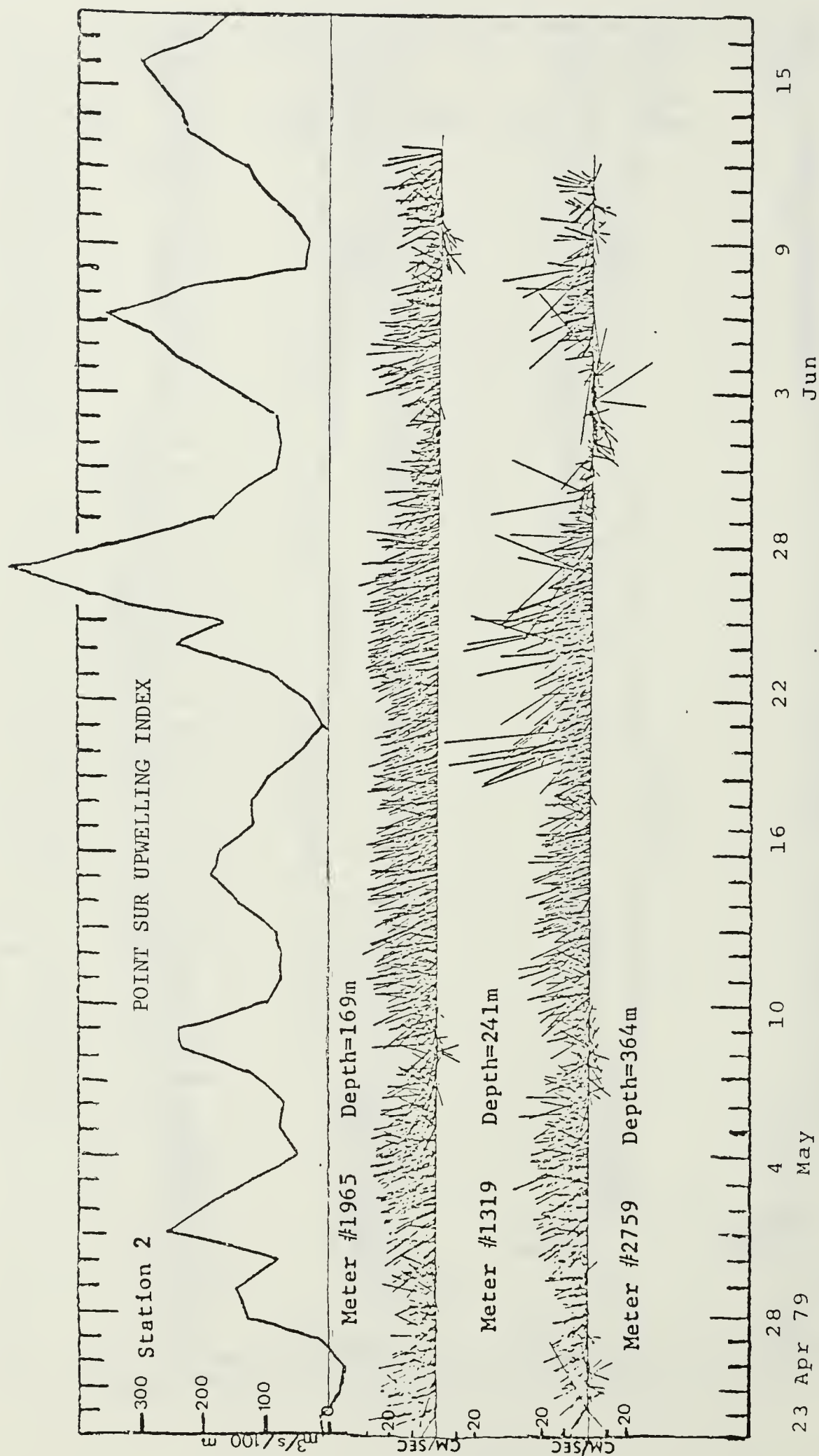


Figure 11. Point Sur Upwelling Index and stickplots of hourly current vectors for the current meters at Station 2 deployed on 23 April 1979.

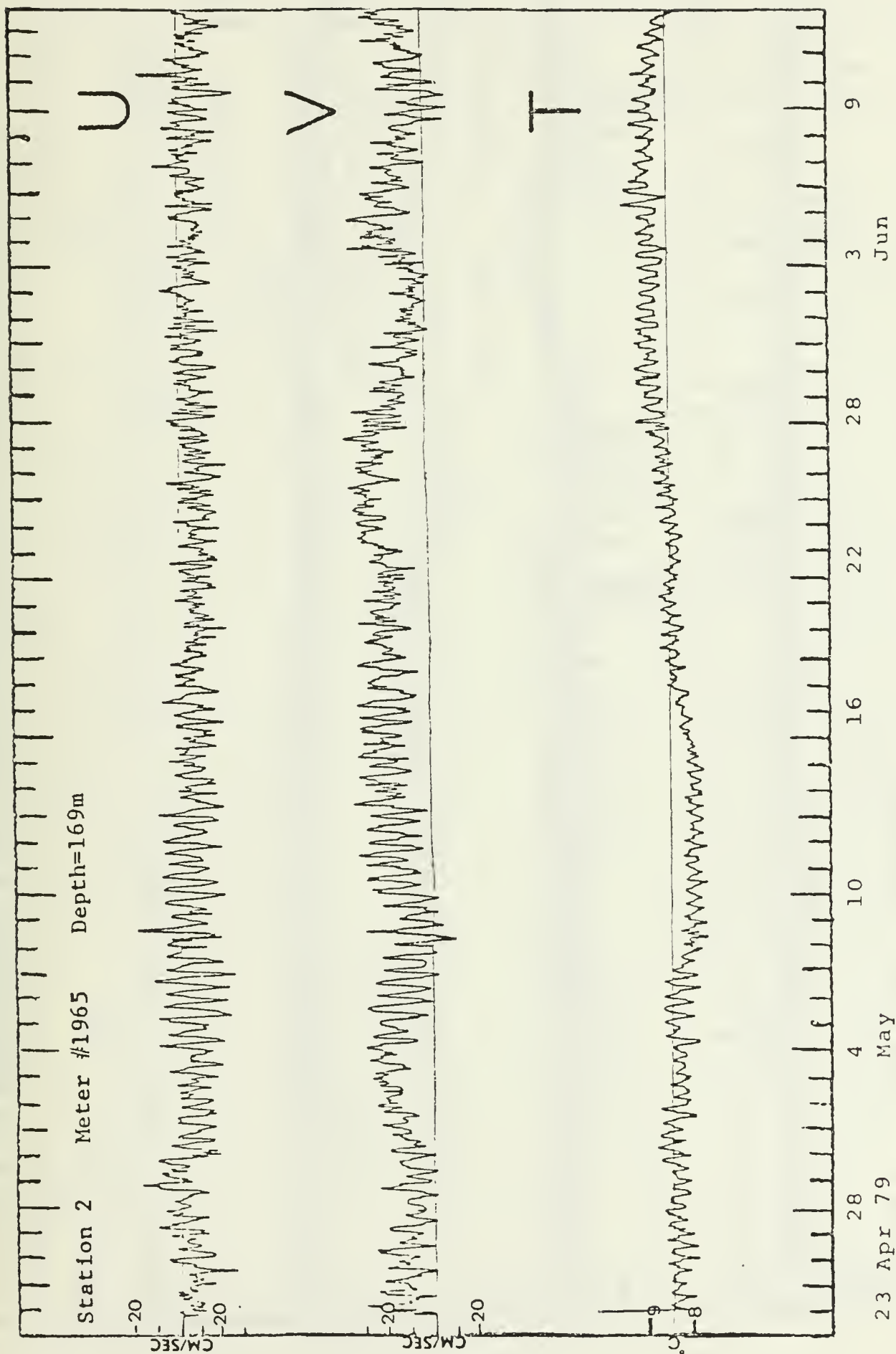


Figure 12. U component, V component, and temperature plots versus time for the current meter at 169 m depth at Station 2 deployed on 23 April 1979.

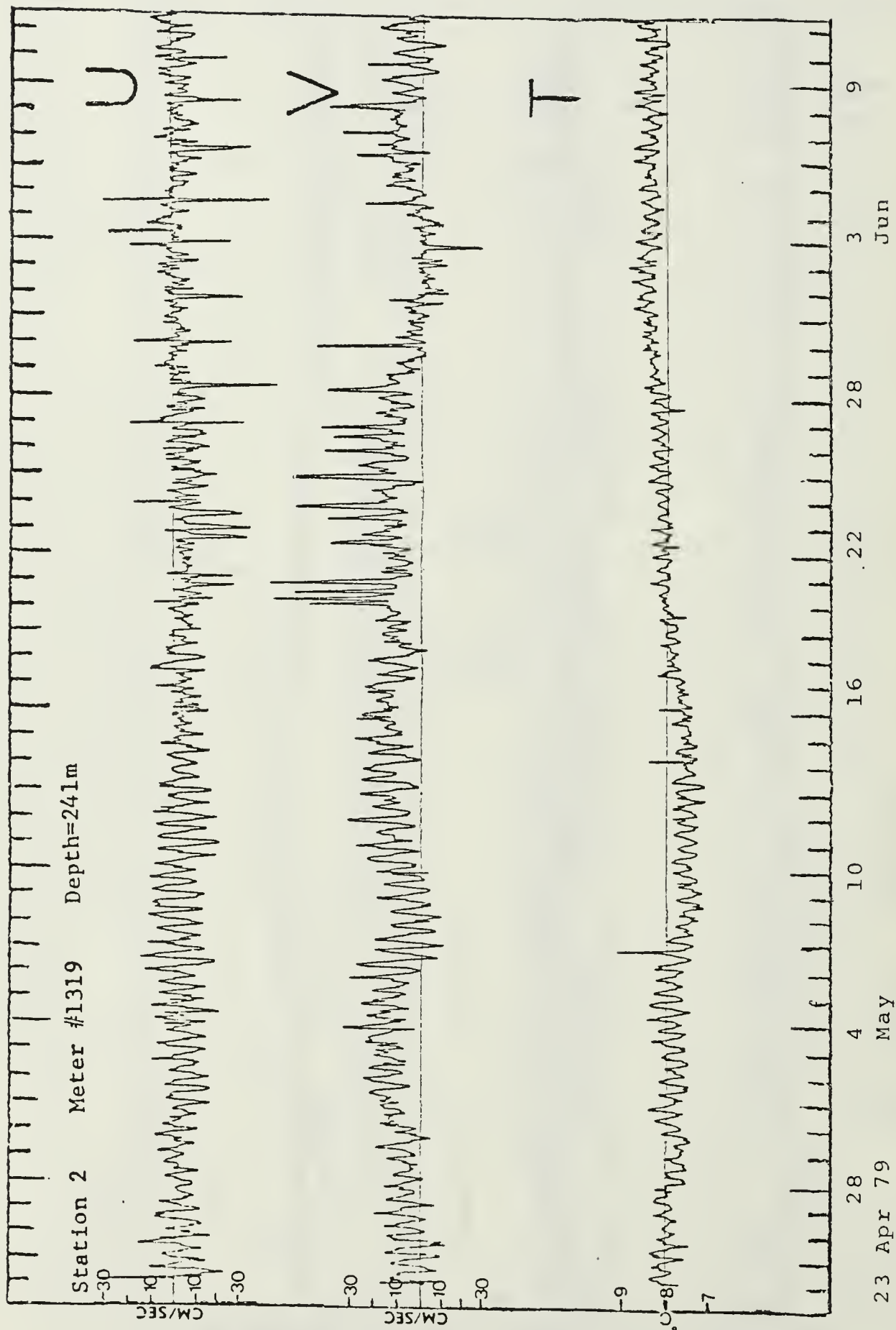


Figure 13. U component, V component, and temperature plots versus time for the current meter at 241 m depth at Station 2 deployed on 23 April 1979.



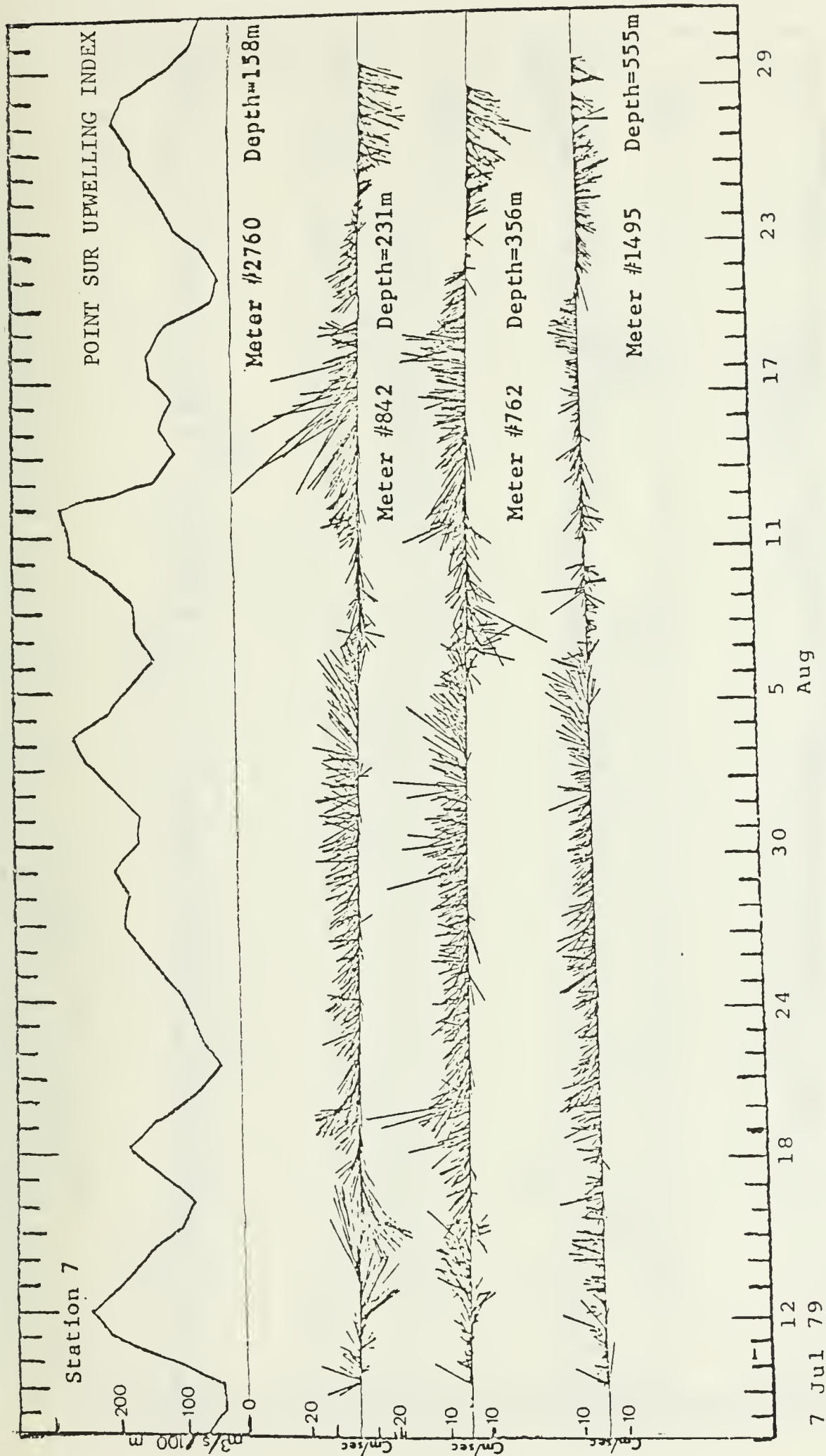


Figure 14. Point Sur Upwelling Index and stickplots of hourly current vectors for the current meters at Station 7 deployed on 7 July 1979.



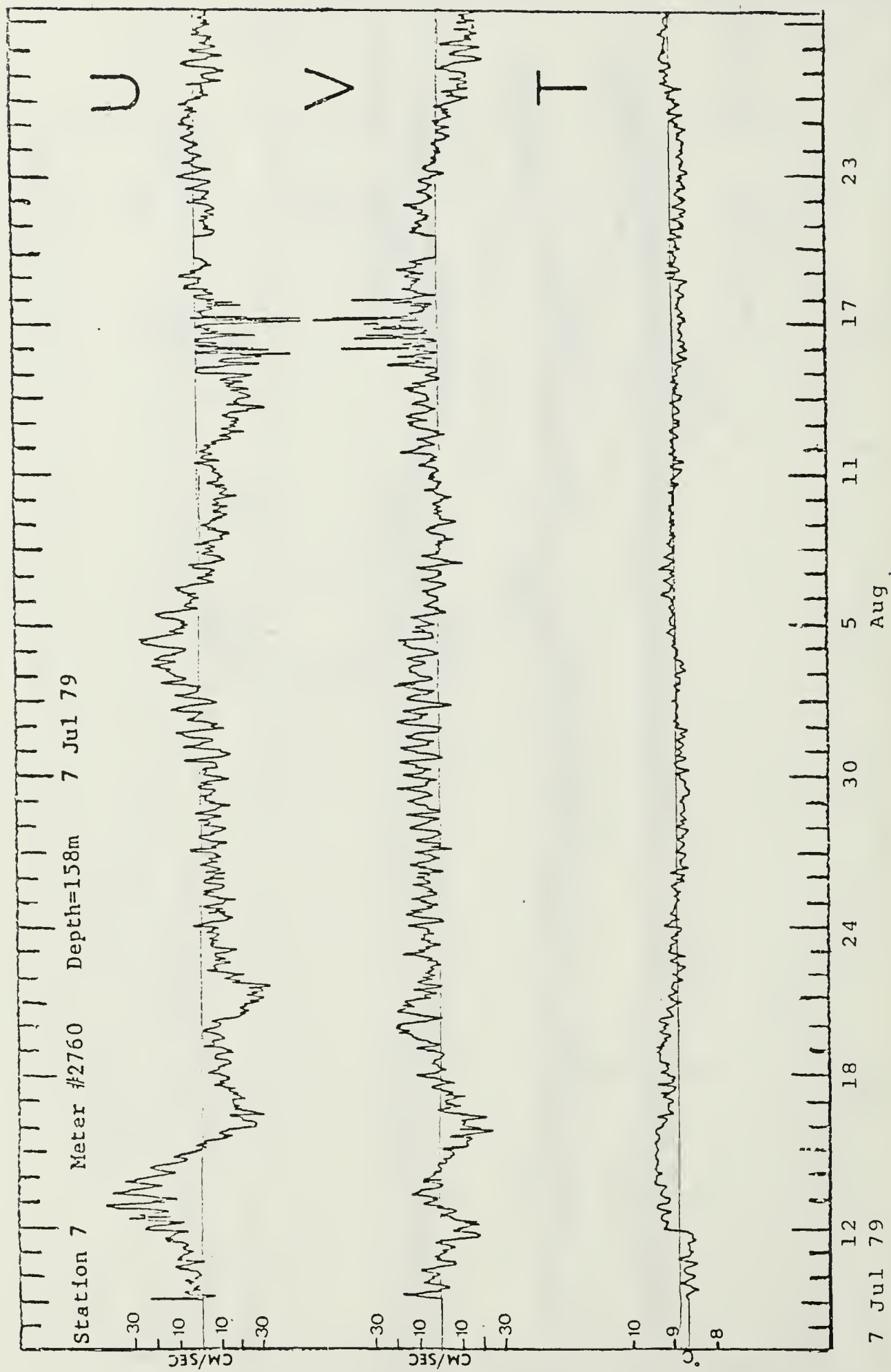


Figure 15. U component, V-component, and temperature plots versus time for the current meter at 158 m depth at Station 7 deployed on 7 July 1979.

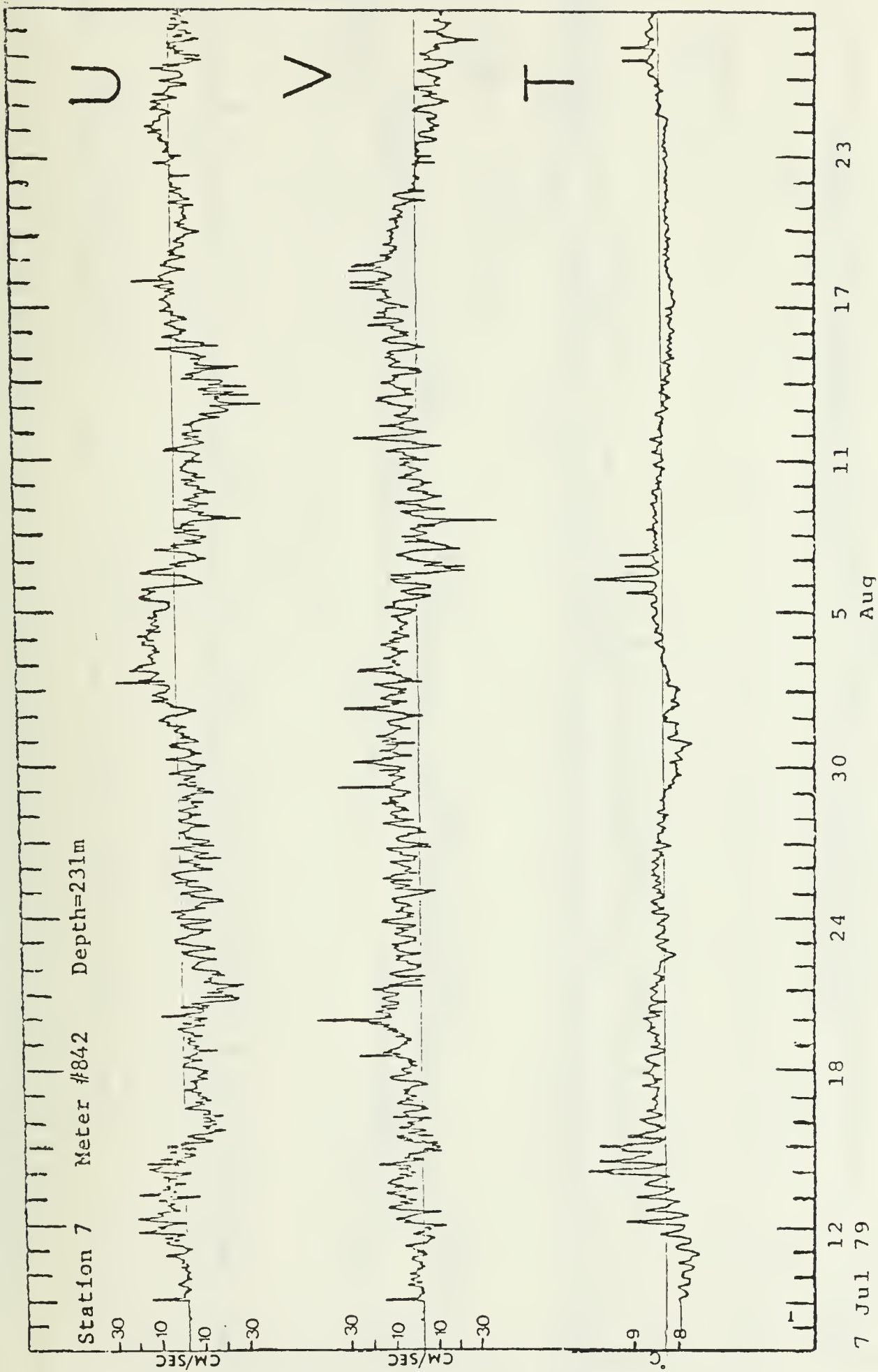


Figure 16. U component, V component, and temperature plots versus time for the current meter at 231 m depth at Station 7 deployed on 7 July 1979.

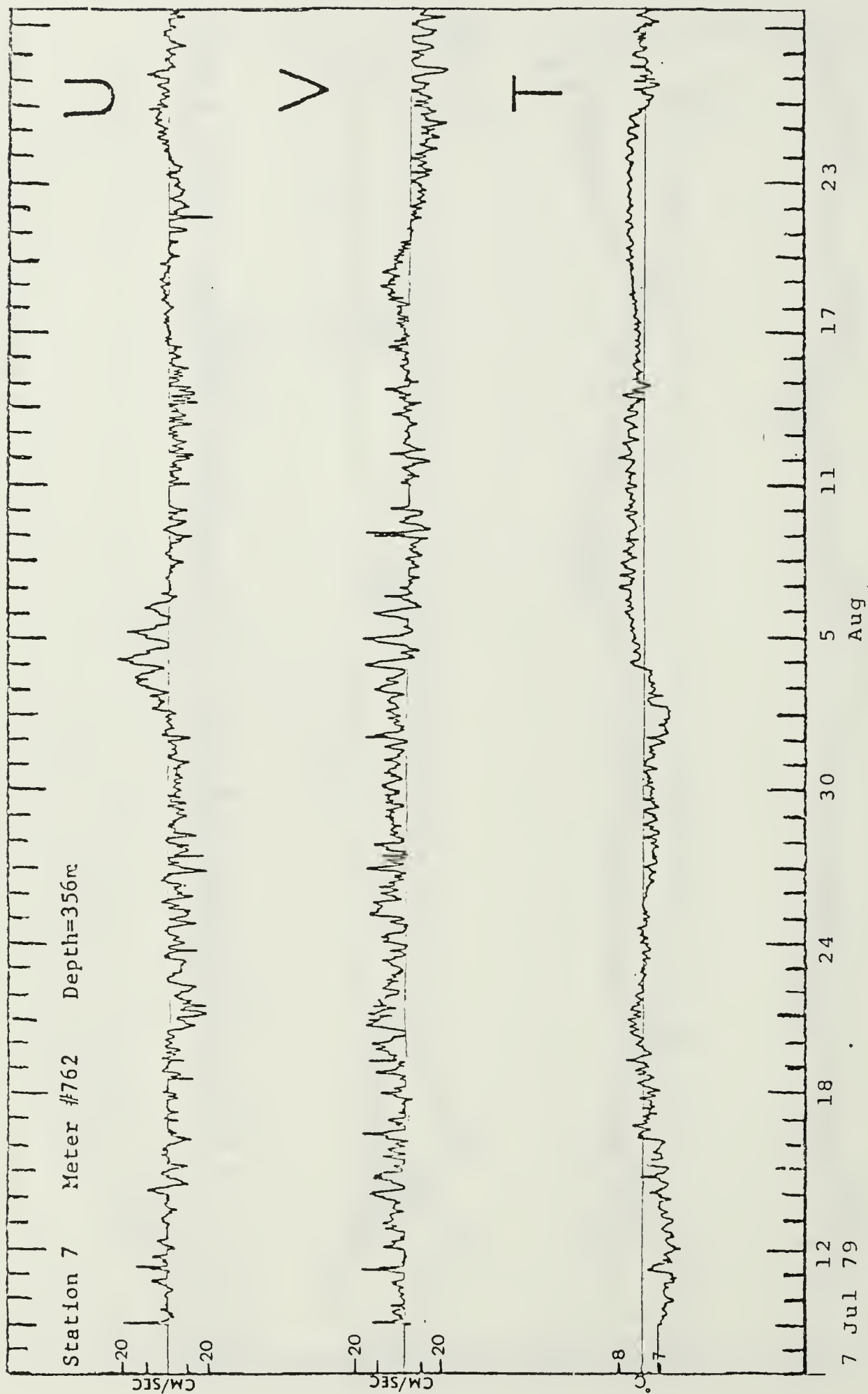


Figure 17. U component, V component, and temperature plots versus time for the current meter at 356 m depth at Station 7 deployed on 7 July 1979.

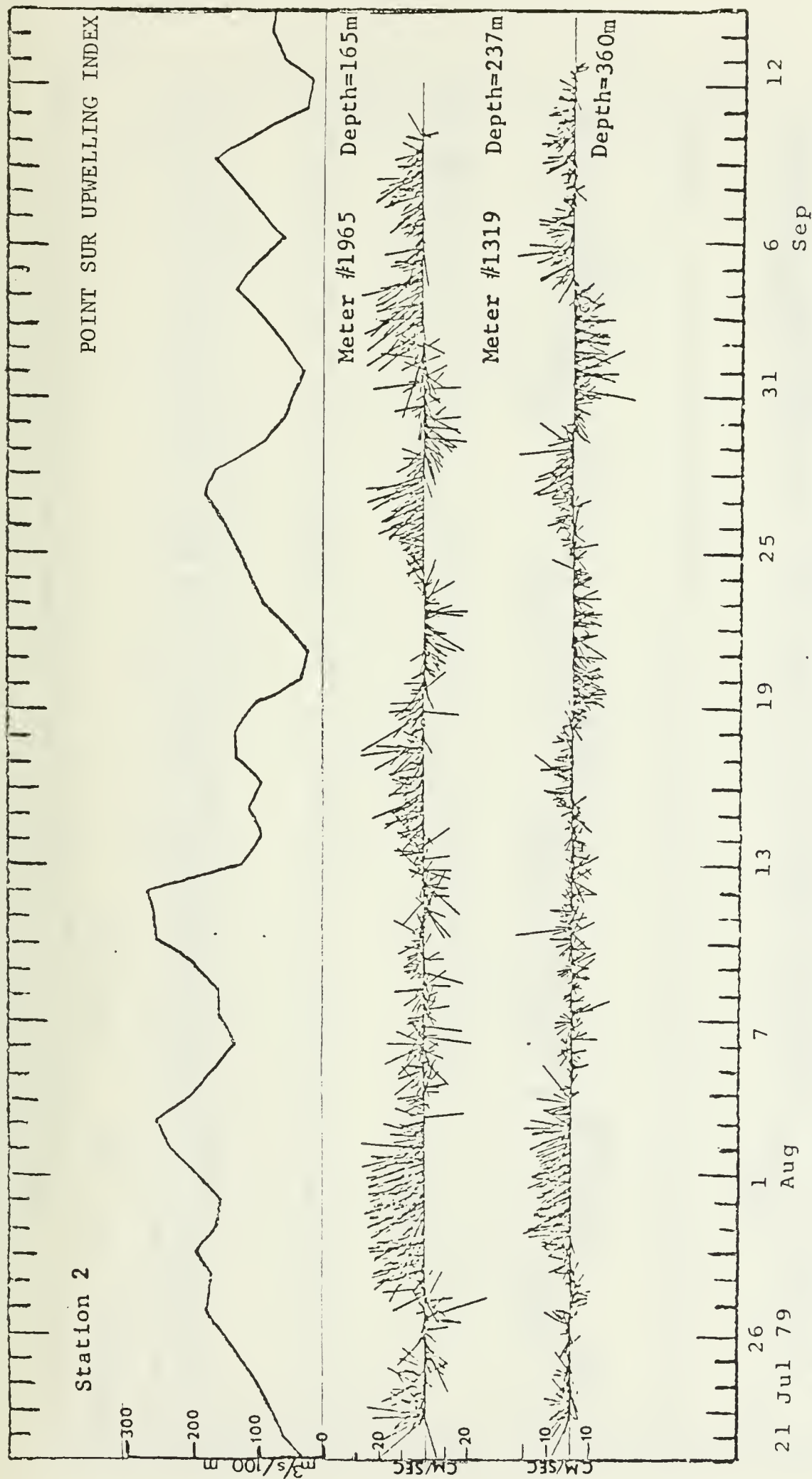


Figure 18. Point Sur Upwelling Index and stickplots of hourly current vectors for the current meters at Station 2 deployed on 21 July 1979.

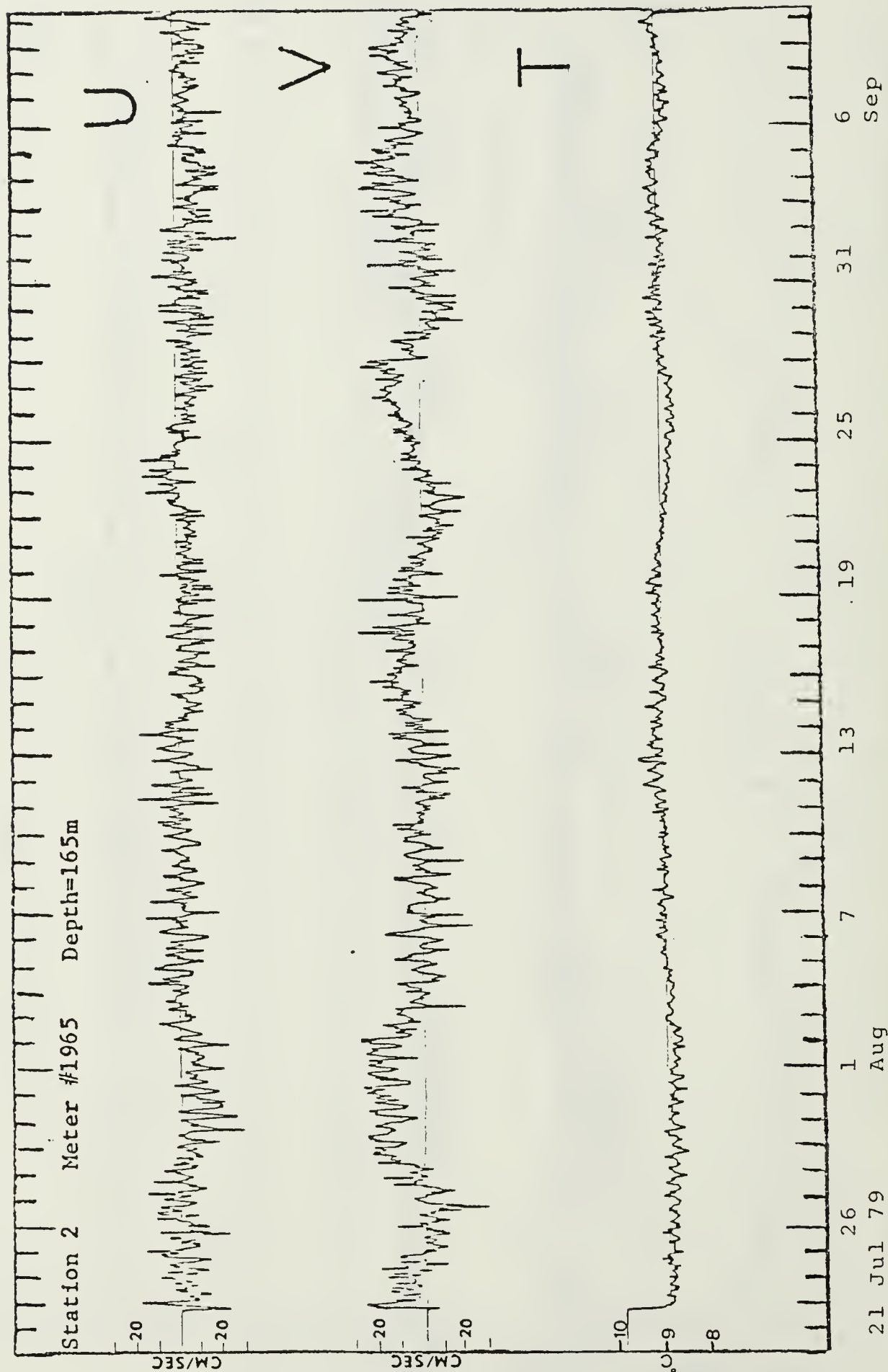


Figure 19. U component, V component, and temperature plots versus time for the current meter at 165 m depth at Station 2 deployed on 21 July 1979.



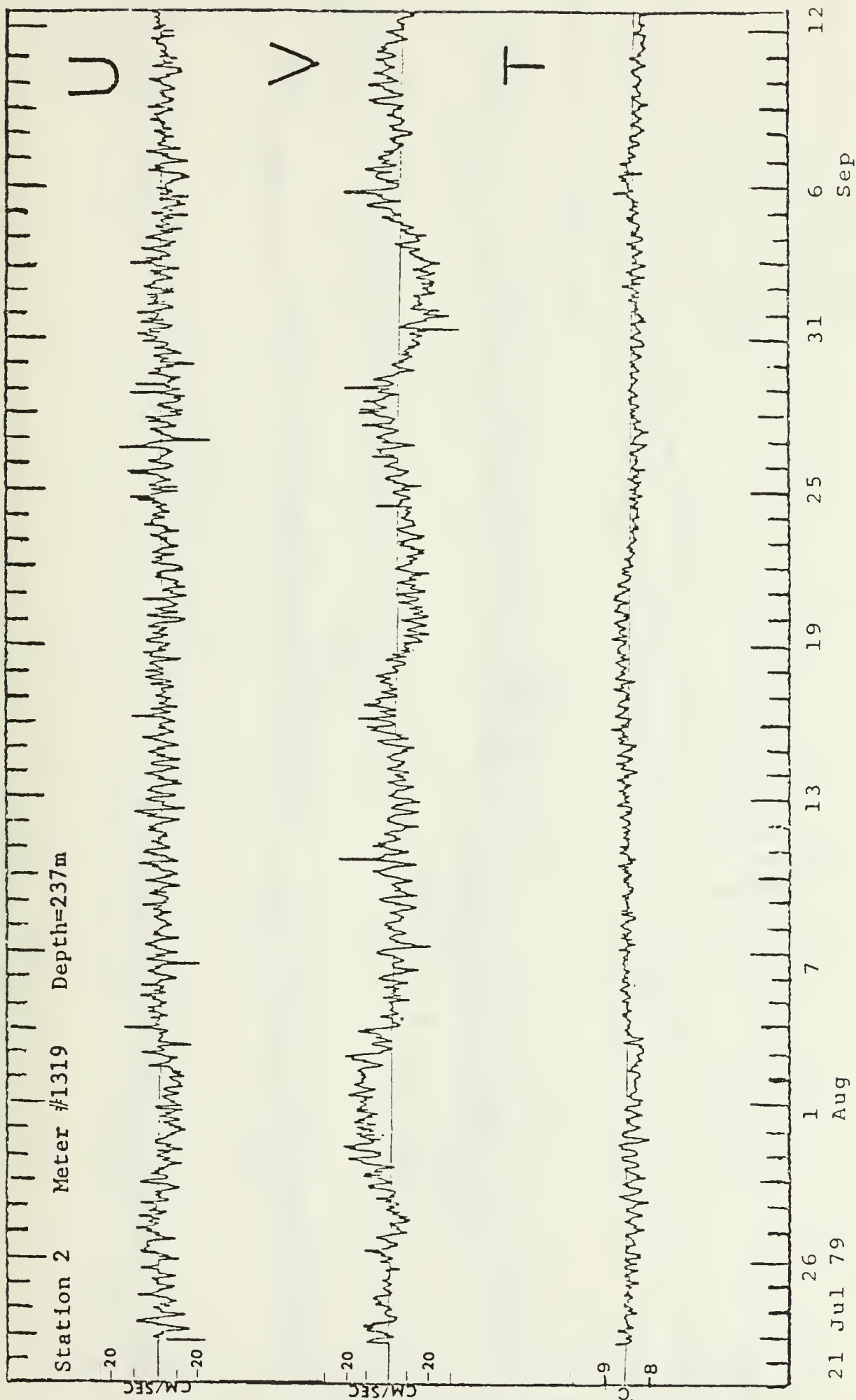


Figure 20. U component, V component, and temperature plots versus time for the current meter at 237 m depth at Station 2 deployed on 21 July 1979.



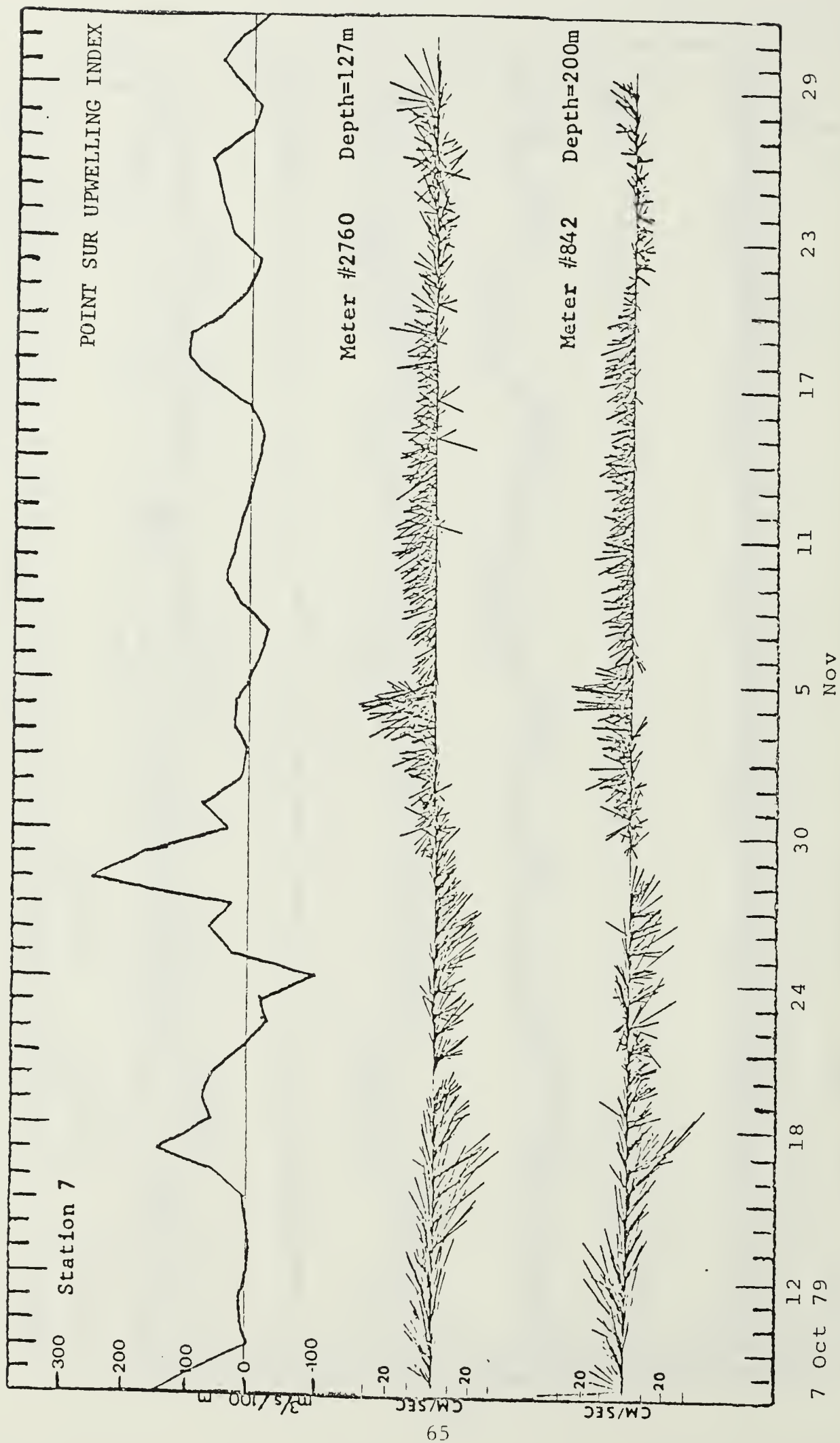


Figure 21. Point Sur Upwelling Index and stickplots of hourly current vectors for the current meters at Station 7 deployed on 7 October 1979.

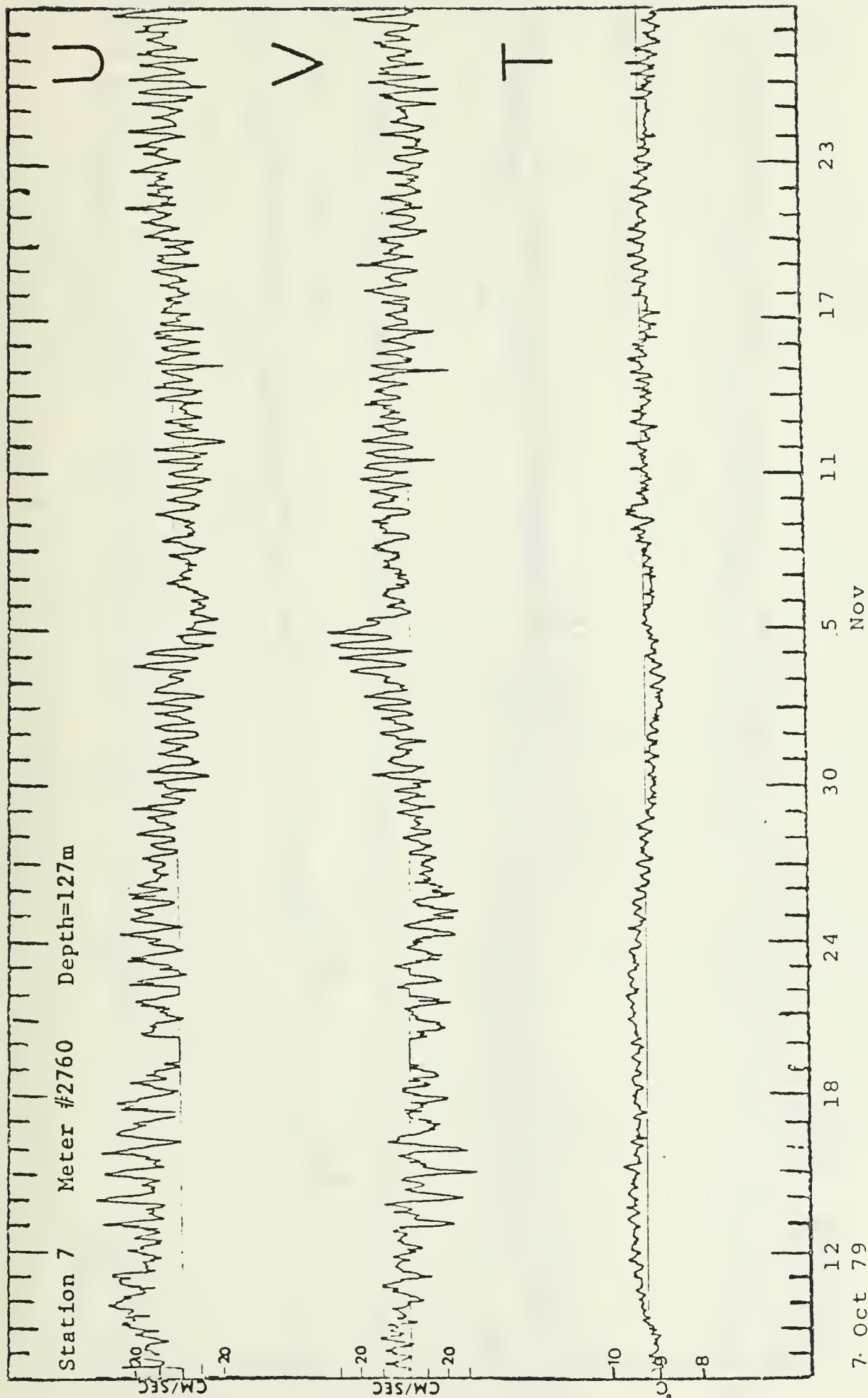


Figure 22. U component, V component, and temperature plots versus time for the current meter at 127 m depth at Station 7 deployed on 7 October 1979.

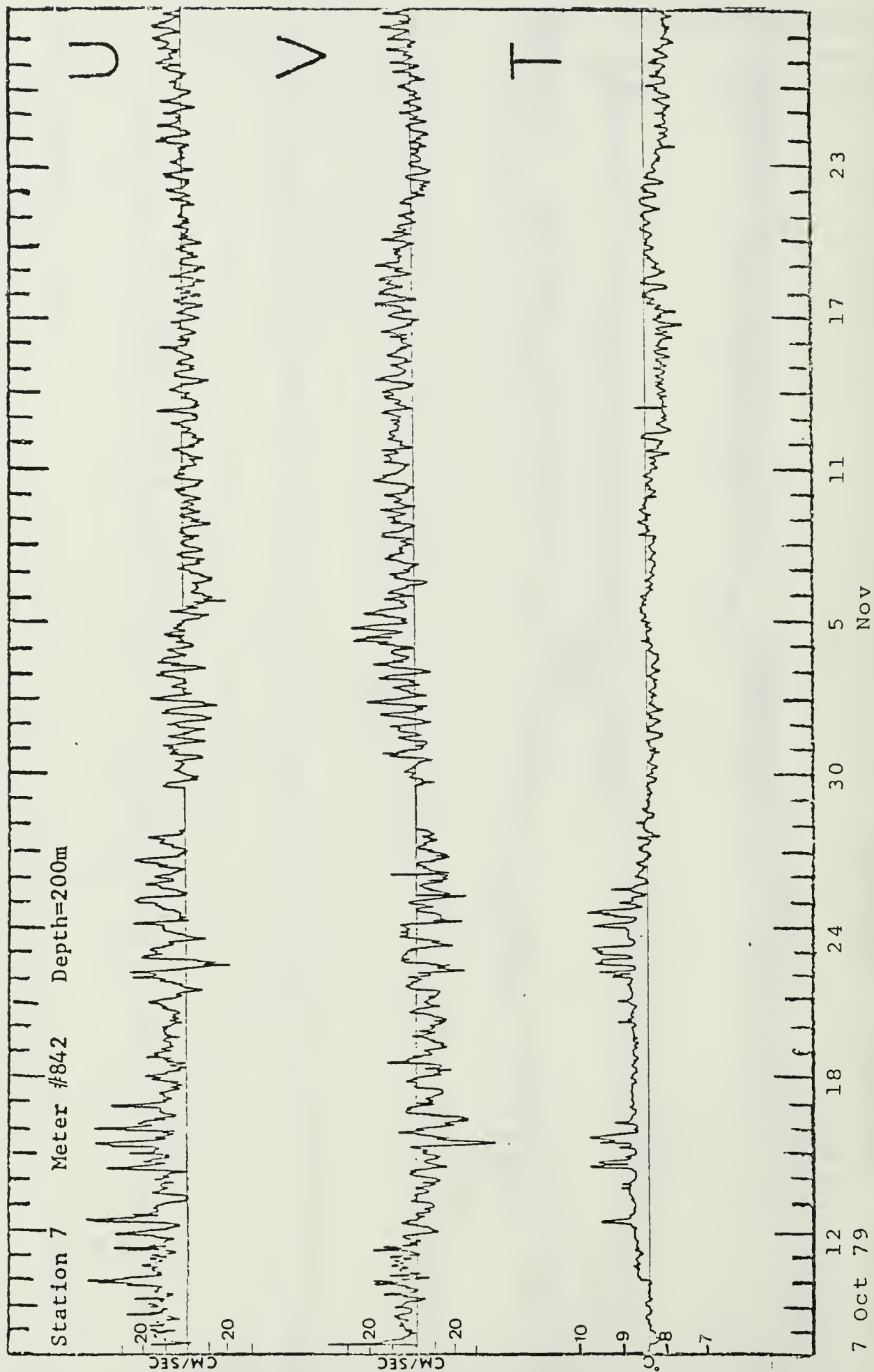


Figure 23. U component, V component, and temperature plots versus time for the current meter at 200 m depth at Station 7 deployed on 7 October 1979.

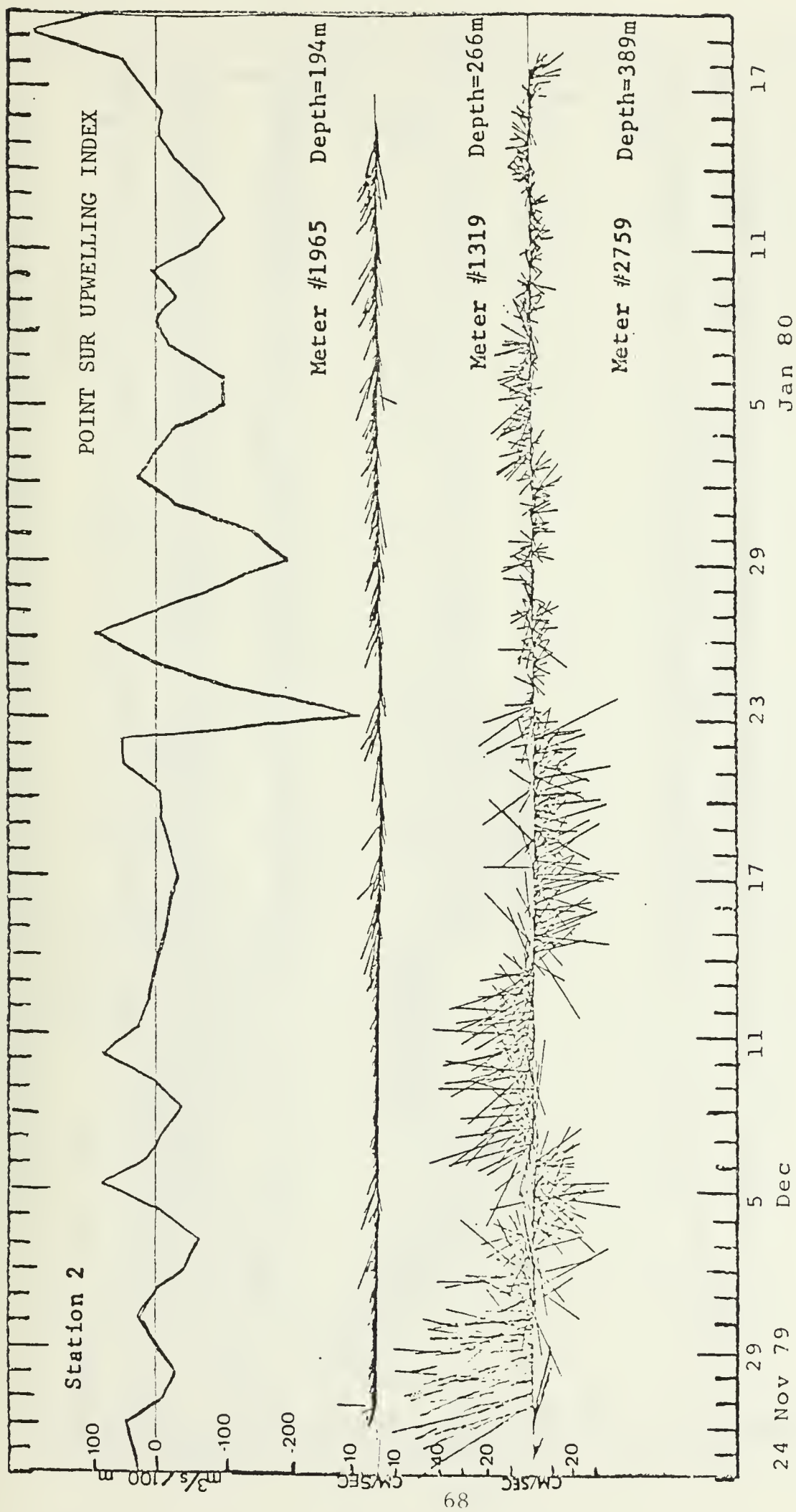


Figure 24. Point Sur Upwelling Index and stickplots of hourly current vectors for the current meters at Station 2 deployed on 24 November 1979.

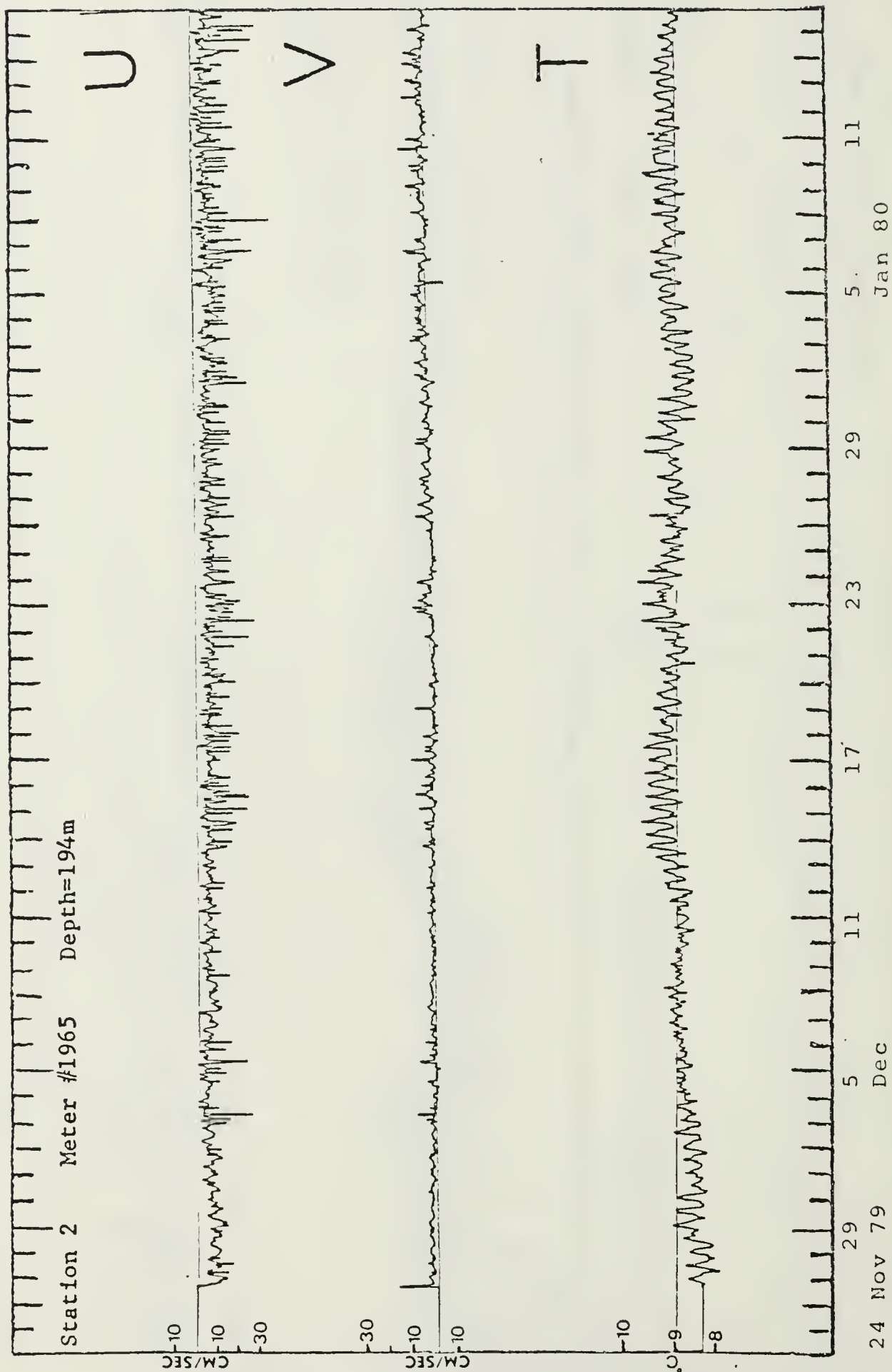


Figure 25. U component, V component, and temperature plots versus time for the current meter at 194 m depth at Station 2 deployed on 24 November 1979.



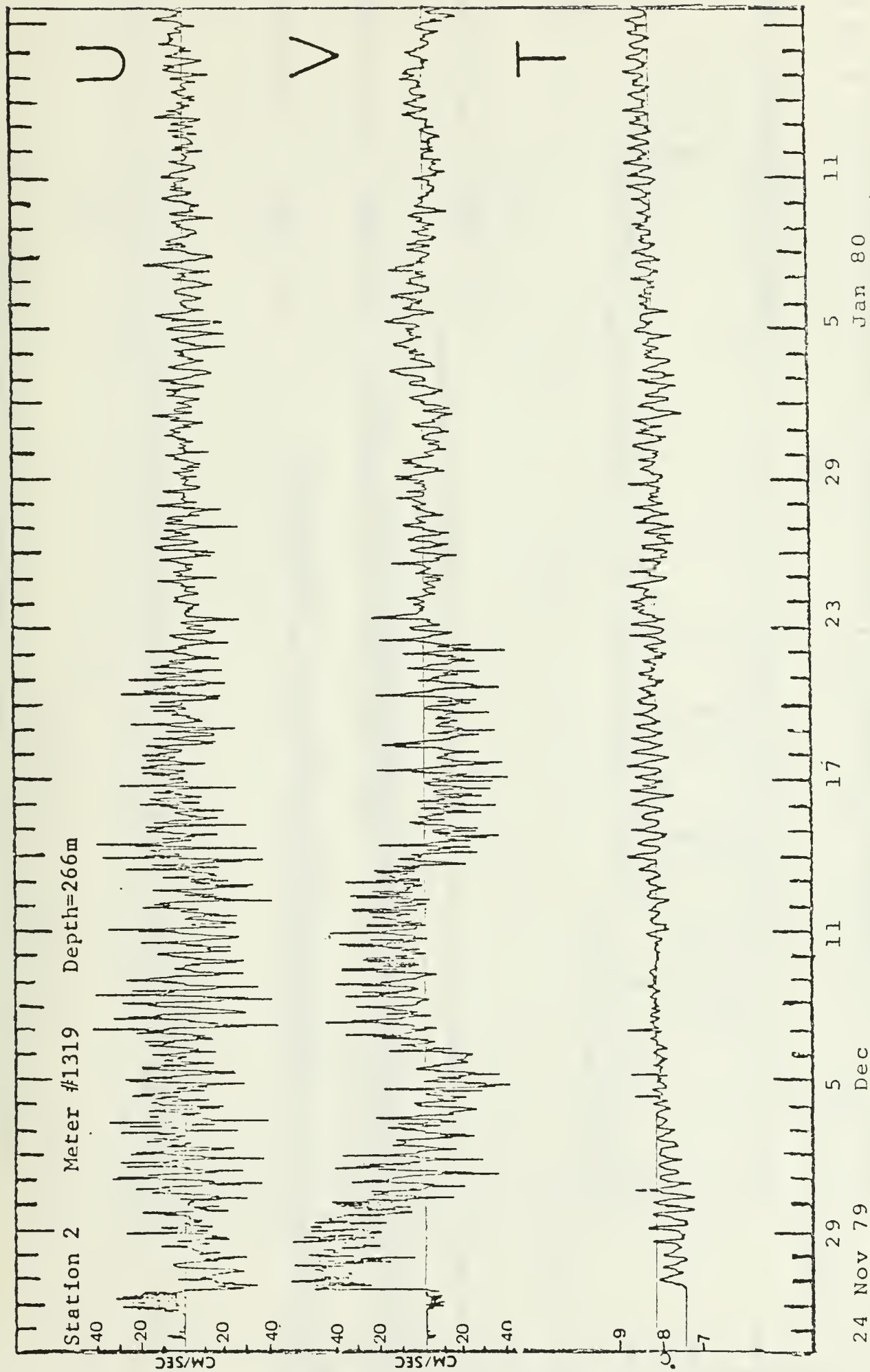


Figure 26. U component, V component, and temperature plots versus time for the current meter at 266 m depth at Station 2 deployed on 24 November 1979.



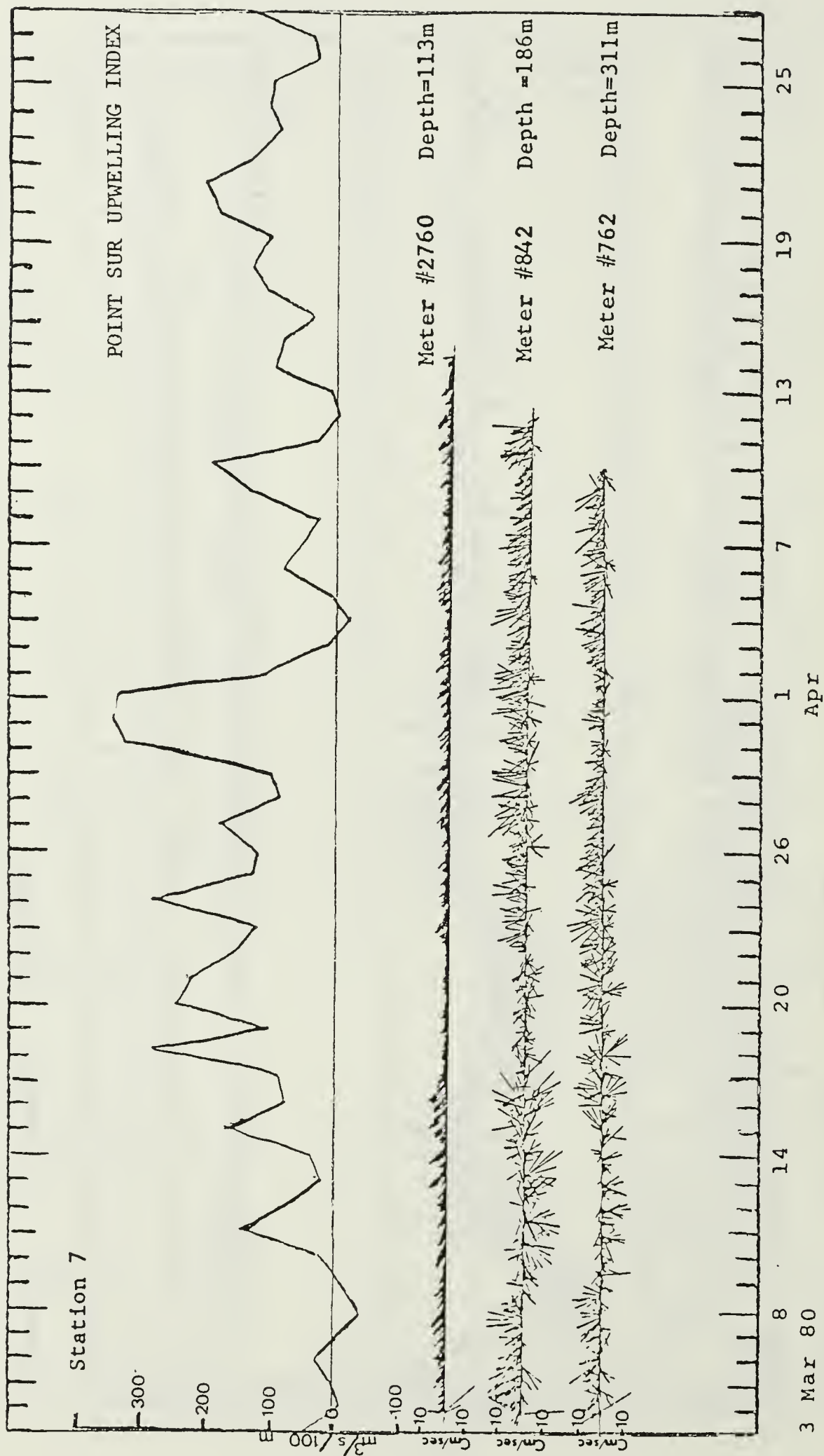


Figure 27. Point Sur Upwelling Index and stickplots of hourly current vectors for the current meters at Station 7 deployed on 3 March 1980.

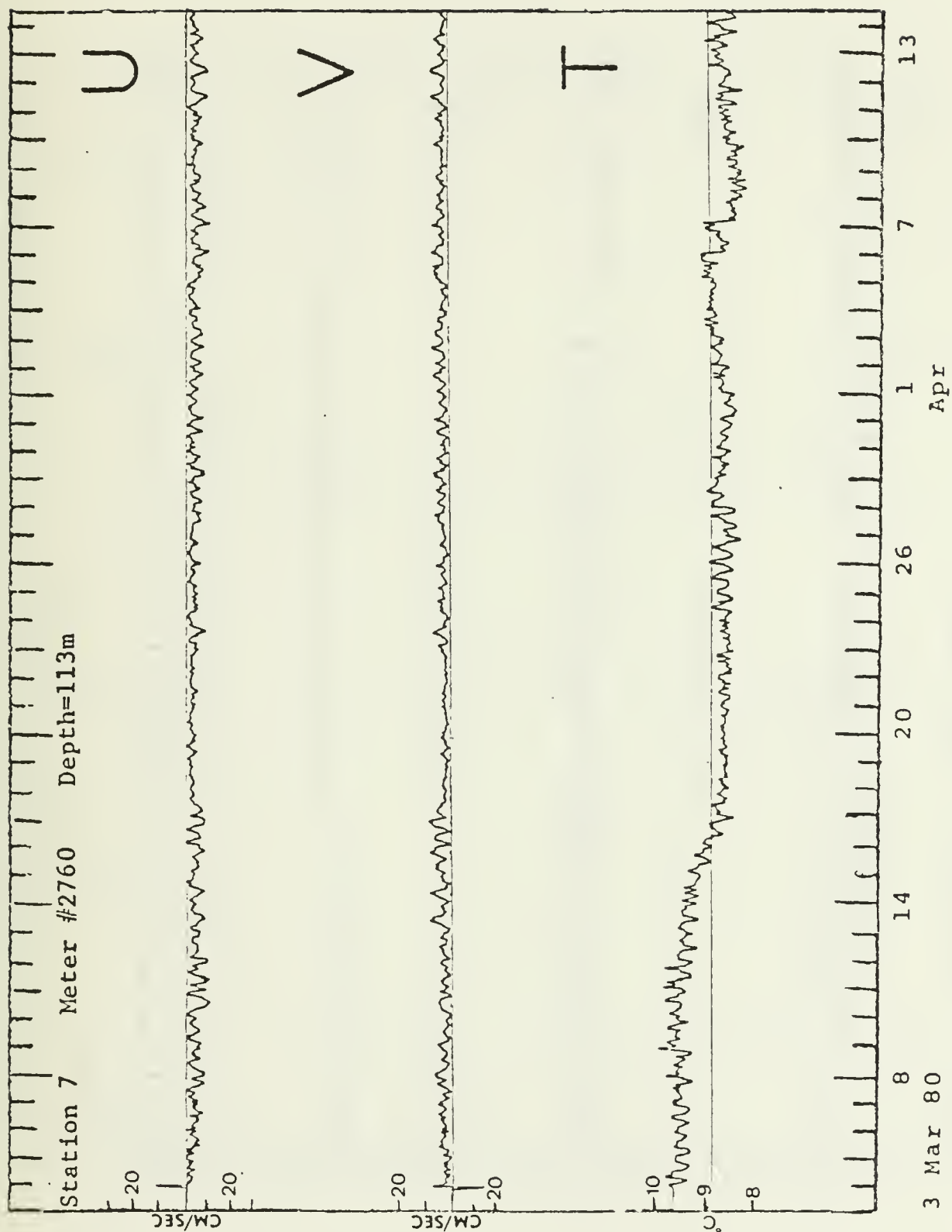


Figure 28. U component, V component, and temperature plots versus time for the current meter at 113 m depth at Station 7 deployed on 3 March 1980.

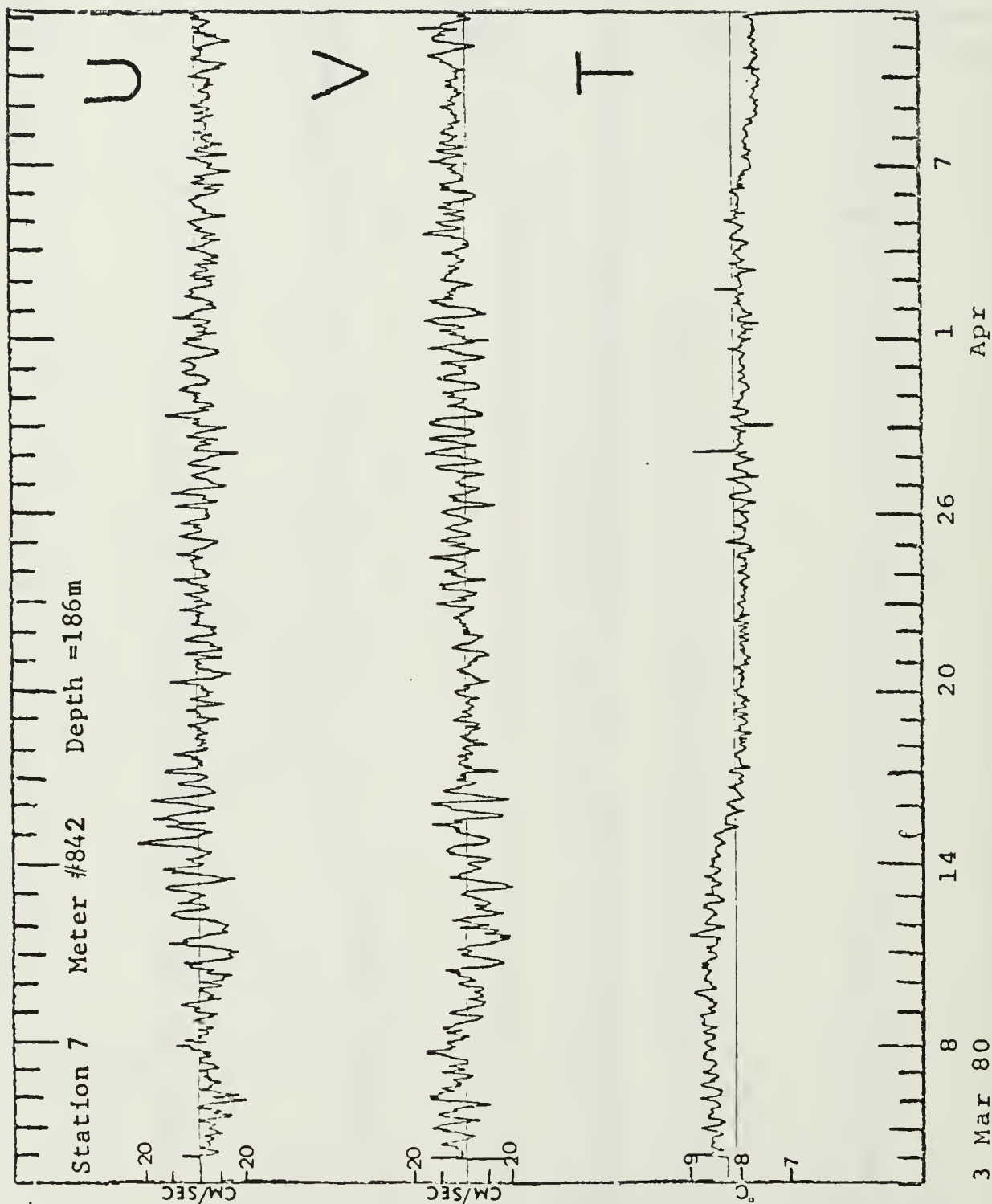


Figure 29. U component, V component, and temperature plots versus time for the current meters at 186 m depth at Station 7 deployed on 3 March 1980.

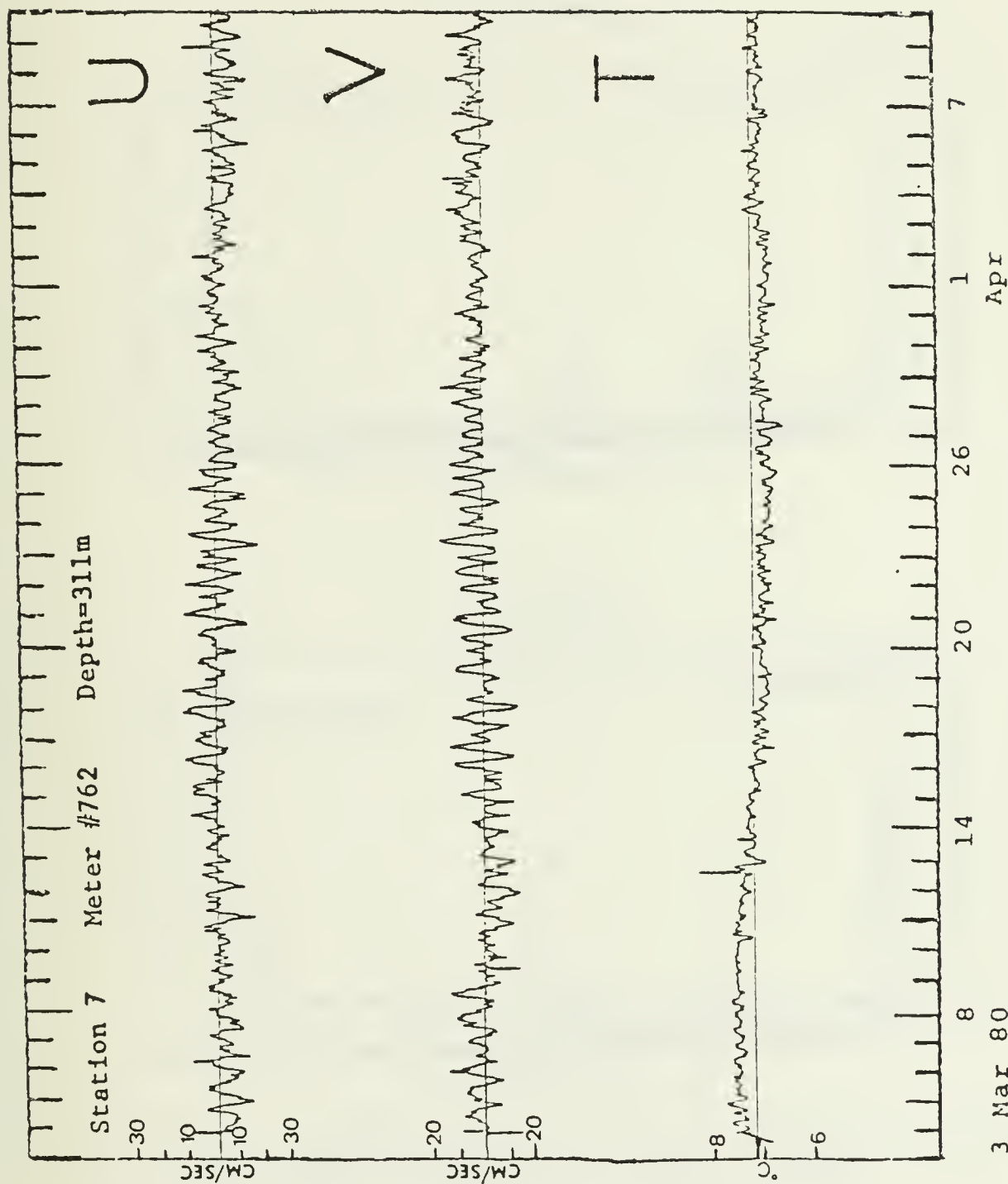


Figure 30. U component, V component, and temperature plots versus time for the current meter at 311 m depth at Station 7 deployed on 5 January 1979.

APPENDIX B: SPECTRUM ANALYSES OF ALONGSHORE FLOW AND  
ON/OFFSHORE FLOW

Station 7      Meter #762      Depth=152m      5 Jan 79

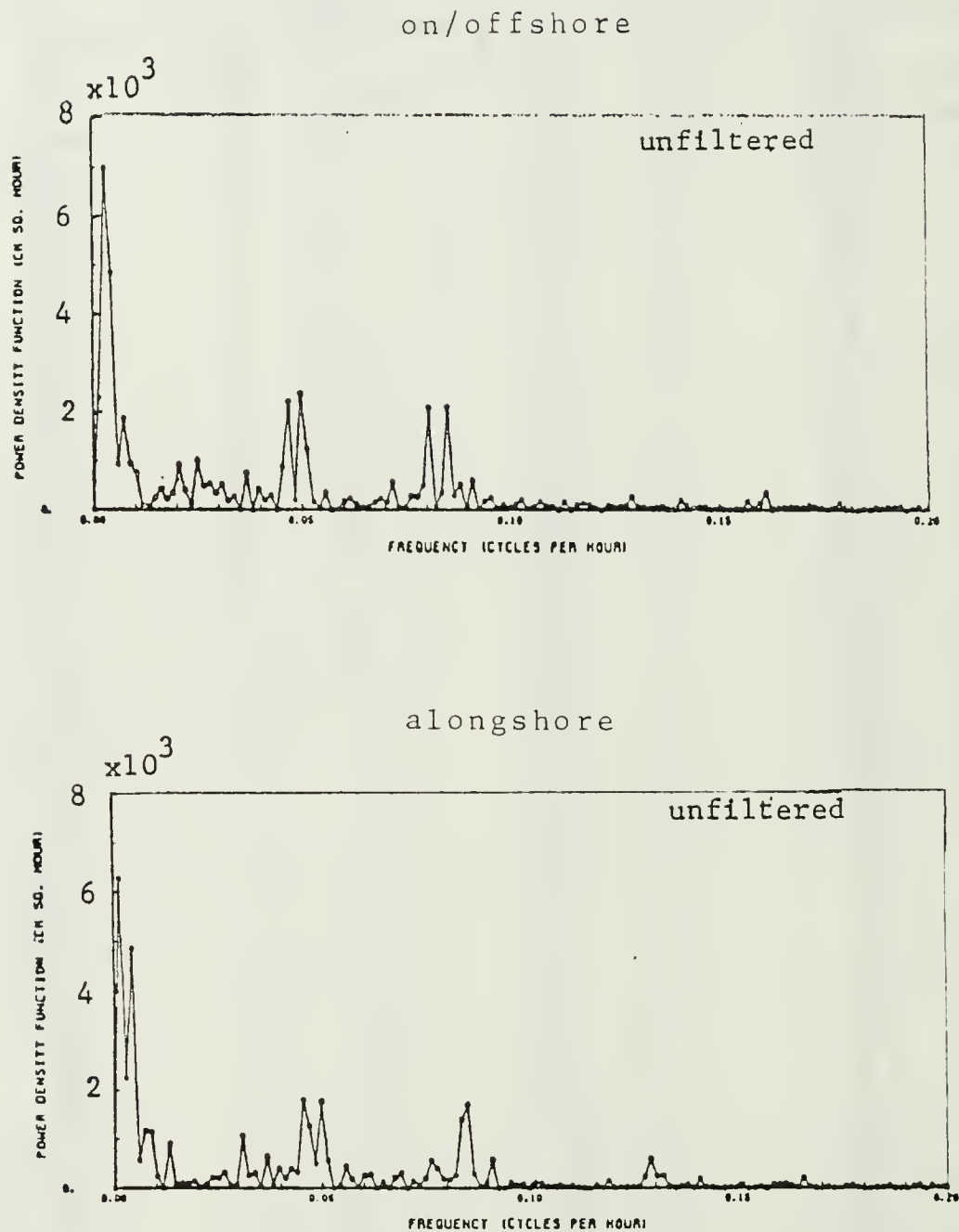


Figure 31. Energy density spectrum of current meter at 152 m depth at Station 7 deployed on 5 January 1979.

Station 7      Meter #842      Depth=223m      5 Jan 79

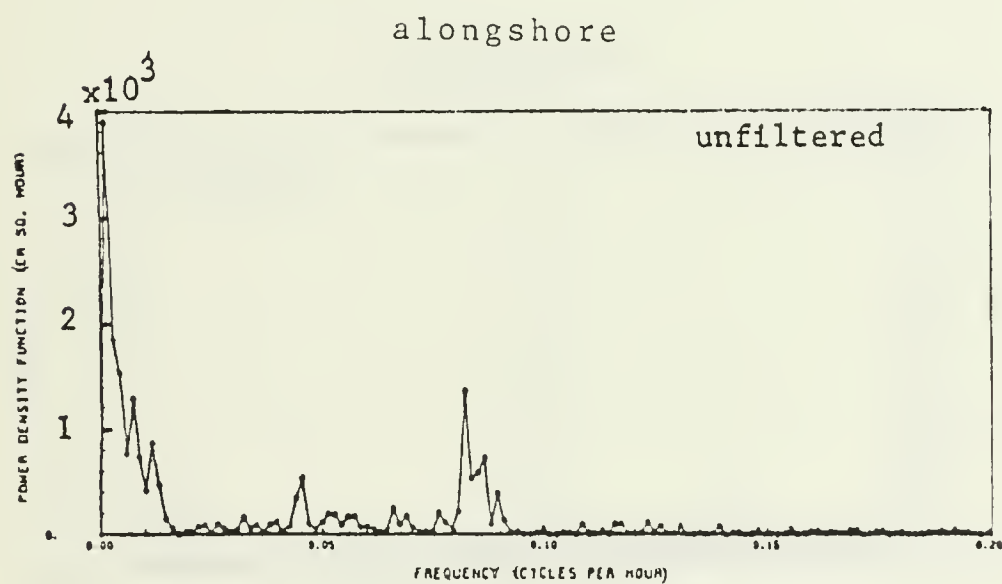
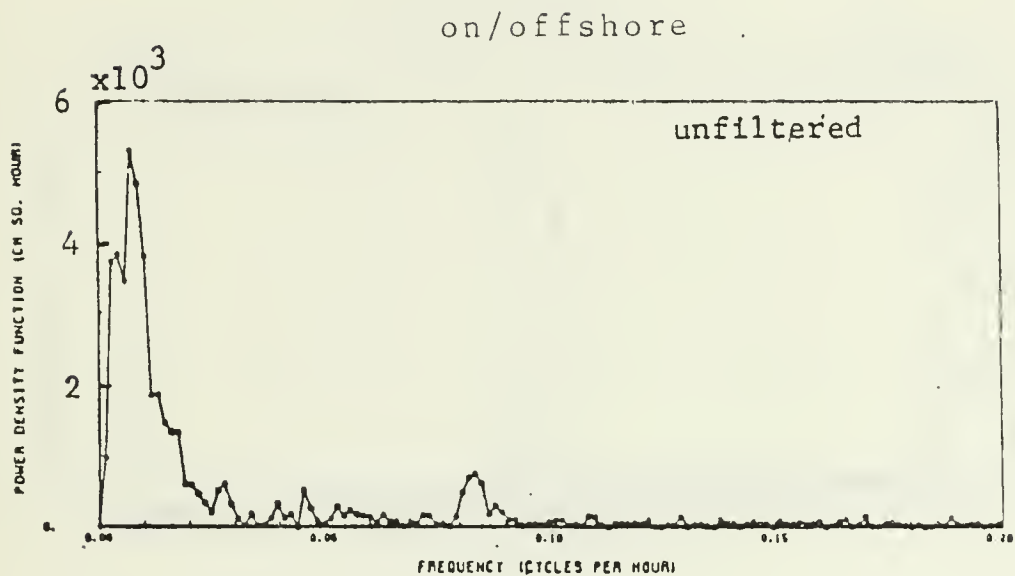


Figure 32. Energy density spectrum of current meter at 223 m depth at Station 7 deployed on 5 January 1979.



Station 2      Meter #1965      Depth=169m      23 Apr 79

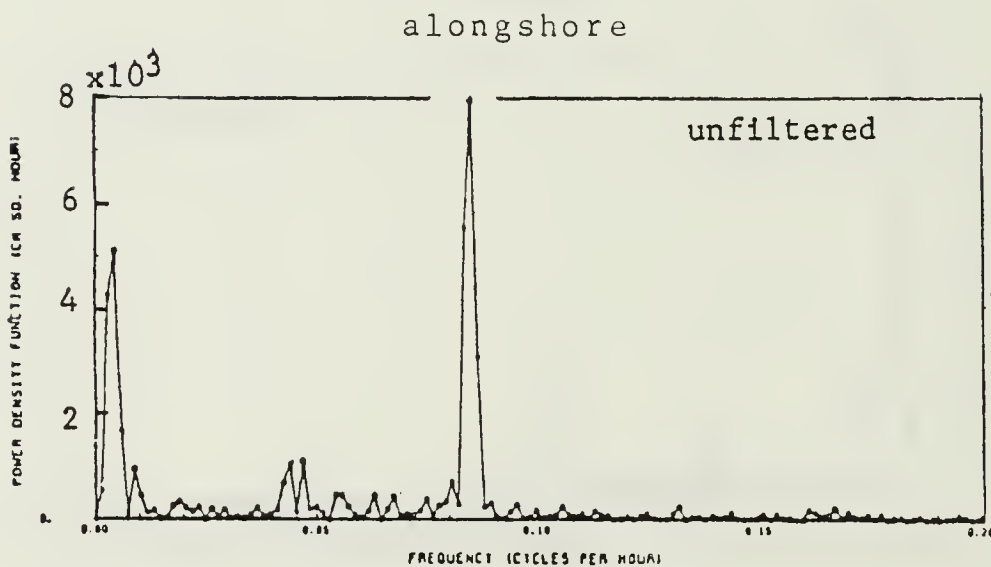
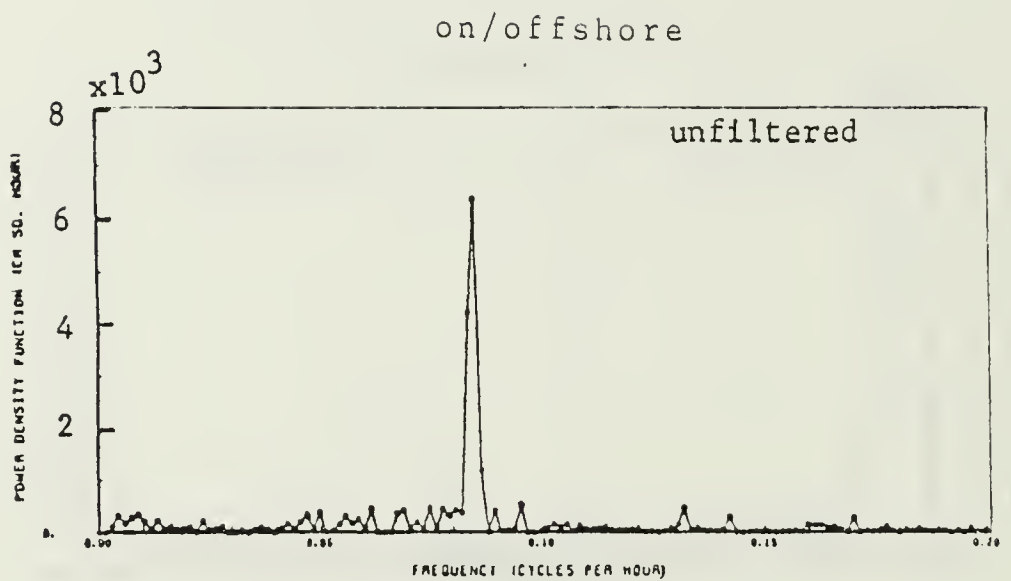


Figure 33. Energy density spectrum of current meter at 169 m depth at Station 2 deployed on 23 April 1979.

Station 2    Meter #1319    Depth=241m    23 Apr 79

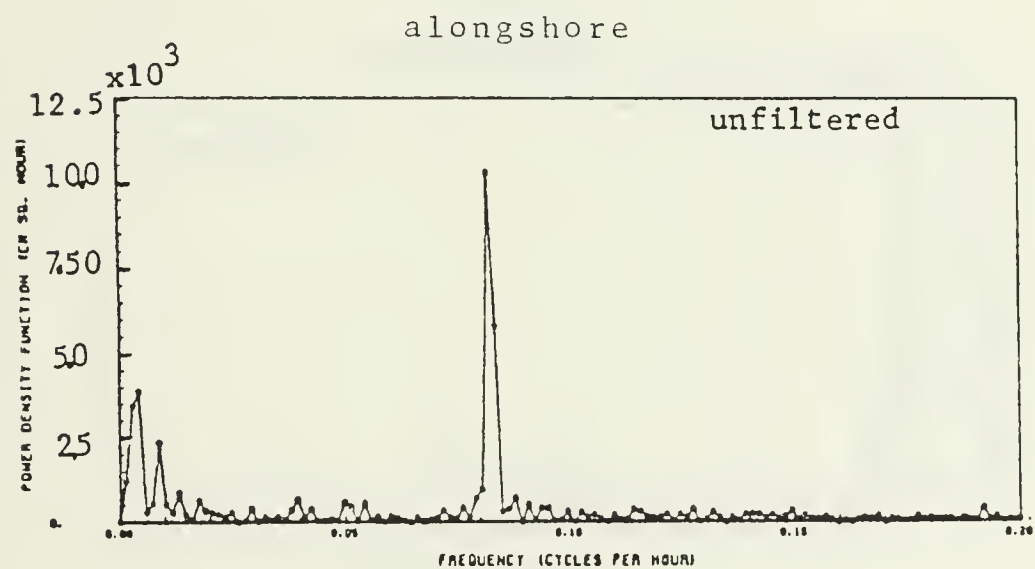
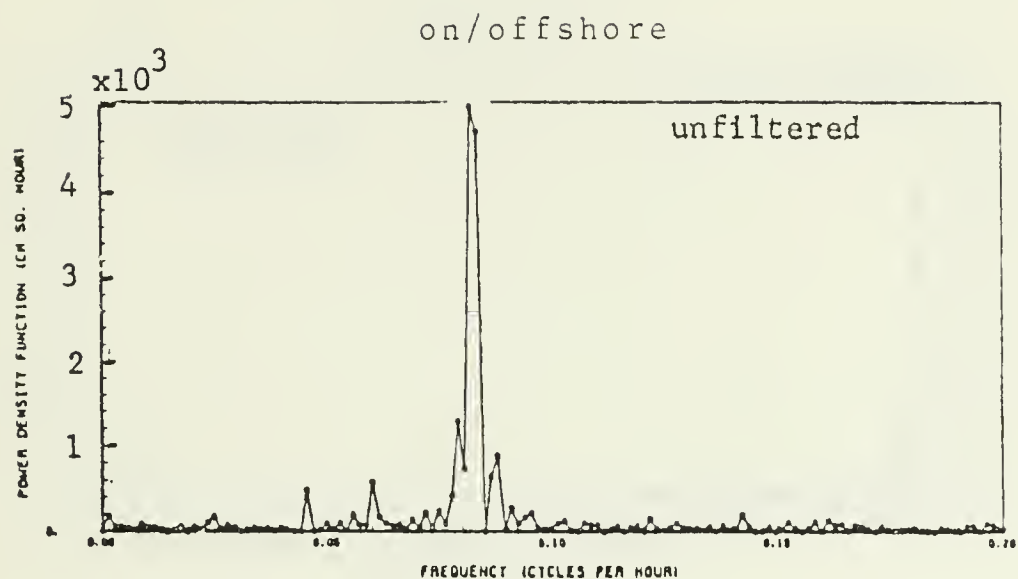


Figure 34. Energy density spectrum of current meter at 241 m depth at Station 2 deployed on 23 April 1979.

Station 7      Meter #2760      Depth=158m      7 Jul 79

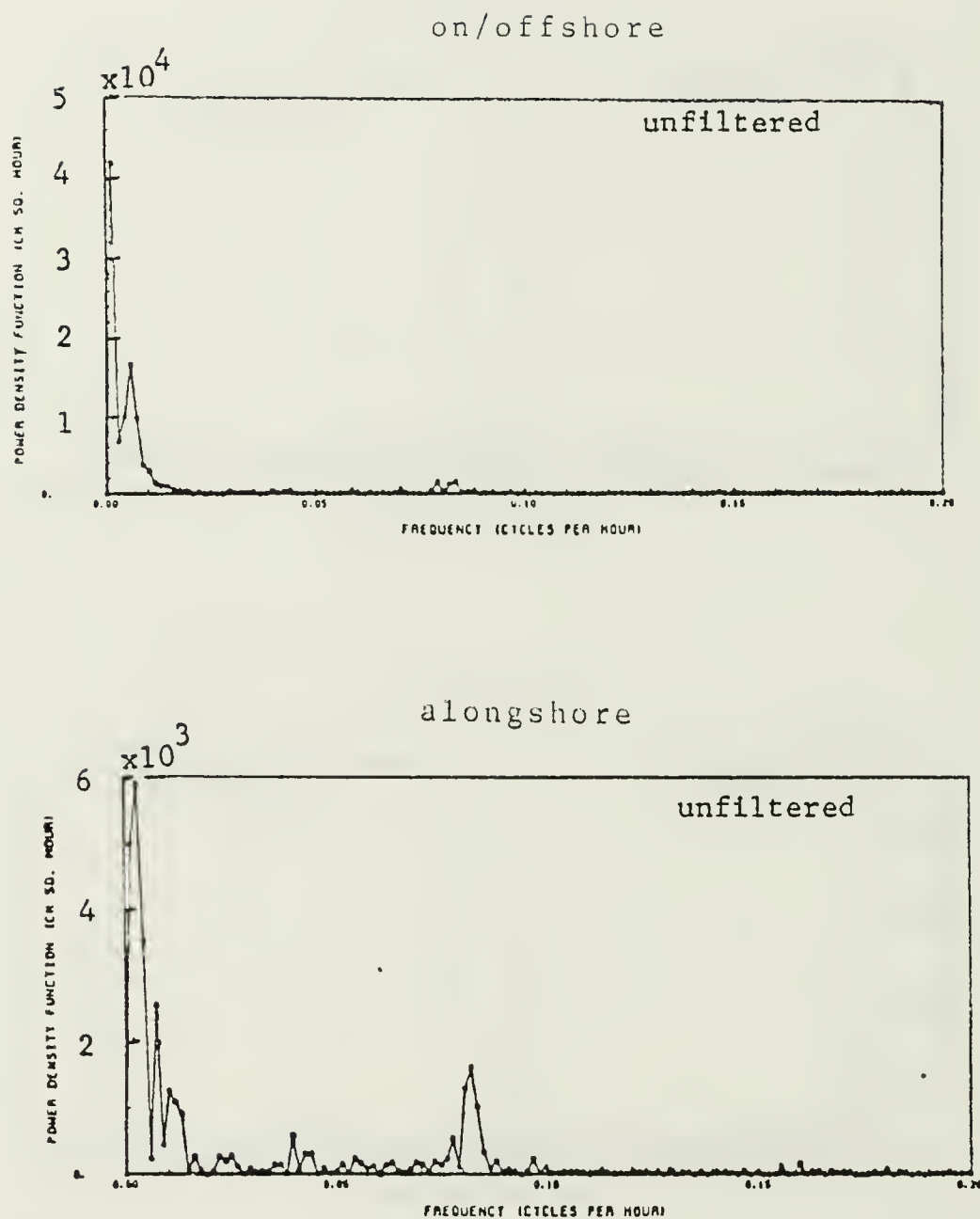


Figure 35. Energy density spectrum of current meter at 158 m depth at Station 7 deployed on 7 July 1979.

Station 7    Meter #842    Depth=231m    7 Jul 79

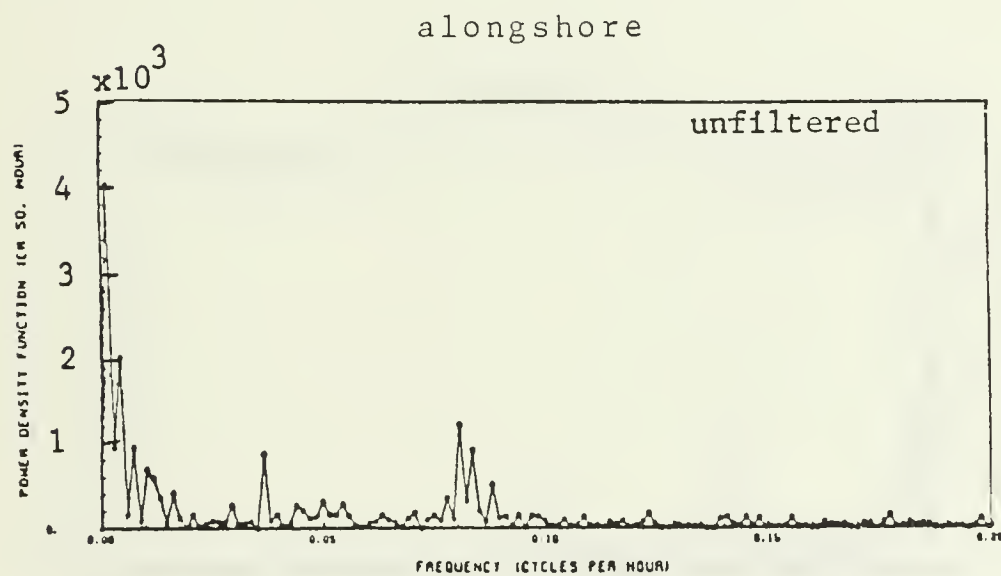
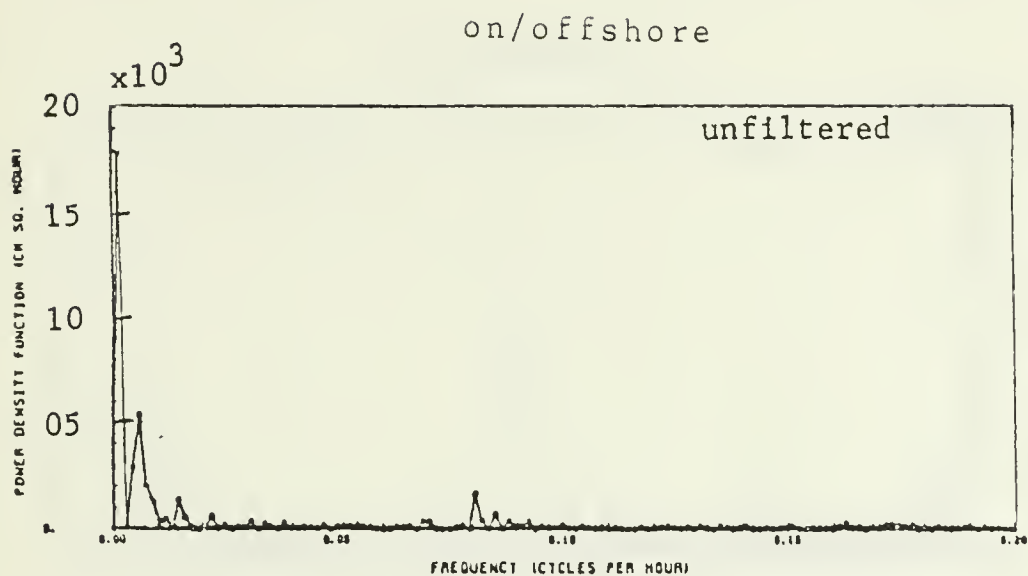


Figure 36. Energy density spectrum of current meter at 231 m depth at Station 7 deployed on 7 July 1979.

Station 7      Meter #762      Depth=356m      7 Jul 79

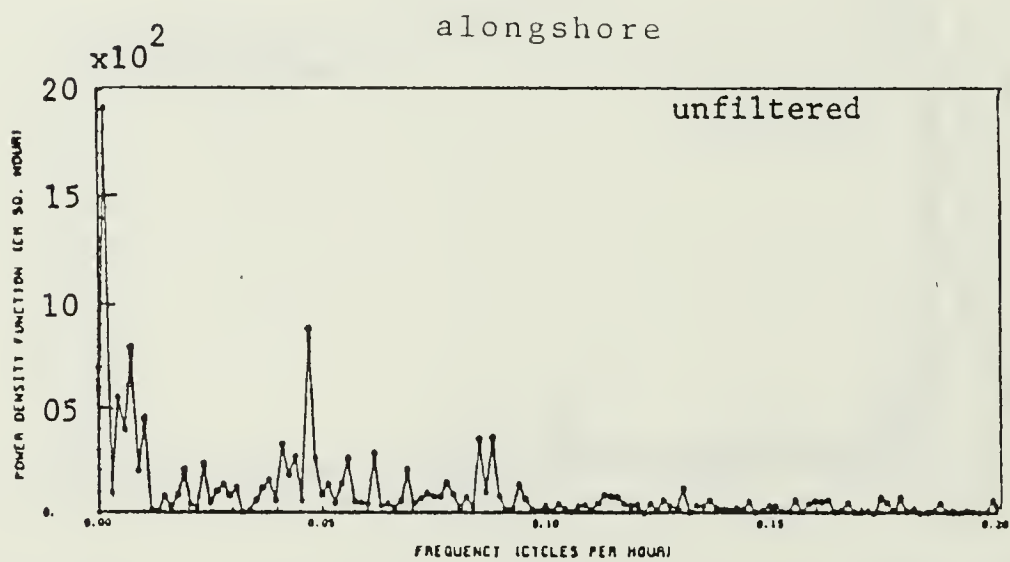
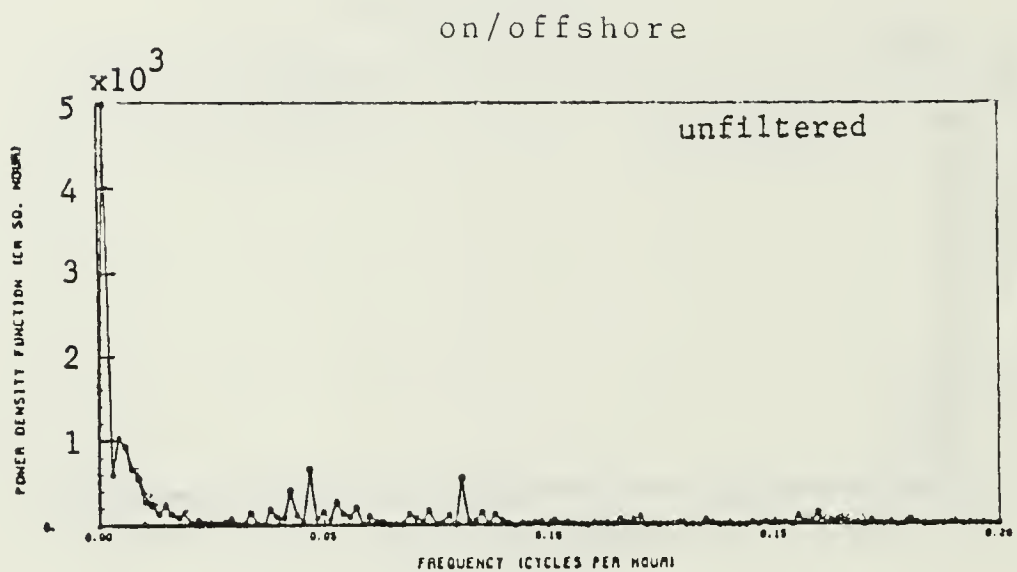


Figure 37. Energy density spectrum of current meter at 356 m depth at Station 7 deployed on 7 July 1979.

Station 2      Meter #1965      Depth=165m      21 Jul 79

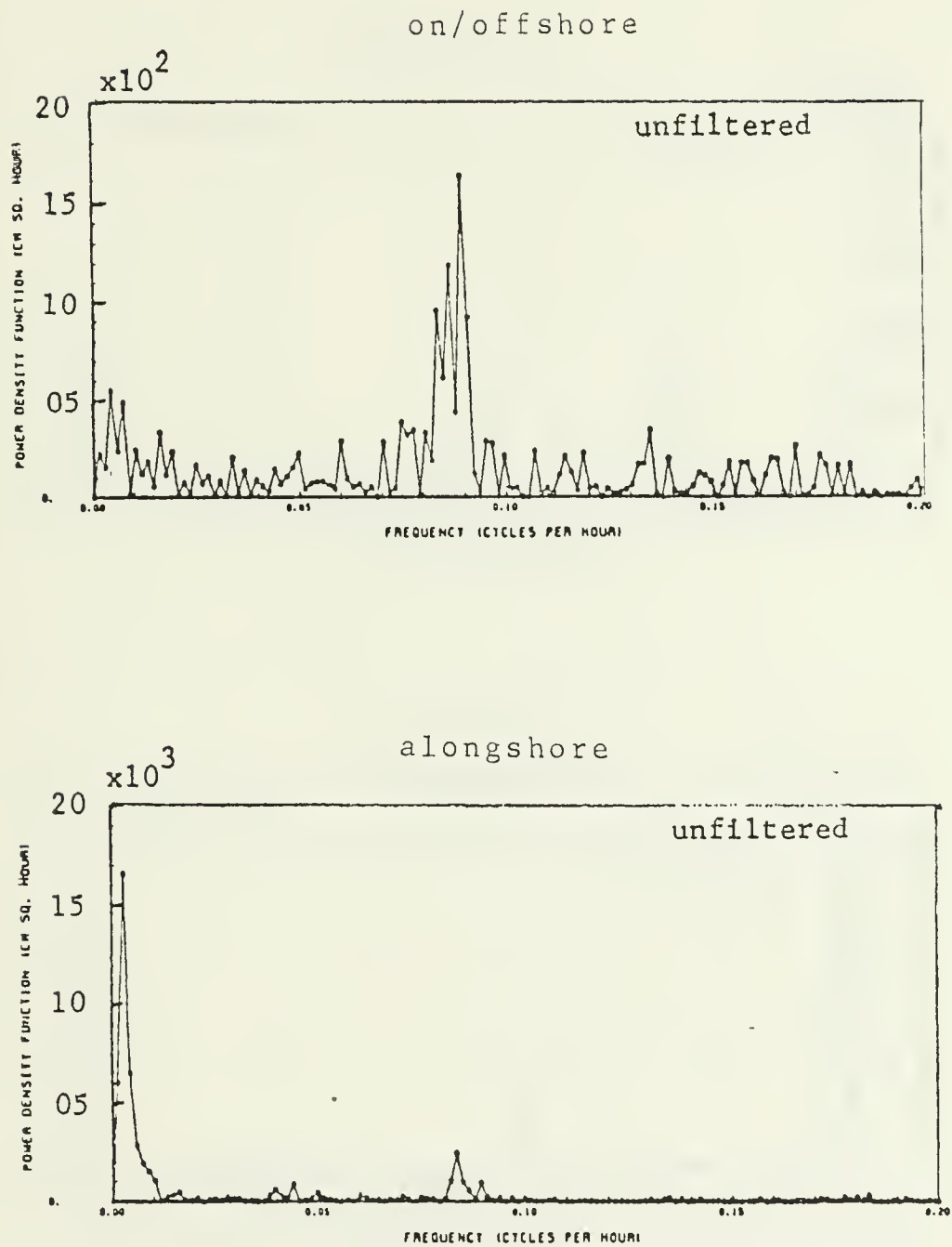


Figure 38. Energy density spectrum of current meter at 165 m depth at Station 2 deployed on 21 July 1979.



Station 2      Meter #1319      Depth=237m      21 Jul 79

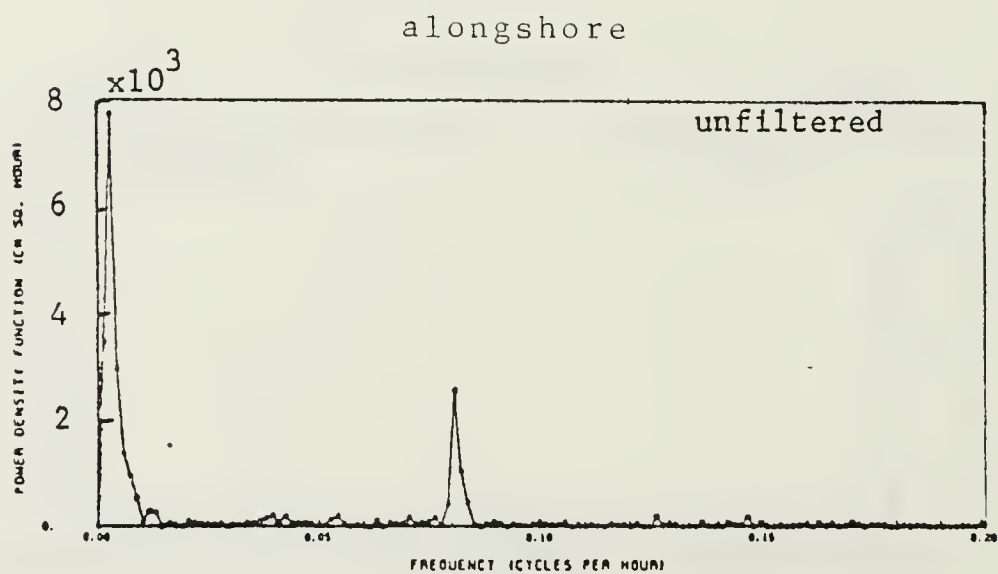
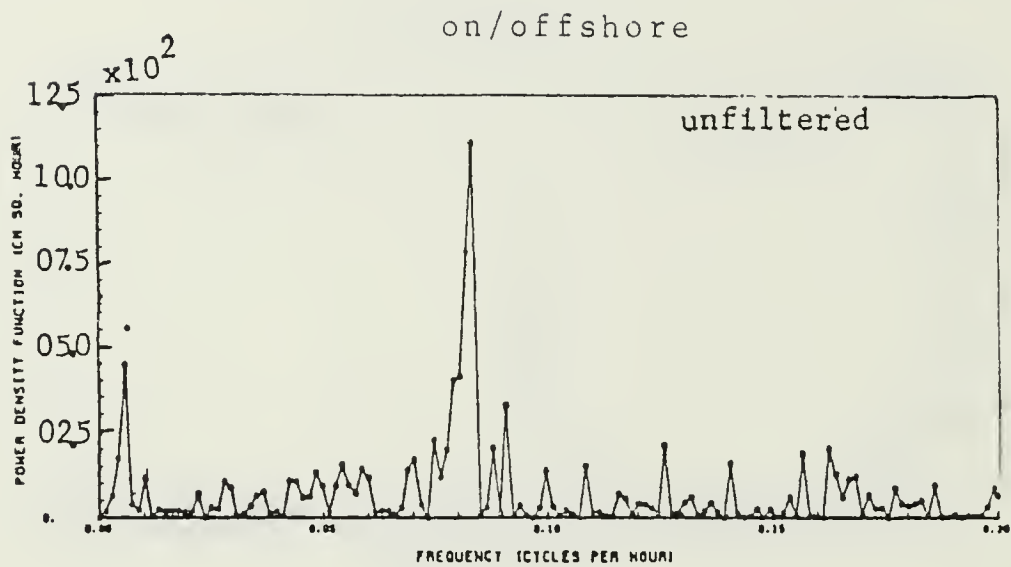


Figure 39. Energy density spectrum of current meter at 237 m depth at Station 2 deployed on 21 July 1979.

Station 7    Meter #2760    Depth=127m    7 Oct 79

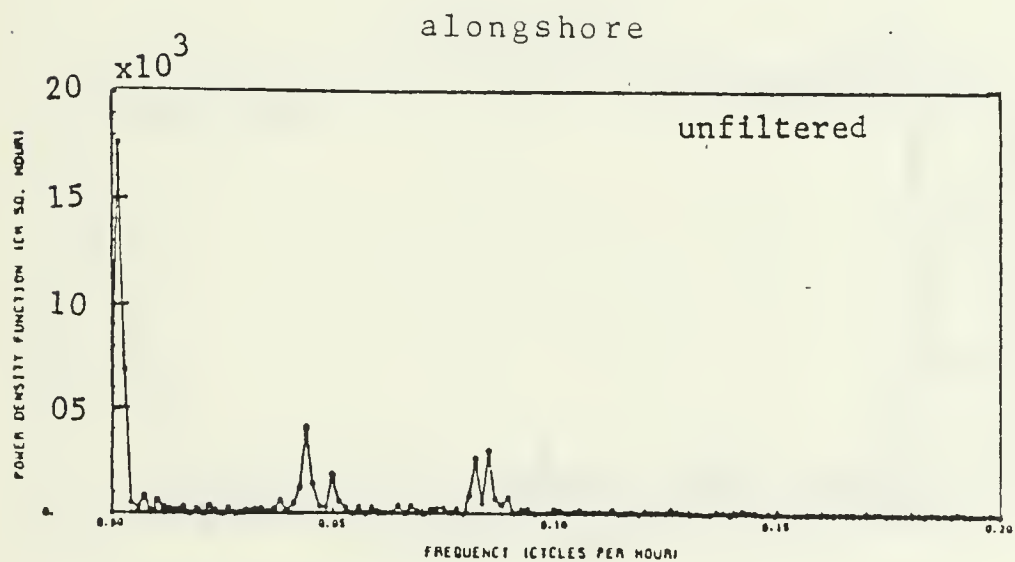
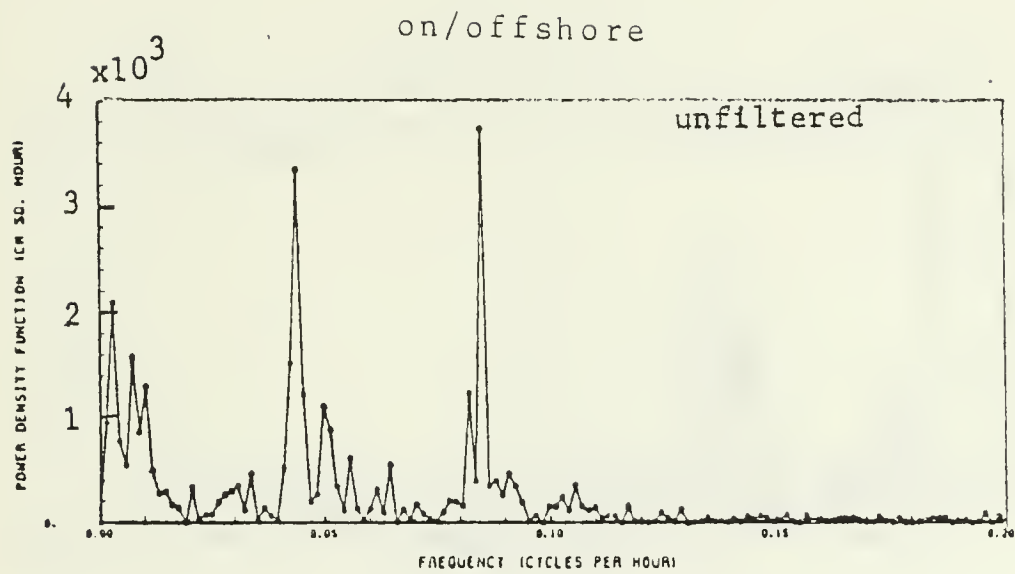


Figure 40. Energy density spectrum of current meter at 127 m depth at Station 7 deployed on 7 October 1979.

Station 7      Meter #842      Depth=200m      7 Oct 79

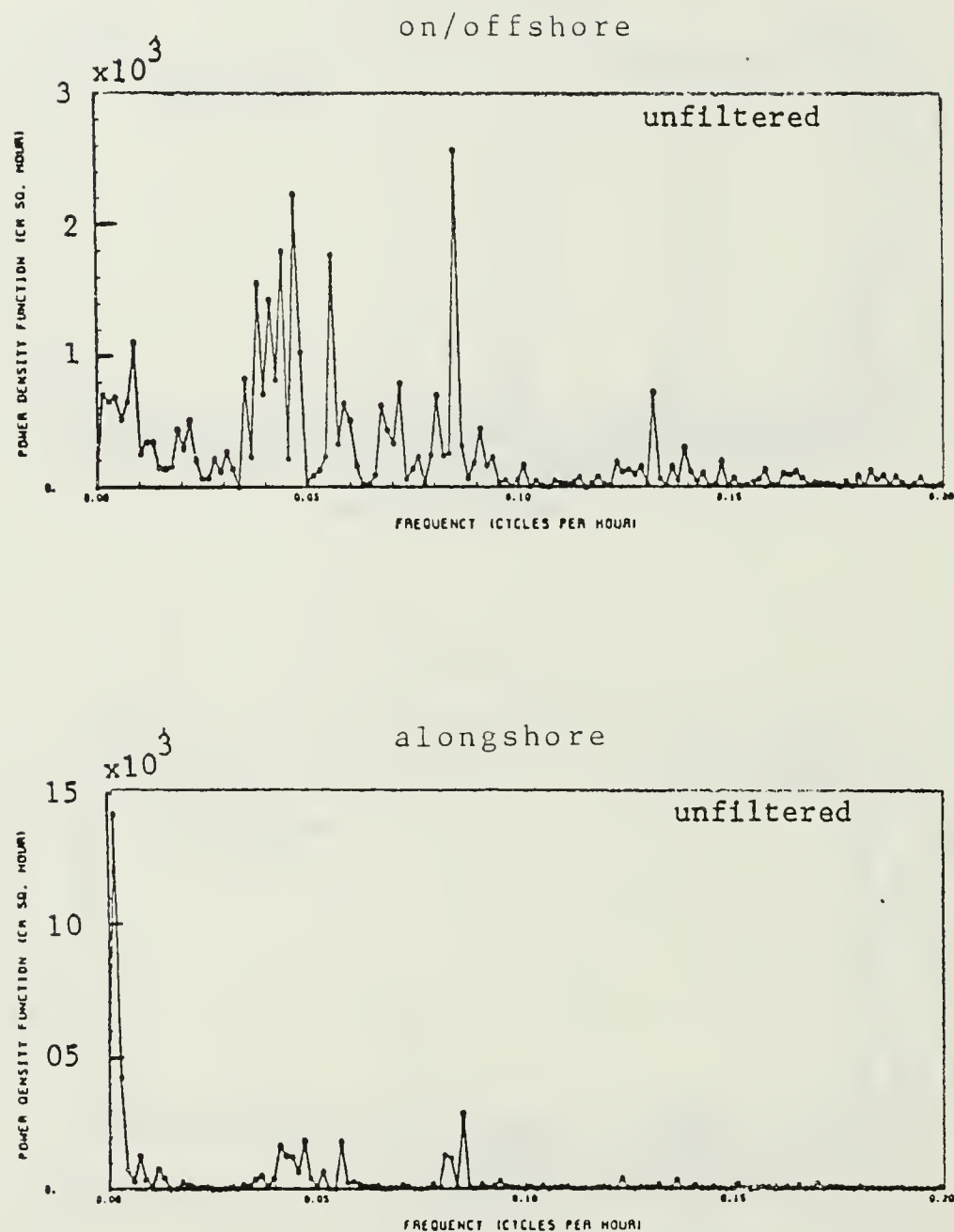


Figure 41. Energy density spectrum of current meter at 200 m depth at Station 7 deployed on 7 October 1979.

Station 2      Meter #1965      Depth=194m      24 Nov 79

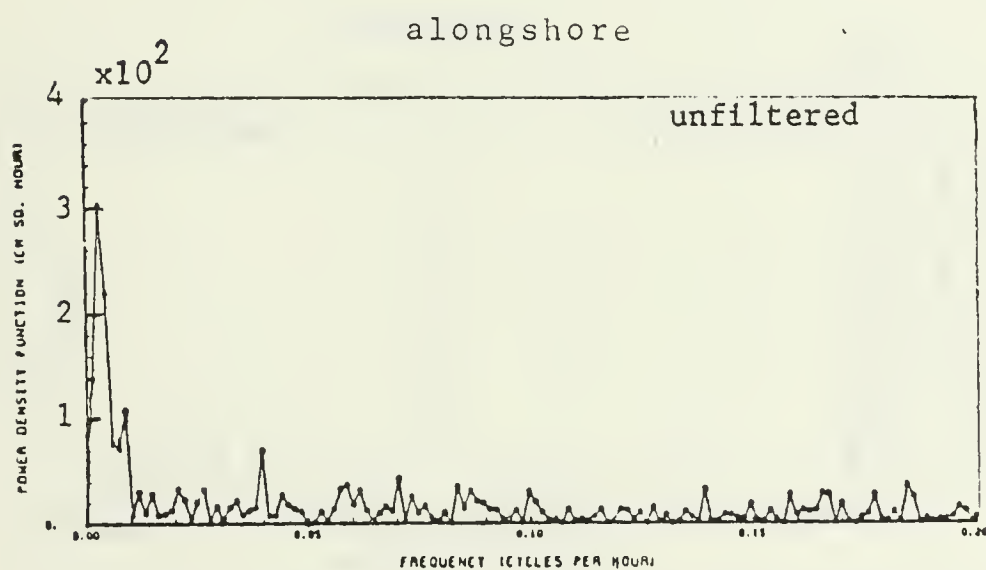
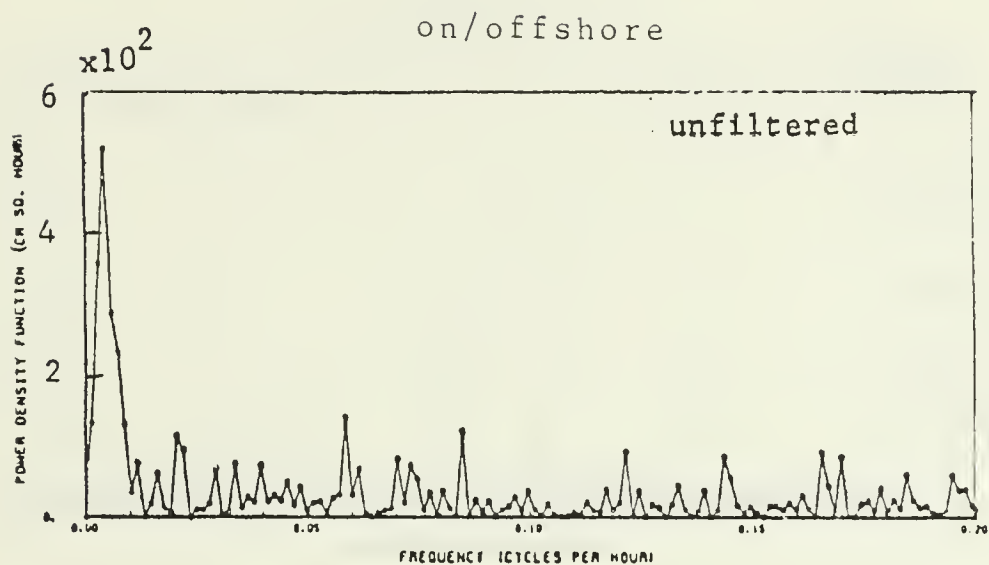


Figure 42. Energy density spectrum of current meter at 194 m depth at Station 2 deployed on 24 November 1979.

Station 2      Meter #1319      Depth=266m      24 Nov 79

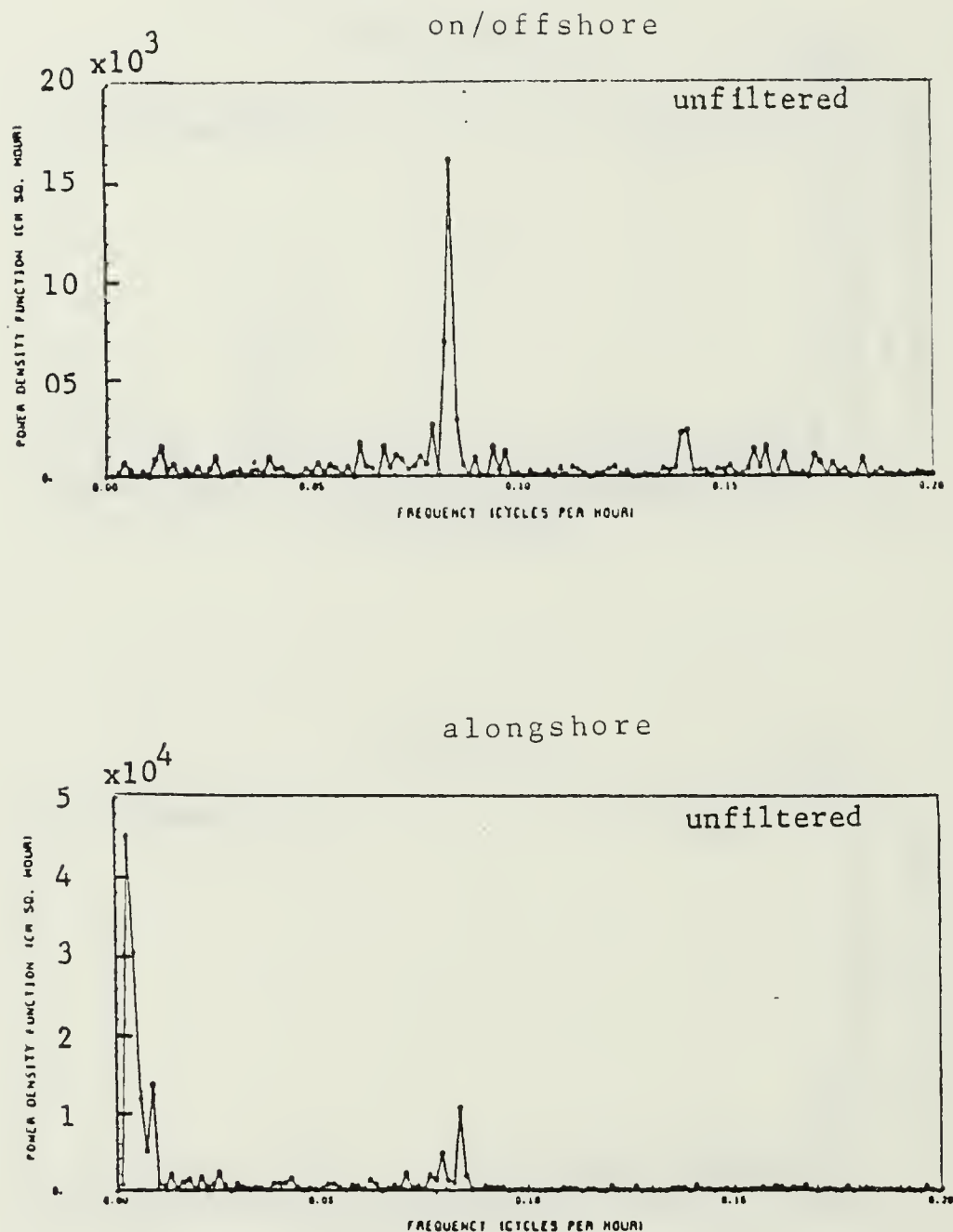
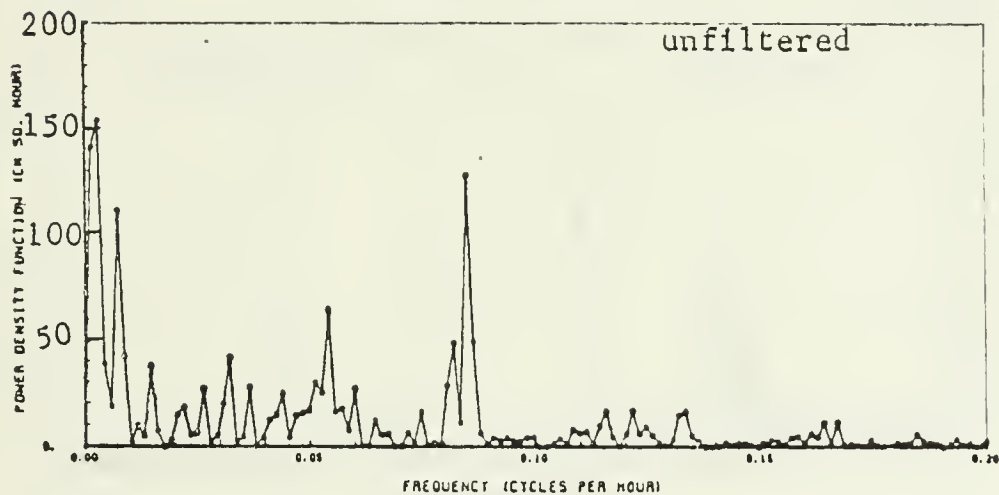


Figure 43. Energy density spectrum of current meter at 266 m depth at Station 2 deployed on 24 November 1979.

Station 7      Meter #2760      Depth=113m      3 Mar 80

on/offshore



alongshore

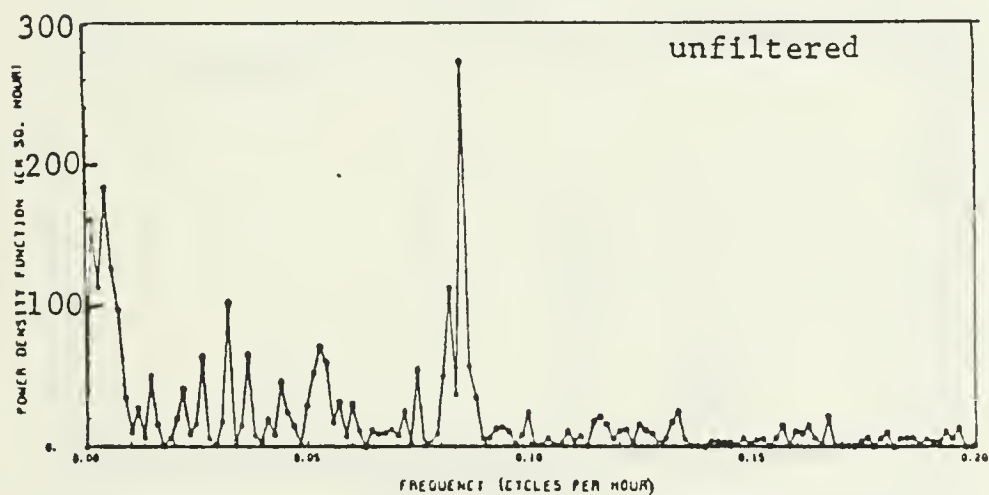


Figure 44. Energy density spectrum of current meter at 113 m depth at Station 7 deployed on 3 March 1980.



Station 7      Meter #842      Depth =186m      3 Mar 80

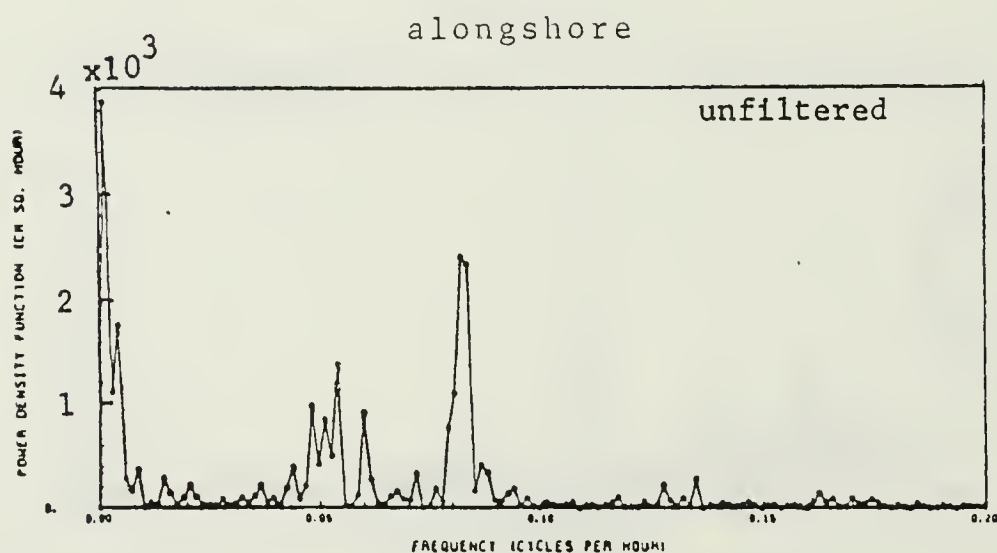
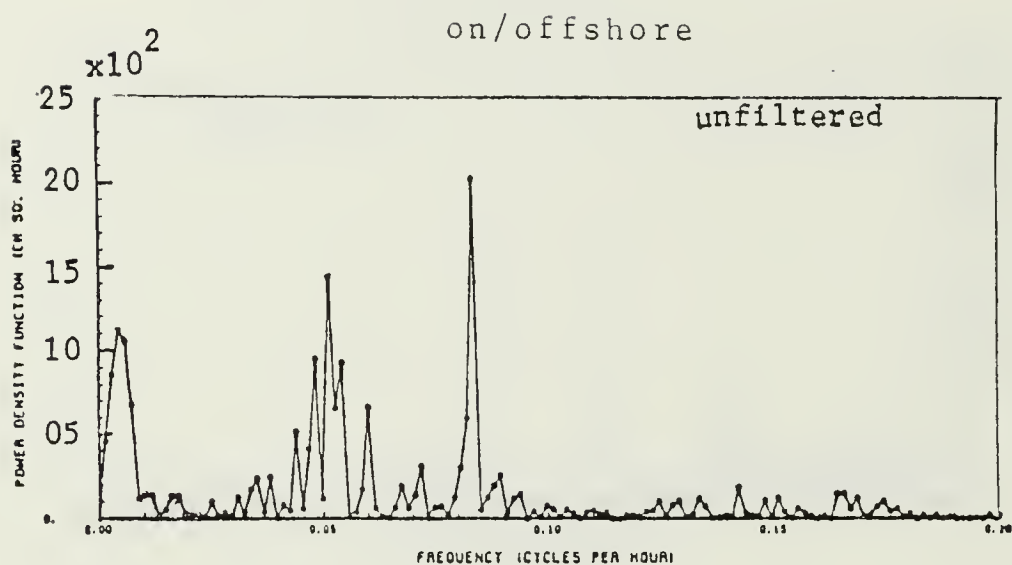


Figure 45. Energy density spectrum of current meter at 186 m depth at Station 7 deployed on 3 March 1980.

Station 7    Meter #762    Depth=311m    3 Mar 80

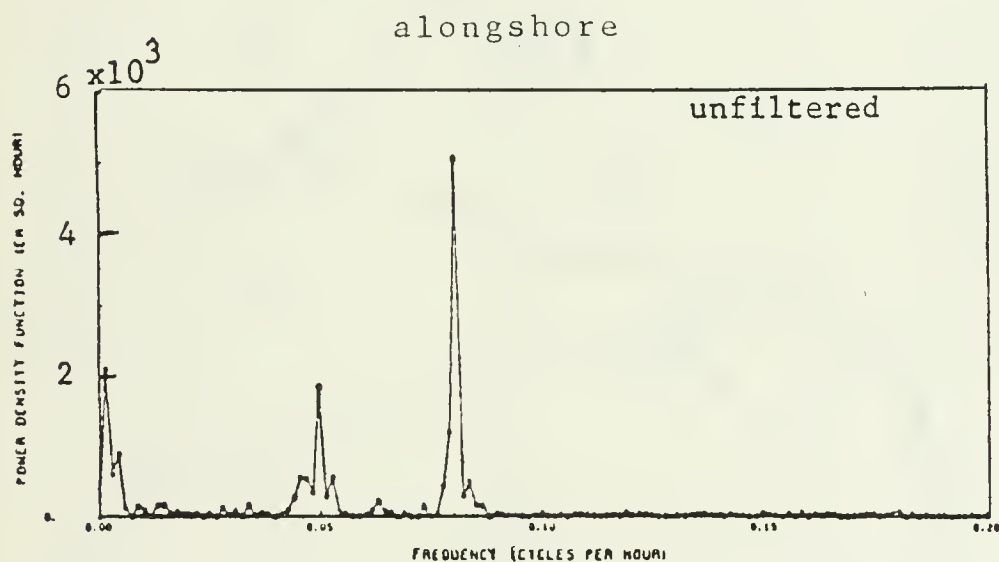
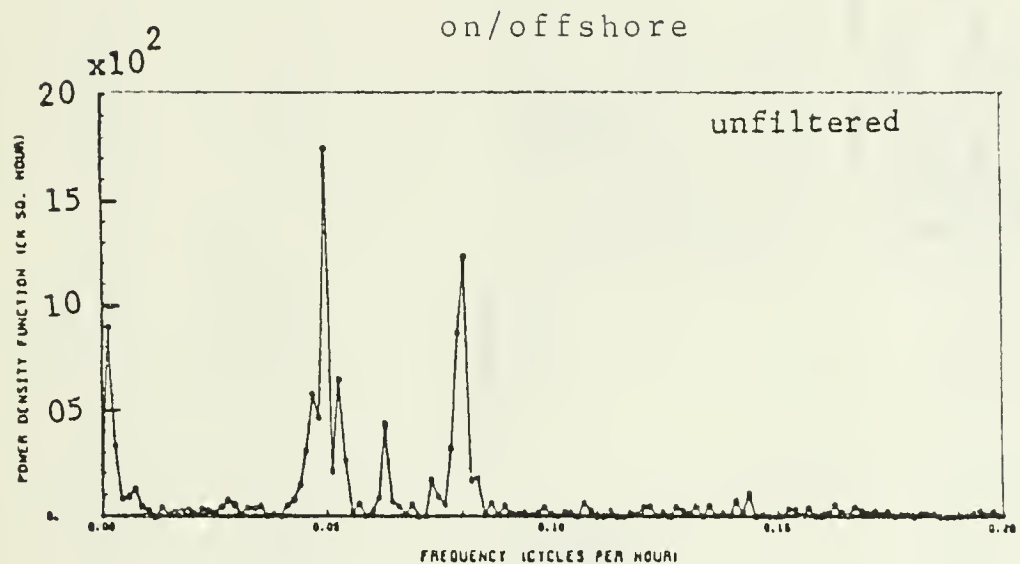


Figure 46. Energy density spectrum of current meter at 311 m depth at Station 7 deployed on 3 March 1980.

# APPENDIX C: PROGRESSIVE VECTOR DIAGRAMS

Station 7  
 Meter #762  
 Depth=152m  
 9 Jan-28 Feb  
 $\bar{\theta}=354.8$   
 $\bar{V}=4.6$  cm/sec  
 + every 3 days

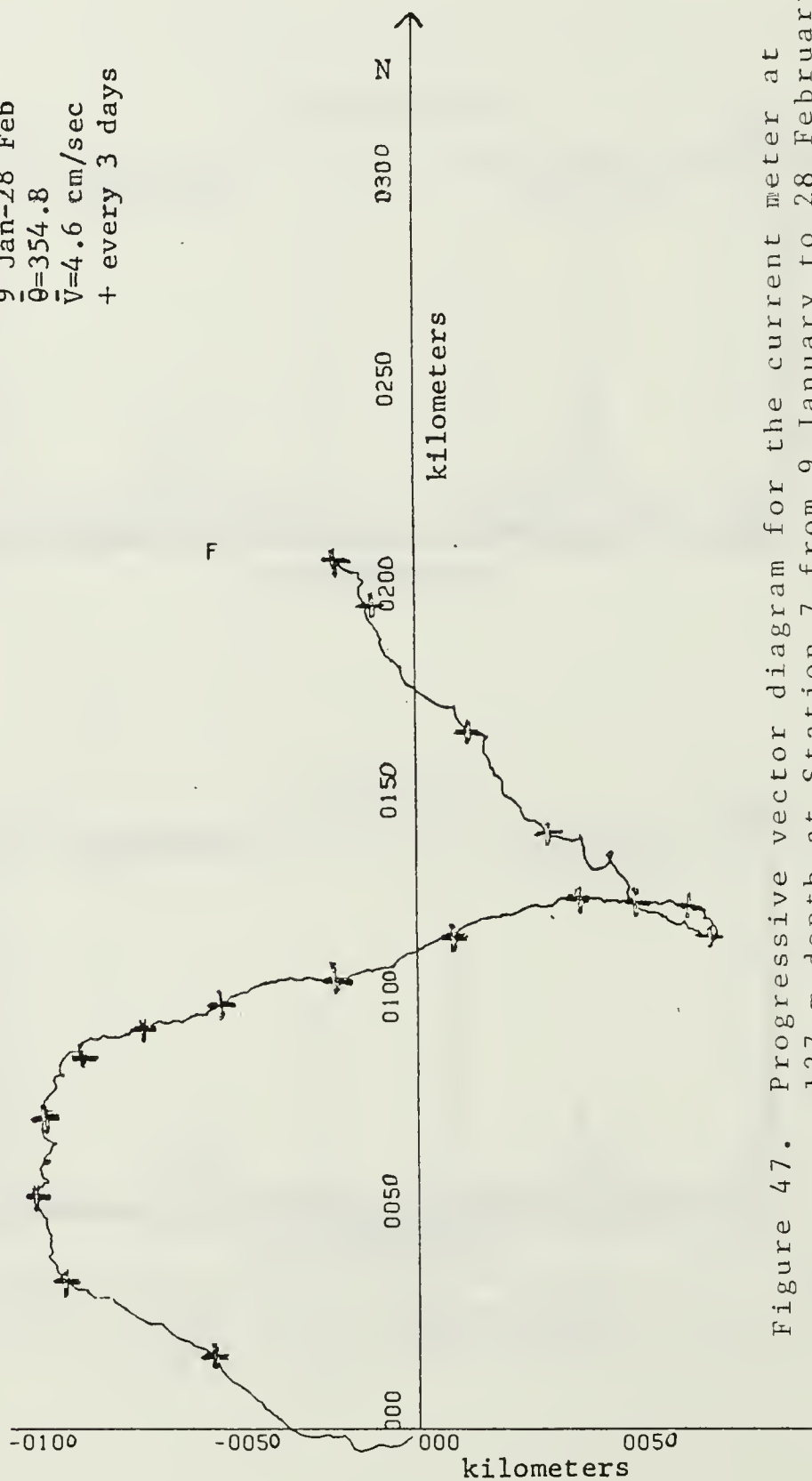


Figure 47. Progressive vector diagram for the current meter at 127 m depth at Station 7 from 9 January to 28 February 1979.

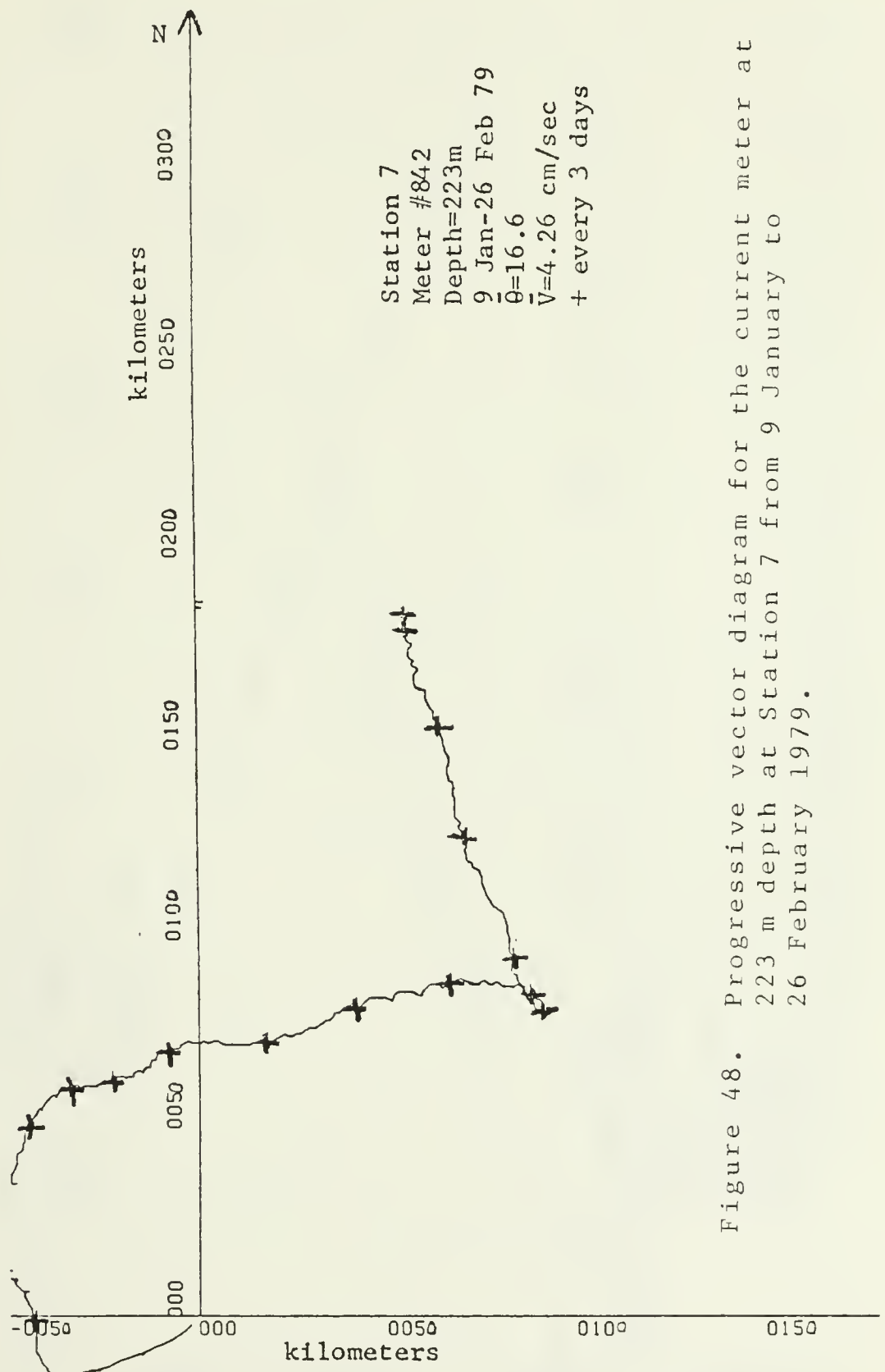


Figure 48. Progressive vector diagram for the current meter at 223 m depth at Station 7 from 9 January to 26 February 1979.

Station 2  
 Meter #1965  
 Depth=169m  
 24 Apr-13 June 79  
 $\bar{\theta}=341.2$   
 $\bar{V}=16.01$  cm/sec  
 + every 3 days

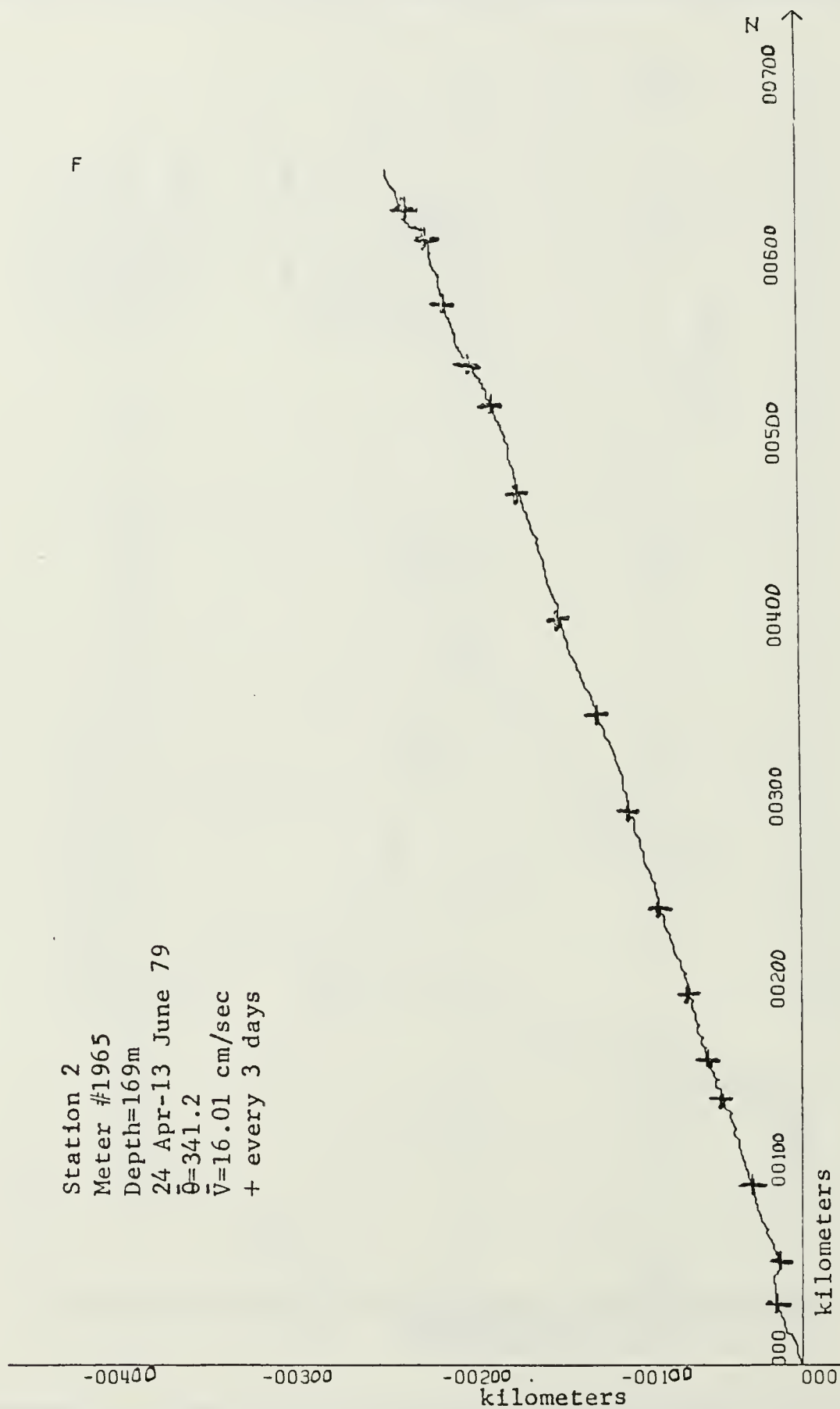


Figure 49. Progressive vector diagram for the current meter at 169 m depth at Station 2 from 24 April to 13 June 1979.

Station 2  
 Meter #1319  
 Depth=241m  
 24 Apr-12 June 79  
 $\bar{\theta}=340.4$   
 $\bar{V}=11.11$  cm/sec  
 + every 3 days

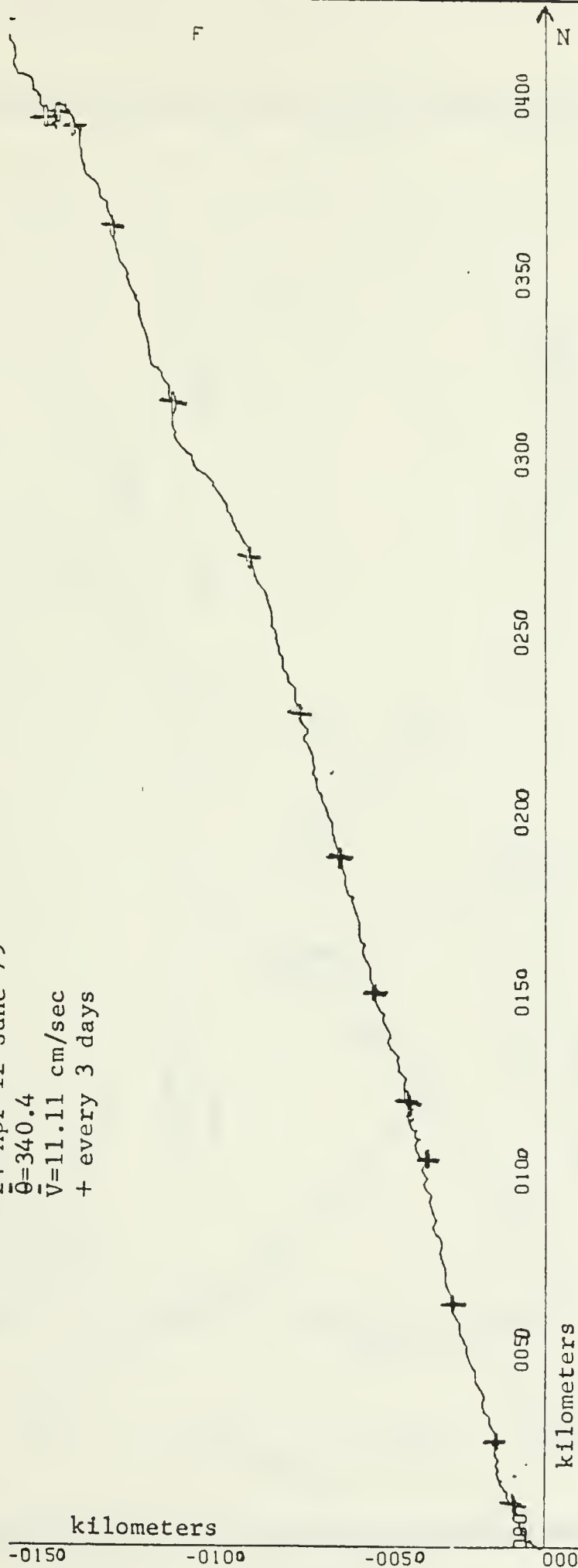


Figure 50. Progressive vector diagram for the current meter at 241 m depth at Station 2 from 24 April 12 June 1979.



Station 7  
 Meter #2760  
 Depth=158m  
 9 Jul-30 Aug 79  
 $\bar{\theta}=312.2$   
 $\bar{V}=4.51$  cm/sec  
 + every 3 days

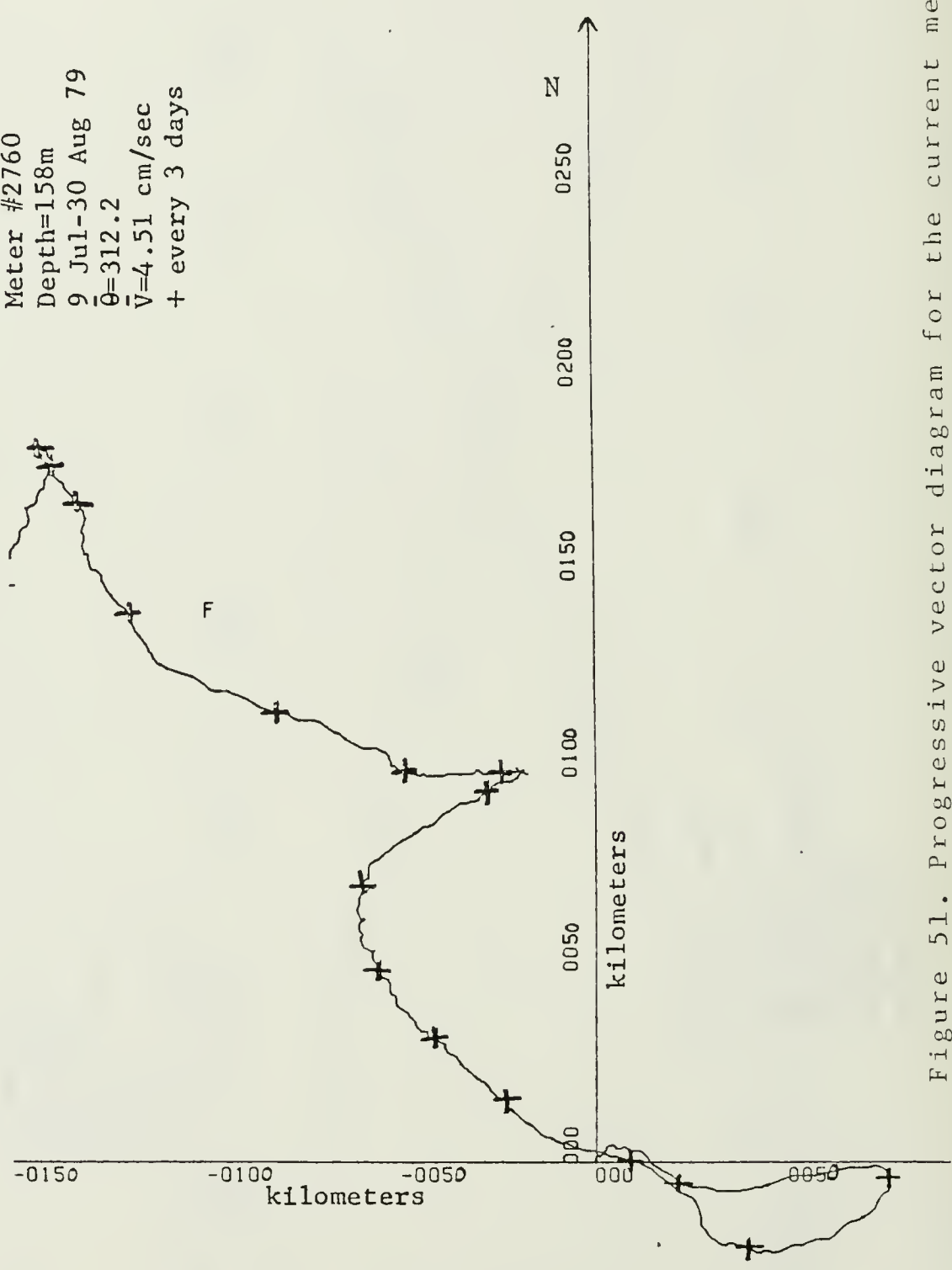


Figure 51. Progressive vector diagram for the current meter at  
 158 m depth at Station 7 from 9 July to 30 August  
 1979.

Station 7  
 Meter #842  
 Depth=231m  
 9 Jul-29 Aug 79  
 $\bar{\theta}=330.6$   
 $\bar{V}=5.84$  cm/sec  
 + every 3 days

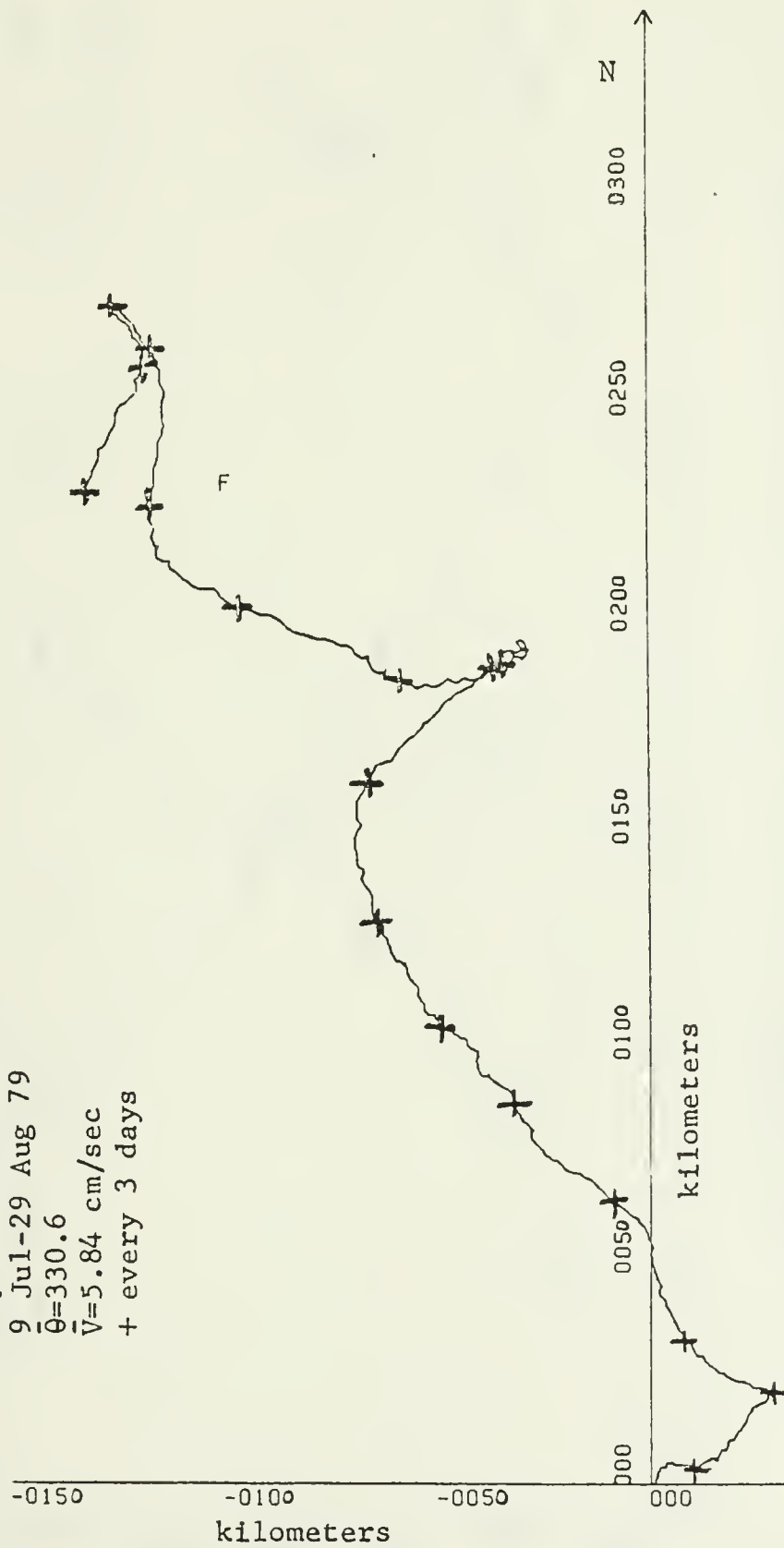


Figure 52. Progressive vector diagram for the current meter at  
 231 m depth at Station 7 from 9 July to 29 August 1979.

Station 7  
 Meter #362  
 Depth=356m  
 9 Jul-30 Aug 79  
 $\bar{\theta}=338.6$   
 $\bar{V}=2.77$  cm/sec  
 + every 3 days

F

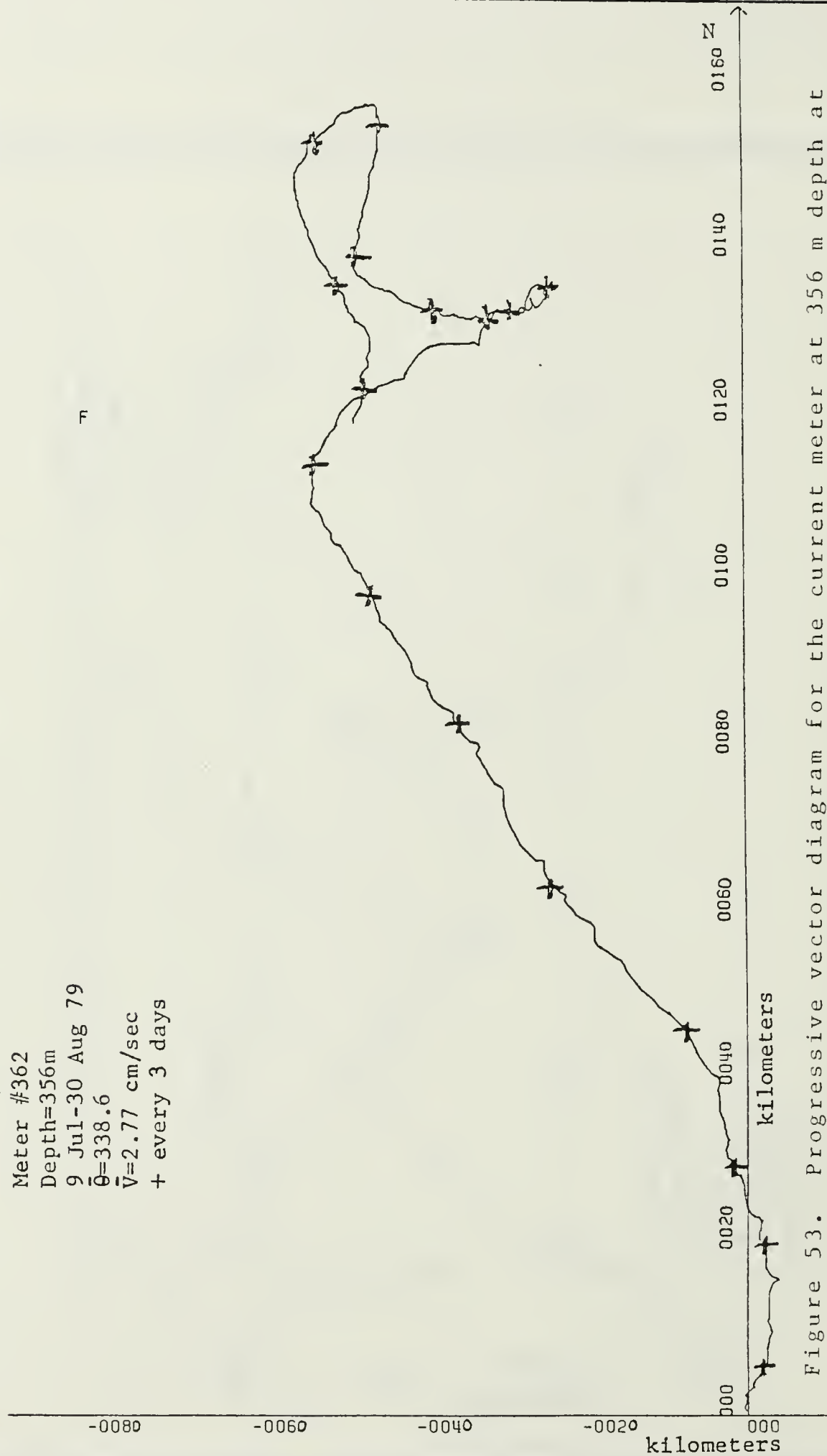


Figure 53. Progressive vector diagram for the current meter at 356 m depth at Station 7 from 9 July to 30 August 1979.

Station 2  
 Meter #1965  
 Depth=165m  
 23 Jul-11 Sep 79  
 $\bar{\theta}=325.1$   
 $\bar{V}=6.13$  cm/sec  
 + every 3 days

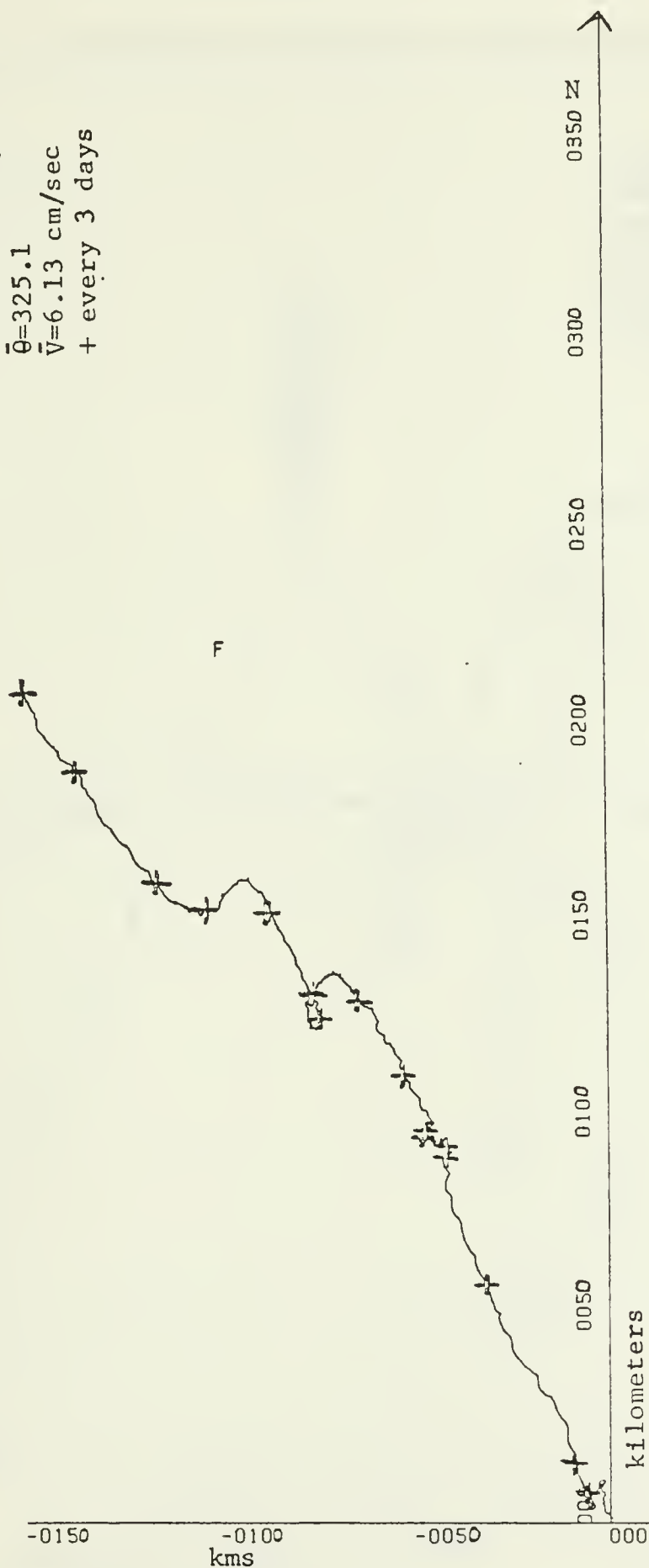


Figure 54. Progressive vector diagram for the current meter at 165 m depth at Station 2 from 23 July to 11 September 1979.

Station 2  
 Meter #1319  
 Depth=237m  
 23 Jul-13 Sep 79  
 $\bar{\theta}=314.3$   
 $\bar{V}=1.47$  cm/sec  
 + every 3 days

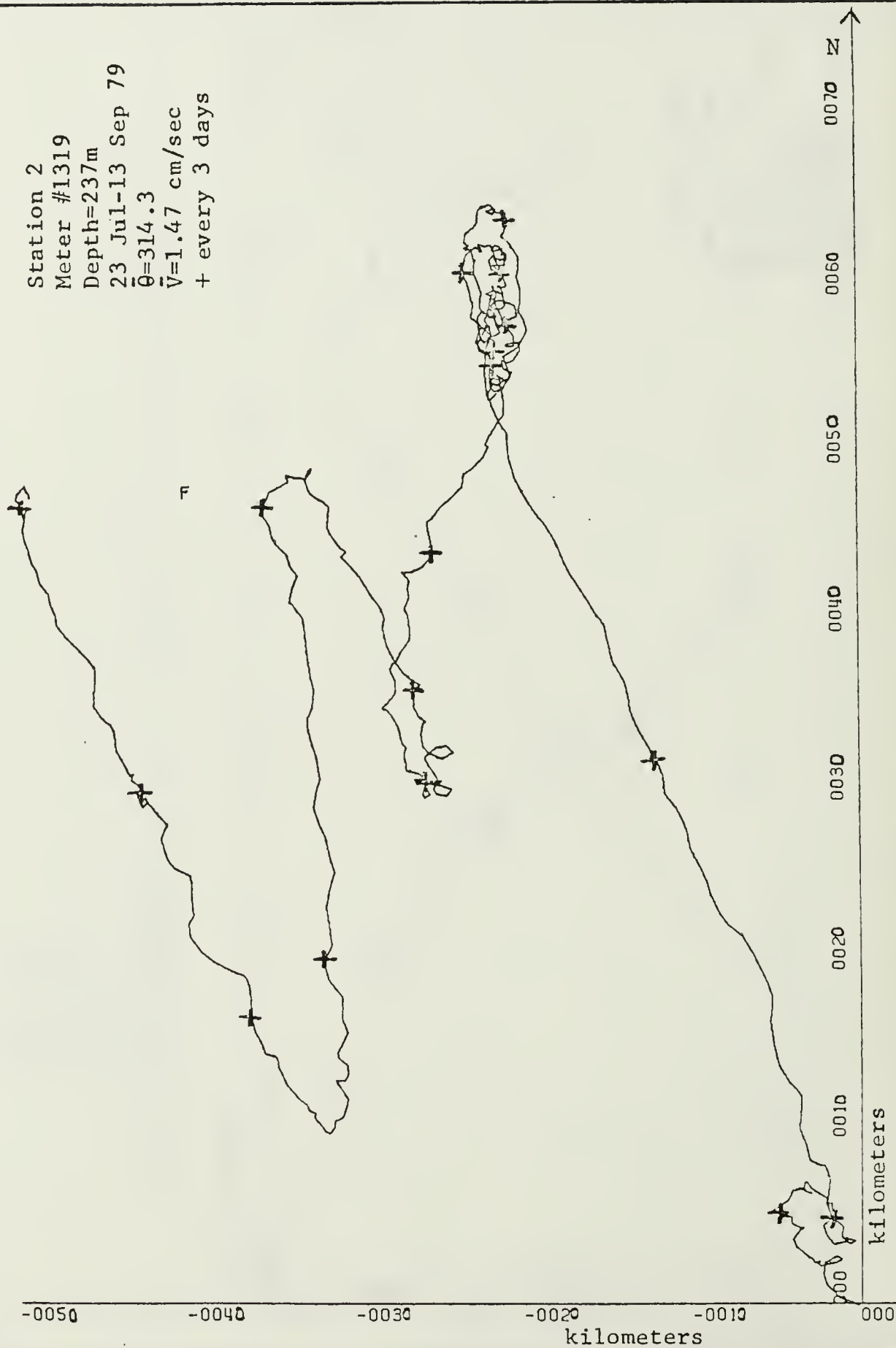


Figure 55. Progressive vector diagram for the current meter at 237 m depth at Station 2 from 23 July to 13 September 1979.

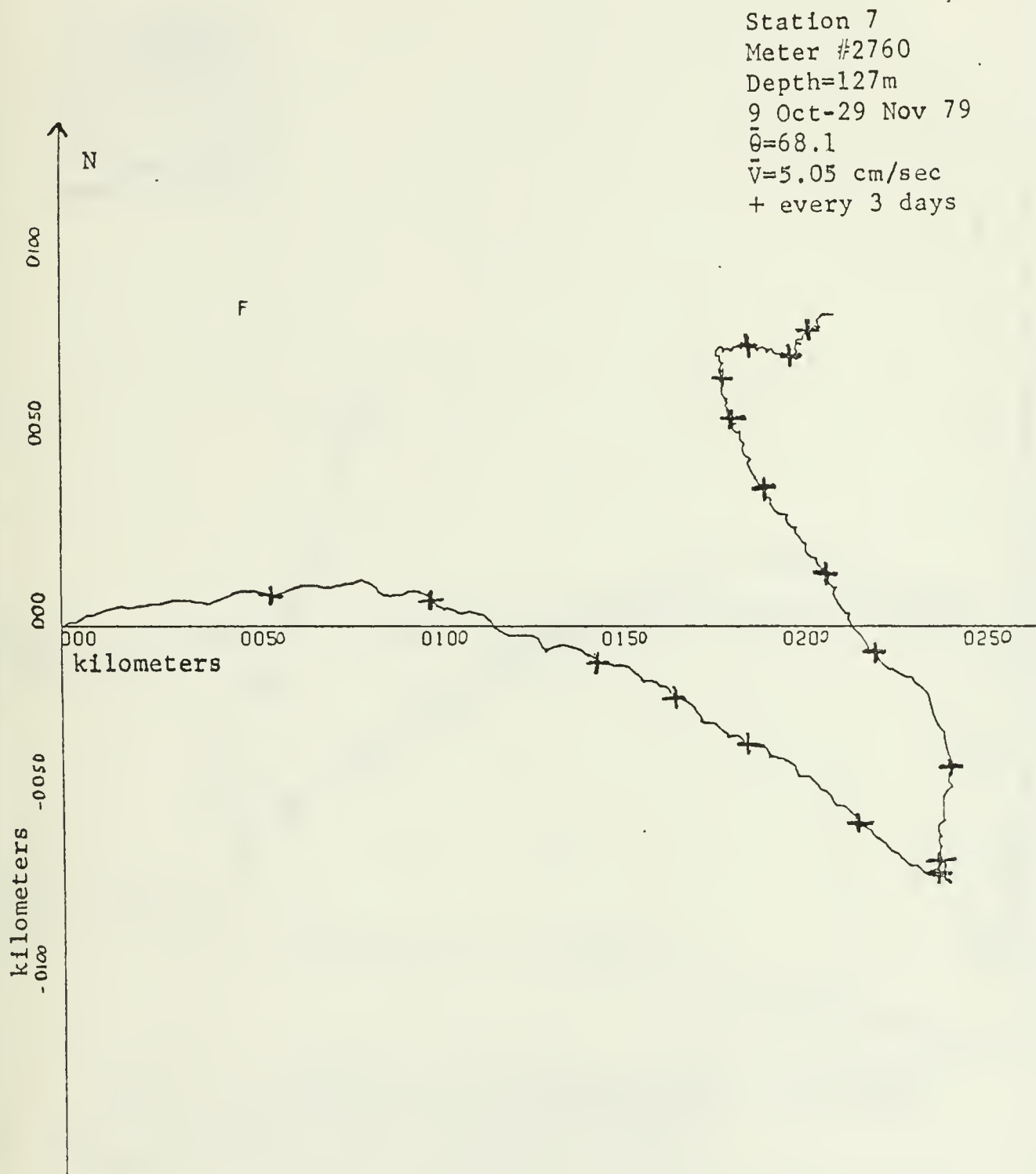


Figure 56. Progressive vector diagram for the current meter at 127 m depth at Station 7 from 9 October to 29 November 1979.



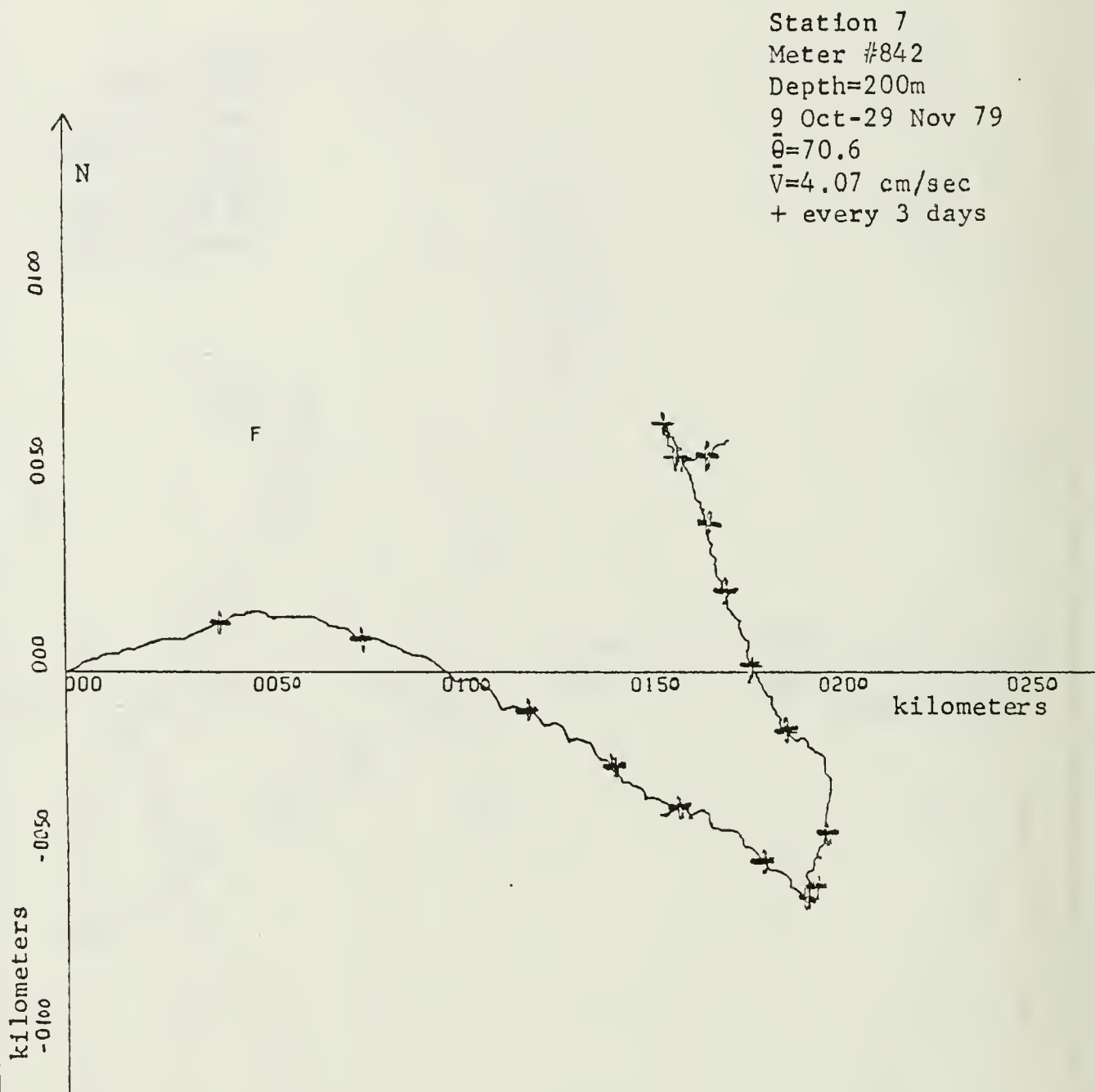


Figure 57. Progressive vector diagram for the current meter at 200 m depth at Station 7 from 9 October to 29 November 1979.

Station 2  
 Meter #1965  
 Depth=194m  
 27 Nov 79-16 Jan 80  
 $\bar{\theta}=279.8$   
 $\bar{V}=6.24$  cm/sec  
 + every 3 days

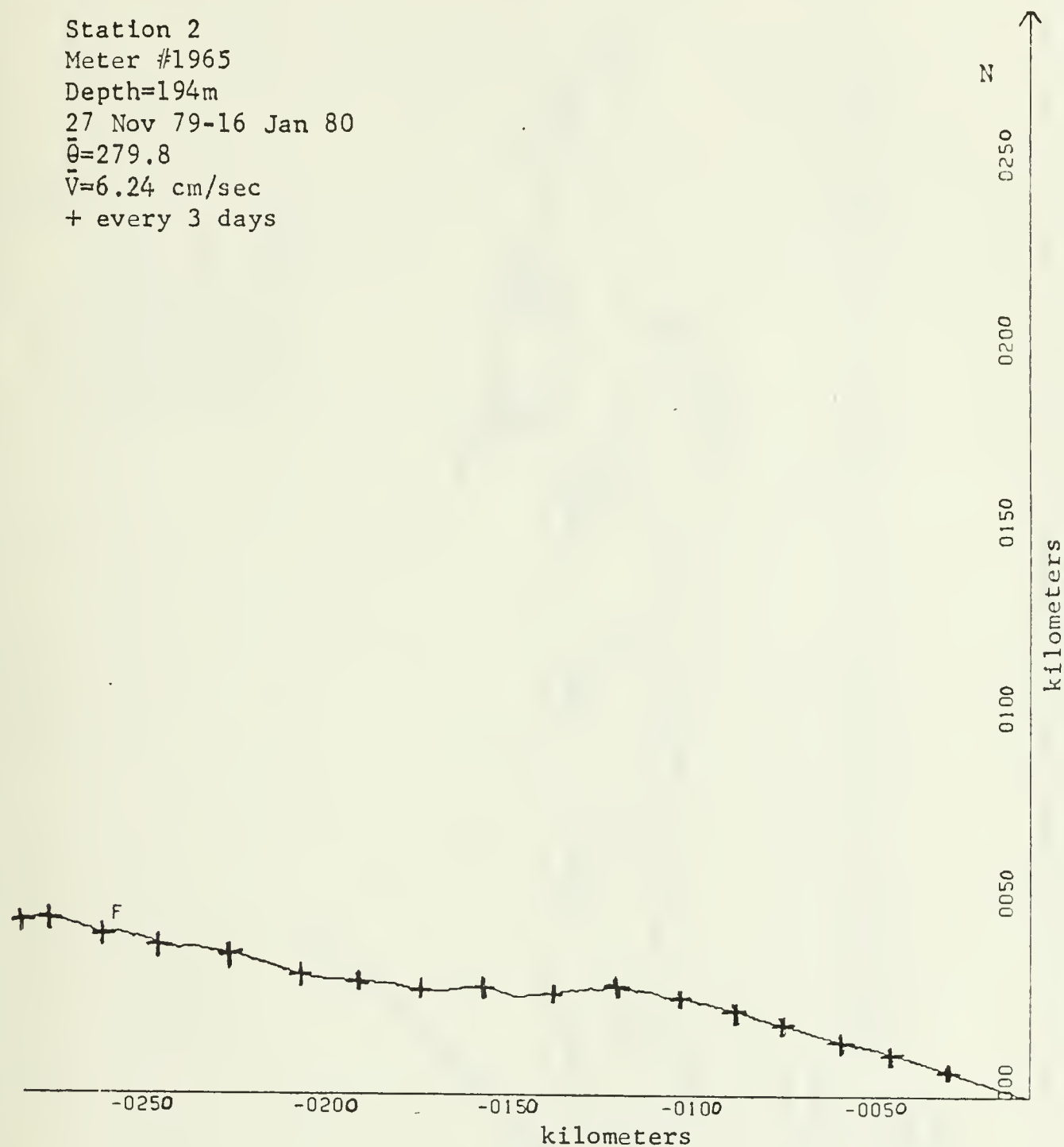


Figure 58. Progressive vector diagram for the current meter at 169 m depth at Station 2 from 27 November 1979 to 16 January 1980.

Station 2  
 Meter #1319  
 Depth=266m  
 27 Nov 79-18 Jan 80  
 $\bar{\theta}=3.1$   
 $\bar{V}=2.66$  cm/sec  
 + every 3 days

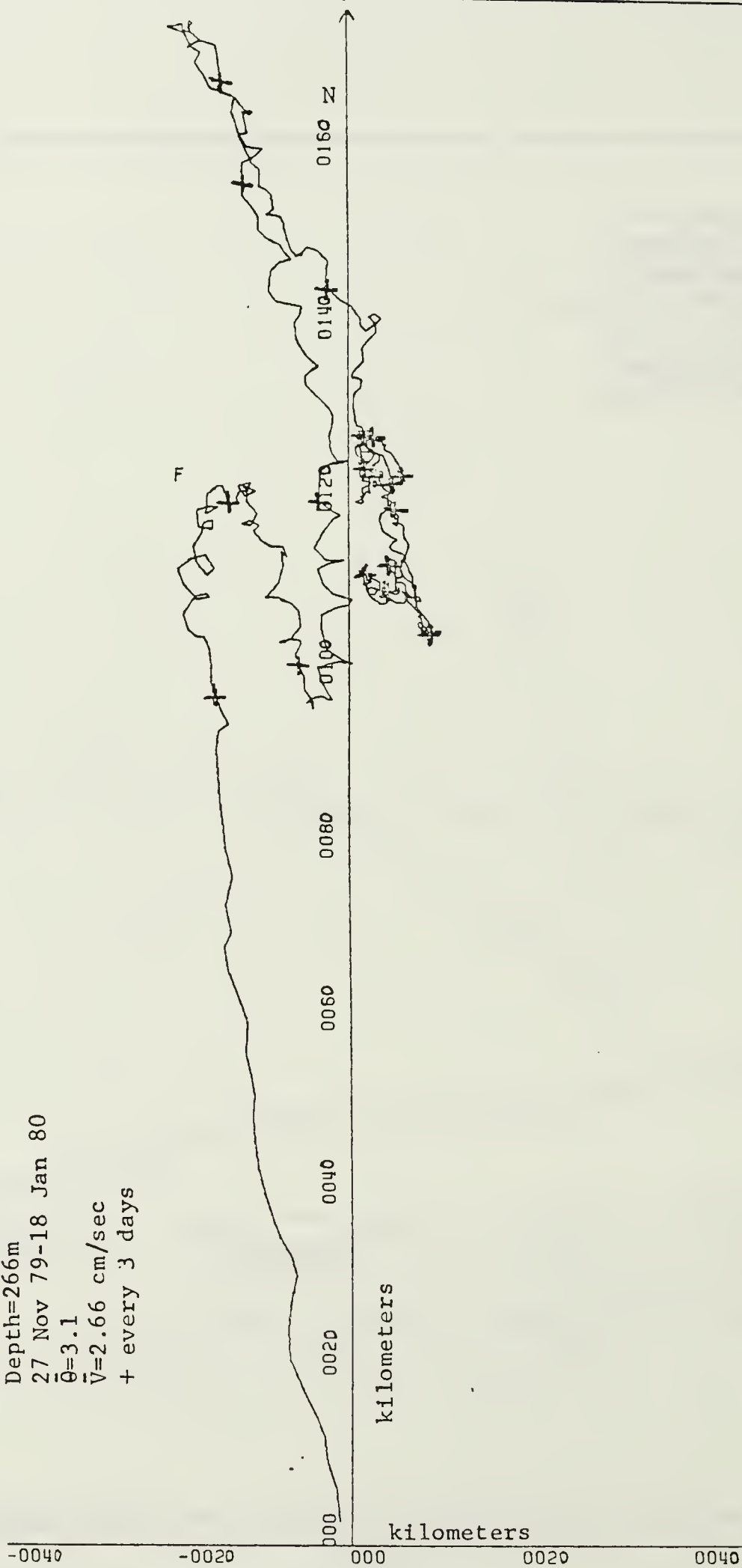


Figure 59. Progressive vector diagram for the current meter at 266 m depth at Station 2 from 27 November 1979 to 18 January 1980.

Station 7  
 Meter #2760  
 Depth=113m  
 4 Mar-15 Apr 80  
 $\bar{\theta}=310.5$   
 $\bar{V}=4.41$  cm/sec  
 + every 3 days

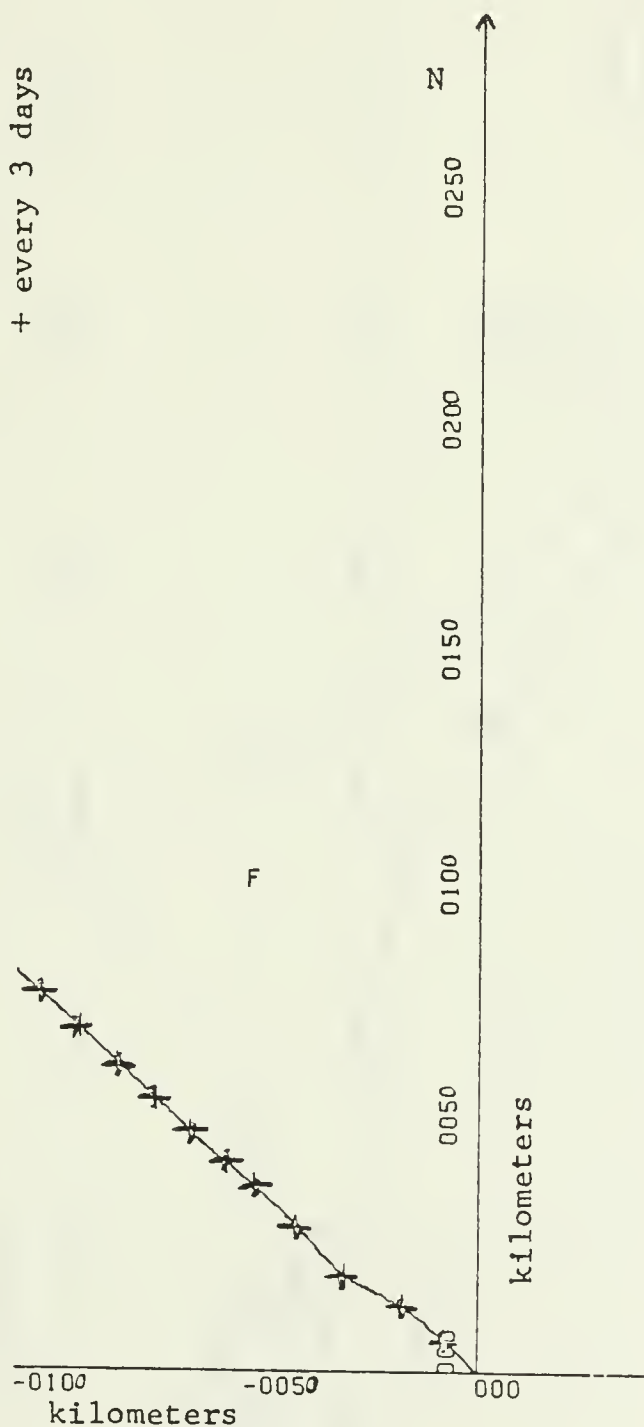


Figure 60. Progressive vector diagram for the current meter at 113 m depth at Station 7 from 4 March to 15 April 1980.

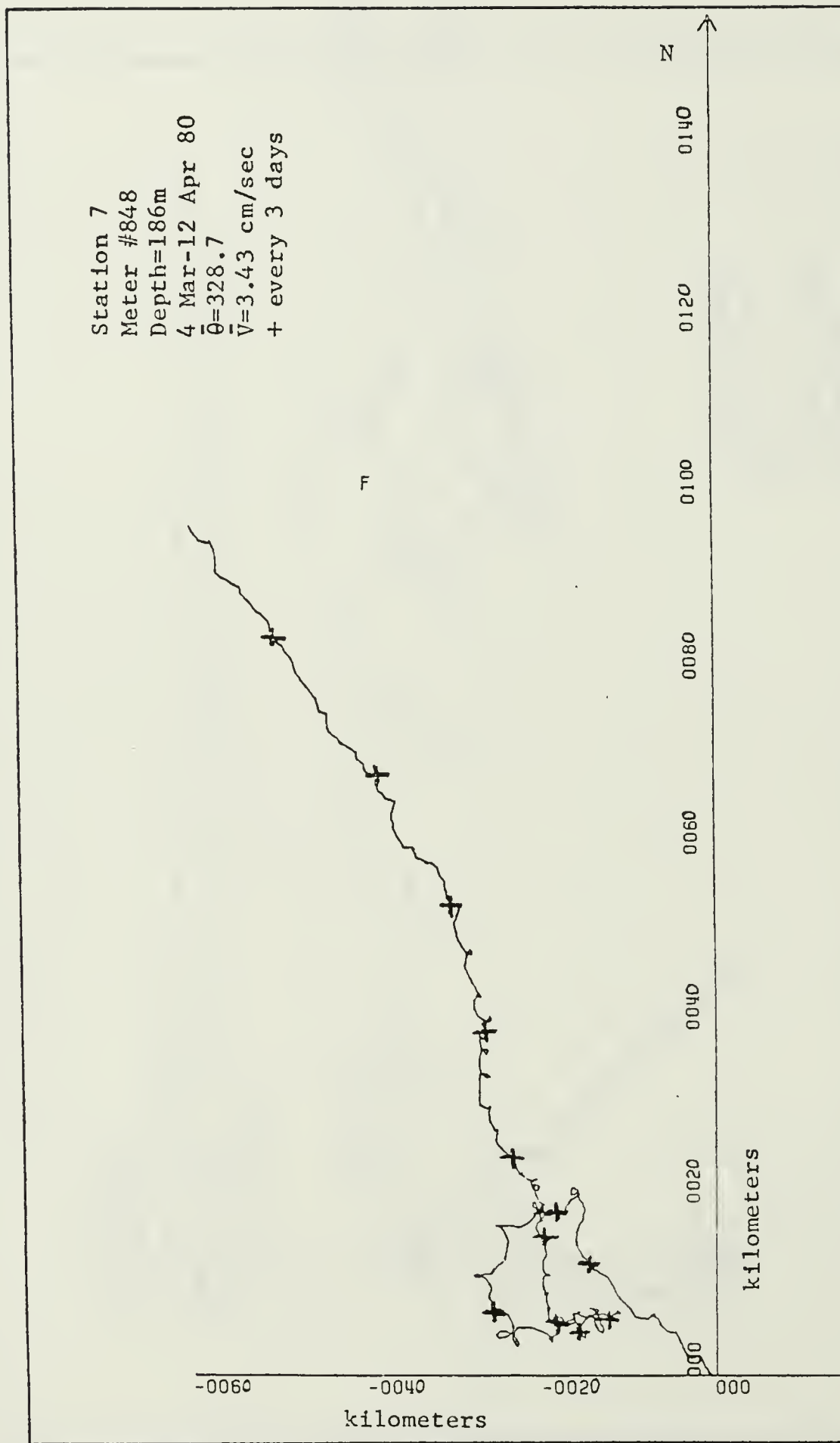


Figure 61. Progressive vector diagram for the current meter at 186 m depth at Station 7 from 4 March to 12 April 1980.

Station 7  
 Meter #762  
 Depth=311m  
 4 Mar-10 Apr 80  
 $\bar{Q}=8.2$   
 $\bar{V}=2.67$  cm/sec  
 + every 3 days

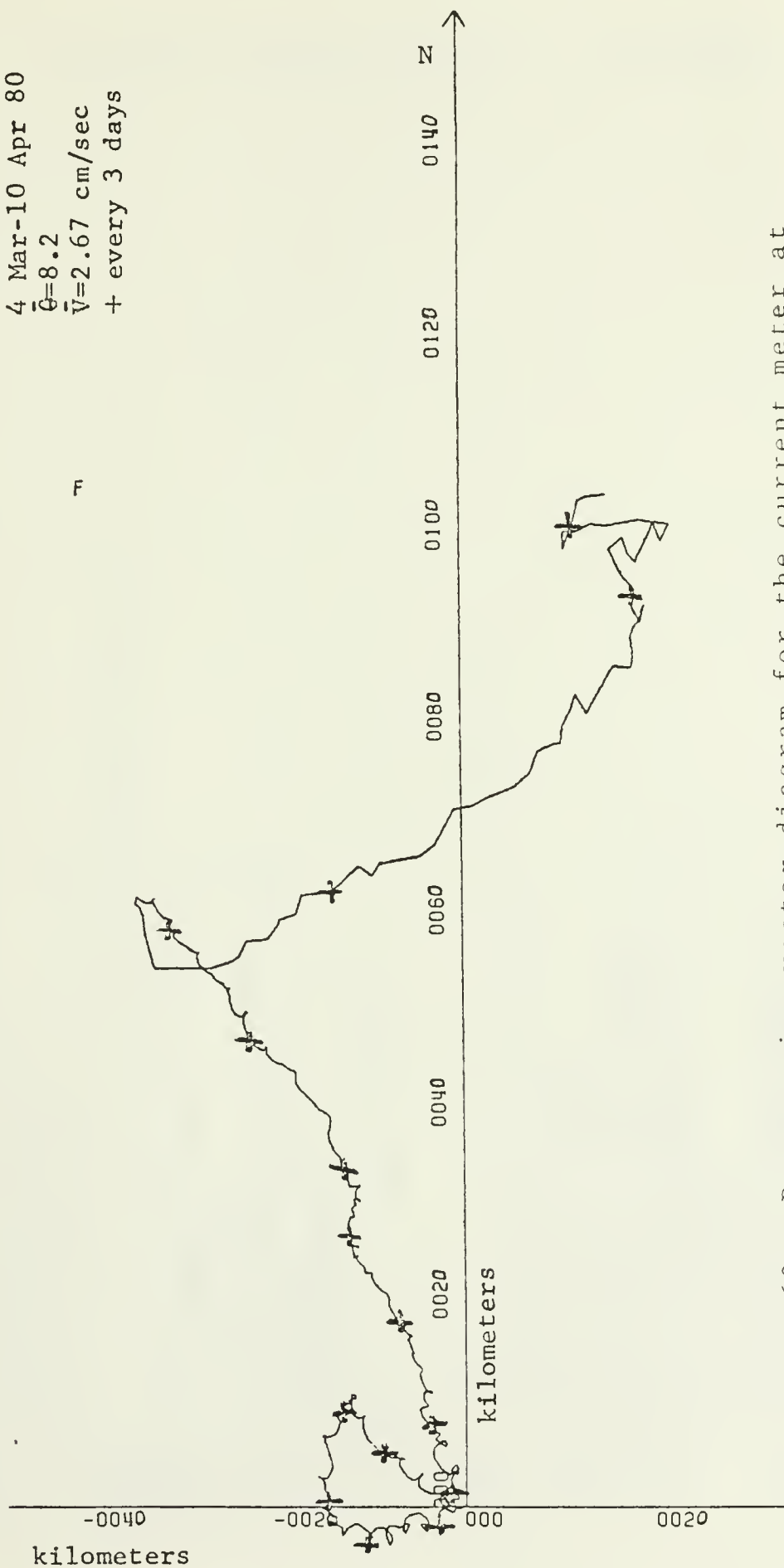


Figure 62. Progressive vector diagram for the current meter at 311 m depth at Station 7 from 4 March to 10 April 1980.



## APPENDIX D: COMPUTER PROGRAM LISTINGS

```

C THIS PROGRAM FORMATS THE MAGNETIC CURRENT METER DATA INPUT
C SO THAT IT IS FORTRAN READABLE. WRITTEN BY FANS OCELMAN NPS
C COMPUTER CENTER.
C
C BITS: PROC CPTICN5(MAIN);
C DCL INPUTF FILE RECORD ENV(CCNSECUTIVE);
C DCL OUTPUTF FILE RECORD ENV(CCNSECUTIVE);
C DCL FIELDX CHAR(512) VARYING STATIC;
C DCL FIELDY(512) CHAR(1) BASED(P);
C DCL 1 SYNCBIT(512) BASEC(P),
C DCL 2 312 311(2),
C DCL 3 312 311(2),
C DCL 4 312 311(2),
C DCL 5 312 311(2),
C DCL 6 312 311(2),
C DCL 7 312 311(2),
C DCL 8 312 311(2),
C DCL 9 312 311(2),
C DCL 10 312 311(2),
C DCL 11 312 311(2),
C DCL 12 312 311(2),
C DCL 13 312 311(2),
C DCL 14 312 311(2),
C DCL 15 312 311(2),
C DCL 16 312 311(2),
C DCL 17 312 311(2),
C DCL 18 312 311(2),
C DCL 19 312 311(2),
C DCL 20 312 311(2),
C DCL 21 312 311(2),
C DCL 22 312 311(2),
C DCL 23 312 311(2),
C DCL 24 312 311(2),
C DCL 25 312 311(2),
C DCL 26 312 311(2),
C DCL 27 312 311(2),
C DCL 28 312 311(2),
C DCL 29 312 311(2),
C DCL 30 312 311(2),
C DCL 31 312 311(2),
C DCL 32 312 311(2),
C DCL 33 312 311(2),
C DCL 34 312 311(2),
C DCL 35 312 311(2),
C DCL 36 312 311(2),
C DCL 37 312 311(2),
C DCL 38 312 311(2),
C DCL 39 312 311(2),
C DCL 40 312 311(2),
C DCL 41 312 311(2),
C DCL 42 312 311(2),
C DCL 43 312 311(2),
C DCL 44 312 311(2),
C DCL 45 312 311(2),
C DCL 46 312 311(2),
C DCL 47 312 311(2),
C DCL 48 312 311(2),
C DCL 49 312 311(2),
C DCL 50 312 311(2),
C DCL 51 312 311(2),
C DCL 52 312 311(2),
C DCL 53 312 311(2),
C DCL 54 312 311(2),
C DCL 55 312 311(2),
C DCL 56 312 311(2),
C DCL 57 312 311(2),
C DCL 58 312 311(2),
C DCL 59 312 311(2),
C DCL 60 312 311(2),
C DCL 61 312 311(2),
C DCL 62 312 311(2),
C DCL 63 312 311(2),
C DCL 64 312 311(2),
C DCL 65 312 311(2),
C DCL 66 312 311(2),
C DCL 67 312 311(2),
C DCL 68 312 311(2),
C DCL 69 312 311(2),
C DCL 70 312 311(2),
C DCL 71 312 311(2),
C DCL 72 312 311(2),
C DCL 73 312 311(2),
C DCL 74 312 311(2),
C DCL 75 312 311(2),
C DCL 76 312 311(2),
C DCL 77 312 311(2),
C DCL 78 312 311(2),
C DCL 79 312 311(2),
C DCL 80 312 311(2),
C DCL 81 312 311(2),
C DCL 82 312 311(2),
C DCL 83 312 311(2),
C DCL 84 312 311(2),
C DCL 85 312 311(2),
C DCL 86 312 311(2),
C DCL 87 312 311(2),
C DCL 88 312 311(2),
C DCL 89 312 311(2),
C DCL 90 312 311(2),
C DCL 91 312 311(2),
C DCL 92 312 311(2),
C DCL 93 312 311(2),
C DCL 94 312 311(2),
C DCL 95 312 311(2),
C DCL 96 312 311(2),
C DCL 97 312 311(2),
C DCL 98 312 311(2),
C DCL 99 312 311(2),
C DCL 100 312 311(2),
C DCL 101 312 311(2),
C DCL 102 312 311(2),
C DCL 103 312 311(2),
C DCL 104 312 311(2),
C DCL 105 312 311(2),
C DCL 106 312 311(2),
C DCL 107 312 311(2),
C DCL 108 312 311(2),
C DCL 109 312 311(2),
C DCL 110 312 311(2),
C DCL 111 312 311(2),
C DCL 112 312 311(2),
C DCL 113 312 311(2),
C DCL 114 312 311(2),
C DCL 115 312 311(2),
C DCL 116 312 311(2),
C DCL 117 312 311(2),
C DCL 118 312 311(2),
C DCL 119 312 311(2),
C DCL 120 312 311(2),
C DCL 121 312 311(2),
C DCL 122 312 311(2),
C DCL 123 312 311(2),
C DCL 124 312 311(2),
C DCL 125 312 311(2),
C DCL 126 312 311(2),
C DCL 127 312 311(2),
C DCL 128 312 311(2),
C DCL 129 312 311(2),
C DCL 130 312 311(2),
C DCL 131 312 311(2),
C DCL 132 312 311(2),
C DCL 133 312 311(2),
C DCL 134 312 311(2),
C DCL 135 312 311(2),
C DCL 136 312 311(2),
C DCL 137 312 311(2),
C DCL 138 312 311(2),
C DCL 139 312 311(2),
C DCL 140 312 311(2),
C DCL 141 312 311(2),
C DCL 142 312 311(2),
C DCL 143 312 311(2),
C DCL 144 312 311(2),
C DCL 145 312 311(2),
C DCL 146 312 311(2),
C DCL 147 312 311(2),
C DCL 148 312 311(2),
C DCL 149 312 311(2),
C DCL 150 312 311(2),
C DCL 151 312 311(2),
C DCL 152 312 311(2),
C DCL 153 312 311(2),
C DCL 154 312 311(2),
C DCL 155 312 311(2),
C DCL 156 312 311(2),
C DCL 157 312 311(2),
C DCL 158 312 311(2),
C DCL 159 312 311(2),
C DCL 160 312 311(2),
C DCL 161 312 311(2),
C DCL 162 312 311(2),
C DCL 163 312 311(2),
C DCL 164 312 311(2),
C DCL 165 312 311(2),
C DCL 166 312 311(2),
C DCL 167 312 311(2),
C DCL 168 312 311(2),
C DCL 169 312 311(2),
C DCL 170 312 311(2),
C DCL 171 312 311(2),
C DCL 172 312 311(2),
C DCL 173 312 311(2),
C DCL 174 312 311(2),
C DCL 175 312 311(2),
C DCL 176 312 311(2),
C DCL 177 312 311(2),
C DCL 178 312 311(2),
C DCL 179 312 311(2),
C DCL 180 312 311(2),
C DCL 181 312 311(2),
C DCL 182 312 311(2),
C DCL 183 312 311(2),
C DCL 184 312 311(2),
C DCL 185 312 311(2),
C DCL 186 312 311(2),
C DCL 187 312 311(2),
C DCL 188 312 311(2),
C DCL 189 312 311(2),
C DCL 190 312 311(2),
C DCL 191 312 311(2),
C DCL 192 312 311(2),
C DCL 193 312 311(2),
C DCL 194 312 311(2),
C DCL 195 312 311(2),
C DCL 196 312 311(2),
C DCL 197 312 311(2),
C DCL 198 312 311(2),
C DCL 199 312 311(2),
C DCL 200 312 311(2),
C DCL 201 312 311(2),
C DCL 202 312 311(2),
C DCL 203 312 311(2),
C DCL 204 312 311(2),
C DCL 205 312 311(2),
C DCL 206 312 311(2),
C DCL 207 312 311(2),
C DCL 208 312 311(2),
C DCL 209 312 311(2),
C DCL 210 312 311(2),
C DCL 211 312 311(2),
C DCL 212 312 311(2),
C DCL 213 312 311(2),
C DCL 214 312 311(2),
C DCL 215 312
```

```

PUT EDIT (X, 'BLOCKS READ',
          XOUT, 'RECORDS WRITTEN')
          (SKIP(1), F(6), A, F(6), A);
STCLEN: PFC(P, I);
DCL OUTI(6) BIT(16) STATIC;
DCL OUTI(6) FIXED BIN(15) BASED();
DCL COUNTER;
DCL PCOUNTER;
DCL INFIELD BIT(16) BASED(P);
DCL INFIELD(CUTFIELD(1));
SUBSTR(OUTFIELD(I), 1, 6) = 'CCCCC0'B;
DO IF=1 TO COUNTER;
SUBSTR(OUTFIELD(I), II+11, 1)=SUBSTR(INFIELD, II+3, 1);
SUBSTR(OUTFIELD(I), II+6, 1)=SUBSTR(INFIELD, II+11);
END;
PUT EDIT(COUTI(I))(X(4), F(6));
IF I = 6 THEN DO;
XOUT = XOUT + 1;
WRITE(COUTI) FRCM(CUTFIELD);
END; /* THE PROGRAM */
END; /* THE PROGRAM */

```

```

C THIS PROGRAM APPLIES CALIBRATION PARAMETERS TO AANDERAA CURRENT
C METER DATA, ACCORDING TO EACH INDIVIDUAL CURRENT METER'S
C SPECIFICATIONS.
C INTEGER # 2 AR(50000)
C REAL XXX(6) /6*.) /
C I1=1
C I2=2
C IR=1

C READ IN RAW DATA.
22 READ(2,2),END=90)(AR(I),I=11,I2)
23 FORMAT(6A2)
C I1=I2+1
C I2=I2+6
C GO TO 22

C LOCATE REF NUMBER IN THE RECORD.
C USE A WINDCW CF APPROXIMATELY 20, IN CASE SYNCBIT SLIPS.
90 IF (AR(M).LE.970.AND.AR(M).GE.940) GO TO 5
M=M+1
GO TO 50
C IF REF# OUTSIDE WINDCW, DATA CONSIDERED FAULTY. ZERO OUT ALL
C VALUES.
C IF (AR(M).GE.971.AND.AR(M).LE.939) GO TO 10
C 5
C CALIBRATION PARAMETERS APPLIED. FORMULAS ARE FROM AANDERAA
C OPERATION MANUAL. SALINITY AND PRESSURE SENSORS ARE NOT USED.
C T=-2.462+ (.02277*AR(M+1))- (.134* (-5))*(AR(M+1)*2))+
C 1 (.1937*(10.**(-8))*(AR(M+1)*3))
C S=0.023*AR(M+4)
C P=10.352*AR(M+5).EQ. 0.) GO TO 50
C IF (AR(M+5).EQ. 0.) GO TO 50
C V=1.0*AR(M+5)
C V=0.0*AR(M)
C REF=AR(M)
C WRITE(6,150) IR,REF,T,S,P,V
C FORMAT('I,4X,I6,6(4X,F7.2)')
C 150 WRITE(6,150) CALIBRATED DATA VALUES (10 MINUTE) TC MASS STORAGE.
C WRITE(1) IR,REF,T,S,P,V
C IR=IR+1
C M=M+6
C IF (M.GT.50000) GO TO 100
C GO TO 5

```

```

10  WRITE (6,150) IR,XXX
    WRITE (1) IR,XXX
    IR=IR+1
    IF (M.(1.50000) GO TO 100
    M=M+6
    GO TO 2
    ENDFILE 1
    STOP
    END
100

```

```

C C C C C
THIS PROGRAM USES TEN MINUTE CALIBRATED DATA VALUES AS INPUT.
MISSING RECORDS ARE FILLED IN AND A BINOMIAL FILTER IS USED TO
CREATE FOURLY VALUES. FOUR PLOTS ARE PRODUCED: CURRENT VS TIME, AND
TEMPERATURE VS TIME.
DIMENSION IR(10000), CIR(10000), SPD(10000), AR(6), REF(10000),
IU(10000), V(10000), T(10000), HRSPD(1700), TRU(10000), THETA(10000),
I FOUR(1700), HOURV(1700), FOURI(1700), IEM(10000)
10 FORMAT (1X, I10, 2F10.2)
J=0
C C C C C
READ DATA FROM MASS STORAGE
20 READ(L,END=25) II,AR
IK(II)=II
REF(II)=AR(1)
TEM(II)=AR(2)
SALES=AR(3)
PRRES=AR(4)
CIR(II)=AR(5)
SPD(II)=AR(6)
GO TO 20
25 CONTINUE
NNPTS=IR(II)
CREATE ARTIFICIAL VALUES FOR MISSING RECORDS. (THIS SUBROUTINE
LEAVES THE REFERENCE NUMBER ZERO FOR READY IDENTIFICATION OF
ARTIFICIAL VALUES.)
NNPTS=NNPTS-2
DO 7 I=3, NNPTS
WARNING: CURRENT SPEEDS GREATER THAN 100 CM/SEC ARE NOT ACCEPTED
HERE BUT SUBSTITUTED WITH INTERPOLATED VALUES.
IF (SPD(I).GE.100) GC TO 6
IF (REF(I).NE.0) GO TO 5
CALL FILLER (I,SPD,CIR,SPDCUT,JROUT)
SPD(I)=SPDCUT
CIR(I)=JROUT
INSURE TEMPERATURE VALUES ARE WITHIN ACCEPTABLE LIMITS. AVGID
IS CURRENT TEMPERATURE FAULTY DATA BY SEARCHING DOWN THE RECORD FOR AN
ACCEPTABLE VALUE.
5 IF (TEM(I).GE.5.0.AND.TEM(I).LE.12.0) GC TO 7
J=I
IF (TEM(J+1).CE.5.0.AND.TEM(J+1).LE.12.0) GO TO 3
J=J+1
GO TO 2
3 TEM=(TEM(I-1)+TEM(J+1))/2.
TEM(I)=INEX

```

```

7  CONTINUE
C  CREATE A REPRESENTATIVE FOURLY CURRENT VALUE FROM THE 10 MINUTE
C  RECORDS.
C
      NPIS6=(NPIS/6)
      CALL RMEAN(NPIS,NPIS6,SPD,DIR,HRSPD,U,V,T,TRU,THETA,IEM,
1  HOURU,HCURV,HOURT,RFOF)
C  CREATE DATA PLOTS.
C
      NPIS=NPIS6
      NPIS2=NPIS+2
      CALL STKFLT(NPIS,NPIS2,IF,HRSPC,HOURU,FCURV,FCURT,RHOF)
      STOP
      END
      SUBROUTINE FILLER (I,SPC,DIR,SPDOUT,CIRCUT)
C  SUBROUTINE FILLER CREATES SPEED AND DIRECTION VALUES FOR THE CURRENT
C  METER RECORD. THIS IS DONE TO PROVIDE REASONABLE APPROXIMATIONS
C  FOR THE OCCASIONAL RECORD MISSED DUE TO INSTRUMENT (METER)
C  MALFUNCTION. THE AVERAGING ROUTINE AVOIDS INCORPORATING FAULTY
C  DATA.
C
      DIMENSION CIR(1),SPC(1)
      J=I
      IF(SPD(J+1).LE.100.)GC IC 5
8      J=J+1
      GO TO 3
9      SPDOUT=(SPD(I-1)+SPD(J+1))/2.
      IF (CIR(I-1).LE.90..AND.CIR(I+1).GT.270.) GC IC 10
      IF (CIR(I-1).GT.270..AND.CIR(I+1).LE.90.) GC IC 10
      IF (CIR(I-1)-DIR(I+1).GT.180.) GO TO 15
      IF (CIR(I+1)-DIR(I-1).GT.180.) GO TO 15
      DIROUT=(CIR(I-1)+DIR(I+1))/2.
      GO TO 20
10  DIROUT=(CIR(I-1)-DIR(I+1))/2.+DIR(I+1)+180.
      IF (DIROUT.GE.360.) DIROUT=DIROUT-360.
      IF (DIROUT.LE.0.) DIROUT=DIROUT+360.
      GO TO 20
15  DIROUT=(CIR(I-1)+DIR(I+1))/2.+180.
      GO TO 20
20  CONTINUE
      RETURN
      END
      SUBROUTINE RMEAN(NPIS,NPIS6,SPC,DIR,HRSPC,U,V,T,TRU,THETA,

```







```

C
HRSPC(NPTS+1)=-40.
HRSPD(NPTS+2)=10.
EVALS=HRSPD(NPTS+2)
EVALS=HRSPD(NPTS+2)
CALL PLOT(3,10,-3)
CALL AXIS(0.,-4.,13,XLEN,0.,0.,20.)
CALL HLINE(0.,XLEN,0.,21111)
WRITE(6,100)
J=0
PLUT IFE DATA.
DO 10 I=1,NPTS
J=J+1
PLUT(1)/DVS
XI=HOURV(I)/DVS
YI=HOURV(I)/DVS
CALL PLOT(X1,Y1,2)
WRITE(6,200) J,I,HRSPJ(I),HOURV(I),HOURT(I),X1,Y1
10 CONTINUE
CALL PLOT(0.,0.,999)
SET UP THE U COMPONENT PLOT.
CALL PLOT(0.,0.,0)
CALL FACTOR(0.35)
HRSPD(NPTS+2)=-40.
EVALS=HRSPD(NPTS+2)
DVS=HRSPD(NPTS+2)
CALL PLOT(0.,0.,10,-3)
CALL AXIS(0.,-4.,13,XLEN,0.,0.,20.)
CALL HLINE(0.,XLEN,0.,21111)
CALL PLOT(0.,0.,-3)
B=0.
PLUT IFE DATA.
DO 11 I=1,NPTS
B=B+1.
XI=HOURV(I)/DVS
YI=HOURV(I)/DVS
CALL PLOT(X1,Y1,2)
11 CONTINUE
CALL PLOT(0.,0.,999)
SET UP THE V COMPONENT PLOT.
CALL PLOT(0.,0.,0)
CALL FACTOR(0.35)
HRSPD(NPTS+2)=-40.
EVALS=HRSPD(NPTS+2)
DVS=HRSPD(NPTS+2)

```

```

C
CALL PLOT(3.,10.,-3)
CALL AXIS(0.,-5.,SAMPLE NUMBER,-13,XLEN,C.,0.,20.)
CALL AXIS(0.,-4.,13+SPEED(C4/SEC),13,YLEN,90.,FVALS,DVS)
CALL HLINE(0.,XLEN,C.,Z1111)
CALL PLOT(0.,0.,-3)
B=0. THE DATA:
DO 12 I=1,NPTS
B=B+.05
X1=B
Y1=HCURV(I)/DVS
CALL PLOT(X1,Y1,2)
CONTINUE
CALL PLOT(0.,0.,999)
SET UP THE TEMPERATURE PLOT.
CALL PLOT(0.,0,0)
CALL PLOT(0.,0,35)
CALL PLOT(3.,10.,-3)
CALL AXIS(0.,-5.,SAMPLE NUMBER,-13,XLEN,C.,0.,20.)
CALL AXIS(0.,-4.,13H(TEMPERATURE),13,16.,90.,5.,.5)
CALL HLINE(0.,XLEN,RHOT,Z1111)
CALL PLOT(0.,RHCT,+3)
B=0. THE DATA:
DO 13 I=1,NPTS
B=B+.05
X1=B
Y1=(HCURV(I)*2.0)-14.
CALL PLOT(X1,Y1,2)
CONTINUE
CALL PLOT(0.,0.,999)
RETURN
END
12
C
13
C

```

```

C DIMENSION REF(10000),DIR(10000),SPD(10000),AR(6),
C 1 ALONG(10000),CROSS(10000),YY(10000),FI(10000),PERIOD(10000),
C 2 FREQUENCY(10000),U(10000),V(10000),IRT(10000),IHT(10000)
C
C PROGRAM TO EVALUATE THE ENERGY DENSITY SPECTRUM OF OBSERVED CURRENTS
C THROUGH THEIR ALONGS-PHASE AND CROSS SHELF COMPONENTS.
C
C 10 FORMAT (1X,I10,2F10.2)
C
C JDATA IS THE (HOURLY) DATA POINT AT WHICH THE ENERGY SPECTRA
C PROGRAM SHOULD BEGIN TO LOOK AT DATA. IT DOES NOT ALWAYS START AT
C 1 SINCE SOME METERS HAVE A LONG LEADER WITH NO RELEVANT VALUES.
C
C JDATA=5
C
C READ RAW DATA FROM MAGNETIC TAPE.
C
C 20 READ(I,END=25) II,AR
C NPTS=II
C REF(II)=AR(1)
C TEM=AR(2)
C SALES=AR(3)
C PRES=AR(4)
C DIR(II)=AR(5)
C SPD(II)=AR(6)
C GO TO 20
C
C 25 CONTINUE
C
C CREATE ARTIFICIAL VALUES FOR MISSING RECORDS. (THIS SUBROUTINE
C LEAVES THE REFERENCE NUMBER ZERO FOR READY IDENTIFICATION OF
C ARTIFICIAL VALUES.)
C
C NPTS=NPTS-2
C GO 5 I=3,NPTS GC TO 6
C IF (SPD(I).GE.100) GC TO 5
C IF (REF(I).NE.0.) GC TO 5
C CALL FILLER(I,SPD,DIR,SPDCUT,CIRCUT)
C SPD(I)=SPDCUT
C DIR(I)=CIRCUT
C
C 5 CONTINUE
C GO 11 I=1,NPTS
C VAR=30.17
C TRT(I)=CIR(I)+VAR
C IF (TRT(I).GE.360.) TRT(I)=TRT(I)-360.
C IHT(I)=IRT(I)*(.017453)
C U(I)=SPD(I)*SIN(THI(I))
C V(I)=SPD(I)*COS(THI(I))
C CROSS(I)=U(I)

```

```

11  ALONG(I)=V(I)
    CCAT INCL=1,4
    DO 30 IF(J.EG.1) GO TO 40
    IF(J.EG.2) GO TO 50
    IF(J.EG.3) GO TO 40
    IF(J.EG.4) GO TO 60
    CALL BCXCAR(ALONG,NPTS,24,1,NOUIT1)
    CALL BCXCAR(ALONG,NPTS,24,1,NOUIT1)
    CALL BCXCAR(ALONG,NPTS,25,1,NOUIT1)
    GO TO 40
50  CALL BCXCAR(CROSS,NPTS,24,1,NOUIT1)
    CALL BCXCAR(CROSS,NPTS,24,1,NOUIT1)
    CALL BCXCAR(CROSS,NPTS,25,1,NOUIT1)
40  N=11
    MS=1
    DT=(1./C.)
    I=1,4500
    JS=1
    IF(J.GE.3) GO TO 41
    YY(I)=ALONG(JSTART)
    GO TO 43
    YY(I)=CROSS(JSTART)
    JSTART=JSTART+1
    CONTINUE
    IF(J.GE.3) GO TO 70
    CALL PREPFA(M,MS,DT,YY,FL,PERIOD,FREQUE,NF)
    IF(J.EG.1) GO TO 80
    CALL FLCT(0.0,C.C,999)
    GO TO 80
70  CALL PREPFA(M,MS,DT,YY,FL,PERIOD,FREQUE,NF)
80  CCAT INCL(C.0,C.0,+999)
    STOP
    ENC
    SUBROUTINE FILLER (I,SPC,CIR,SPCOUT,CIRCUT)

SUBROUTINE FILLER CREATES SPEED AND DIRECTION VALUES FOR THE CURRENT
METER RECORD. THIS IS DONE TO PROVIDE REASONABLE APPROXIMATIONS
FOR THE OCCASIONAL RECORD MISSED DUE TO INSTRUMENT (METER)
MALFUNCTION.

      DIMENSION CIR(1),SPC(1)
      J=1
      IF(SPC(J+1).LE.100.)GO TO 9
      J=J+1

```







```

510 DO 513 I=1,NF
      FL(I)=C.
      IZ=)
      K=0
      DO 21 I27=1,N
        ART(I27)=YYY(I27)
      CONTINUE
      CALL AVERAGE(ART,N,AMEAN)
      DO 22 I28=1,N
        C(I28)=ART(I28)-AMEAN
      CONTINUE
      DO 520 MI=1,MS
        K=K+1
        DO 525 J=1,NM
          IZ=IZ+1
          FLS(J,I)=C(I27)
          WRITE (6,250) K
          CALL IRENC(FLS,NM,CT,U11,U21,U31,U41,URMS1)
          CALL SPEC(FLS,M,INV,S,IFERR)
          WRITE (6,260) U11,U21,U31,U41,URMS1
          DO 540 I=1,NF
            FL(I)=FLS(I)+FL(I)
          CONTINUE
          DO 550 I=1,NF
            FI(I)=FI(I)*Y/(2.*MS)
            IF(I.EG.1)GC TO 23
            PERIOD(I)=((FLCAT(NM))* (CT))/FLOAT(I-1)
            FREQUE(I)=1.0/PERIOD(I)
            IF(FL(I)).LE.10.0)GC TO 55)
          GO TO 24
          PERIOD(I)=FLOAT(NM)
          FREQUE(I)=0.0
          FREQUE(G,270)FI(I),PERIOD(I),FREQUE(I)
          DO 23
          550 CONTINUE
          CALL PLCTG(FREQUE,FI,NF,1,1,1,'FREQUENCY (CYCLES PER HOUR)',27,'PC
          OVER DENSITY FUNCTION (CM SEC. HOUR)',36,G.0,G.2,G.0,G.0,13.0,6.0)
          RETURN
        END
      SUBROUTINE SPEC (FI,M,INV,S,IFERR)
      SUBROUTINE TO CALCULATE THE POWER SPECTRUM OF A SIGNAL USING RHARM
      DIMENSION INV(515),S(515),FI(515)
      CALL RHARM(INV,M,INV,S,IFERR)
      NP=2**N+1
      NF=2**N+1
      NX=2**N+1
      NL=N*NX+1

```

```

500 F1(1)=F1(1)*F1(1)
      DO 500 I=1,NP
        J=2*I+1
        L=I+1
        XR=F1(J)*F1(J)
        XI=F1(J+1)*F1(J+1)
        FI(L)=XR+XI
        CCNT=CCNT+1
        FI(NF)=F1(NL)**2
      RETURN
END
SUBROUTINE TREND(FX,NTS,DT,FMEAN,U2,U3,U4,UFMS)
SUBROUTINE TREND EDITS CALCULATES AND RETURNS DATA
DIMENSION FX(NTS)
EDITING DATA
      FNTS=NTS
      CCMPUTING THE LINEAR TREND
      SUMF=0.0
      DO 101 I=1,NTS
        SUMF=SUMF+FX(I)
      SUMF1=0.0
      DO 102 I=1,NTS
        XI=I
        SUMF1=SUMF1+XI*FX(I)
        XNMI=NTS-1
        XNPI=NTS+1
        XM=(1.0/DT)*(12.0*SUMF1/(FNTS*XNMI*XNPI)-6.0*(SUMF/(XNMI*FNTS)))
        B=SUMF/FNTS-XM*XMPI/2.0
        FMEAN=SUMF/FNTS
      WRITE (6,9) FMEAN,XM,B
      FORNAT (2X, 'MEAN=', F10.5, 3X, 'SLOPE =', F10.5, 2X, 'INTERCEPT =', F10.5
1, //)
      DO 103 I=1,NTS
        XI=I
        FX(I)=FX(I)-(B+XM*XI*DT)
      SUBROUTINE FOR CALCULATING VARIANCE, STD DEV, SKEWNESS, KURTOSIS
      U2=0.0
      U3=0.0
      U4=0.0
      SUMU2=0.0
      SUMU3=0.0
      SUMU4=0.0
      DO 151 I=1,NTS
        U2=FX(I)*FX(I)

```

```

      U3=U2*FX(I)
      U4=U3*FX(I)
      SUMU2=SUMU2+U2
      SUMU3=SUMU3+U3
      SUMU4=SUMU4+U4
      CONTINUE
      FNTS=U1*2/FNTS
      U2=SUMU2/RT(U2)
      U3=SUMU3/(FNTS*U2*URMS)
      U4=SUMU4/(FNTS*U2*U2)
      RETURN
    END
  SUBROUTINE PAGE
    FORMAT ('I')
    WRITE (6,10)
    RETURN
  END
  SUBROUTINE AVERA (A,NPTS, A-MEAN)
    DIMENSION A(NPTS)
    SUM=0.0
    DO 100 I=1,NPTS
      SUM=SUM+A(I)
    CONTINUE
    A-MEAN=SUM/FLOAT(NPTS)
    RETURN
  END

```

151

10

100

[illegible]

```

IF(NSTRT.EQ.0) GC TC 13C
DO 11 J=1,NSTRT
11 REAC(2,12) JUNK
12 FORMAT(A4)
C
C READ DATA
NJ=0
13C DO 13 J=1,N
875 READ(12,875,END=200,ERR=353) U(J),V(J)
13 FORMAT(2F12.5)
NJ=J
C
C IF CCNF IS FALSE, FIND THE EAST AND NORTH COMPONENTS AND PUT
THEM IN U AND V.
14 IF(CCNF) GC TC 16
DO 15 J=1,N
UX=U(J)
VX=V(J)*RAD
U(J)=UX*SIN(VX)
15 V(J)=UX*CCS(VX)
C
C PARAMETERS FOR COMPRESSING DATA
16 NPTS=NP*NX
NXI=NP/NPTS
JEVNPT=NPPTS*NXI
JEVN=NP-JEVNPT
KEVN=JEVN/NP
LEVN=JEVN-KEVN*NP
WRITE(6,161) NP,NPTS,LEVN,JEVN
161 FORMAT(/5X,'PLOTS, LEVN, NPPTS, PCINTS, A CROSS IS PLOTTED EVERY ',I3,' PCINTS, THERE ARE ',I3/5X,' POINTS NOT PLOTTED AND ',I3,' POINTS AFTER THE LAST CROSS.//')
C
C SUM THE COMPONENT DISPLACEMENTS IN KILOMETERS AND STORE NP POINTS
IN CU AND CV
17 SUMU=0.
SUMV=0.
L=0
K=1
CU(1)=C.
CV(1)=C.
XC=LI*3600.*1.E-5
CO 27 Y=1,NXI
20 CO 26 LL=1,NX
L=L+1
DO 25 KK=1,NP
K=K+1

```

```

25 SUMU=SUMU+U(K)*XDDEL
26 SUMV=SUMV+V(K)*XDDEL
27 CV(L)=SUMU
CV(L)=SUMV
PU(M)=SUMU
PV(M)=SUMV
28 IF(JEVEN.EG.O) GO TO 28
DO 292 J=1,NX
L=L+1
CU 29 KK=1,NP
IF(K.GE.N) GO TO 294
K=K+1
SUMU=SUMU+U(K)*XDDEL
SUMV=SUMV+V(K)*XDDEL
292 CV(L)=SUMU
294 CV(L)=SUMV
CV(L)=SUMV
SAVE THE NUMBER OF FLCTIEC FCINTS
NT=EL
FILL THE NEXT 3 WITH THE LAST VALUE TO FILL THE END OF THE
3-COLUMN PRINTOUT IN ALL CASES
28 DO 31 J=1,3
L=L+1
CU(L)=CU(NT)
CV(L)=CV(NT)
31
FORMAT FOR THREE COLUMNS
NPRT=NT/3
IEVN=NT-3*NPRT
IF(IEVN.NE.C) NPRT=NPRT+1
C
PRINT HEADINGS
WRITE(6,55)
53 FORMAT(/,T6,'HOURS',T15,'X(KM)',T24,'Y(KM)',T33,'HOURS',T42,
1,X(KM)',T51,'Y(KM)',T61,'HCURS',T70,'X(KM)',T79,'Y(KM)',/)
C
COMPUTE TIME PARAMETERS
TOTIM=FLCAT(N)*DEL
DELTIM=FLCAT(NP)*DEL
TIM1=DELTIM
TIM2=FLCAT(NPRT)*DELTIM+DELTIM
TIM3=2.*TIM2-DELTIM
DO 50 J=1,NPRT
K2=NPRT+J
K3=K2+NPRT
WRITE(6,55) TIM1,CU(J),CV(J),TIM2,CU(K2),CV(K2),TIM3,CU(K3),CV(K3)

```



[illegible]





```

      REAL*8 ICCODE, BLANK/8F
      REAL*8 ITIT, ICAT8(18)/5HIWIDE, 5HIHIGH, 8FMODEXAX., 5HIIXUP.,
      REYAX., 8FIYRIGHT., 8FX-SCALE=, 8F UNITS, 8HNCCH., 8HY-SCALE=
      UNITS, 8HO ALL X, 8F ACC --, 8H ACC +, 8HVALUES., 8HC ALL Y
      1, 8H UNITS, 14, 8H
      2, 8H UNITS, 14, 8H
      3, 8H UNITS, 14, 8H
      CHECK PREVIOUS OPERATION OF ROUTINE, IF ANY. CODES ARE
      ITTEST = 0 IF PREVIOUS GRAPH, IF ANY, COMPLETED
      ITTEST = 1 IF PREVIOUS GRAPH, NOT COMPLETED
      ITTEST = 2 IF ERROR FOUND WHILE MCCURV WAS CNE, CR IF
      MCCURV WAS ILLEGAL.

      IPCINT = ITYPE
      IF(ITEST - 2)1000,1001,1000
      IF(MCCUR)1003,1002,1003
      ITTEST = 0
      GO TO 1000
      IF(MCCUR - 1)1004,1002,1004
      LAST = 2
      RETURN
      SET UP ERROR RETURN ROUTINE. ENTRY AT STATEMENT 1005.
      1005 IF(ITEST)1005,1006,1005
      1006 IF(MCCUR)1007,1008,1007
      1007 PRINT 1100
      1100 FORMAT ( ' 59H NO FURTHER GRAPH OUTPUT UNTIL MCCURV NEXT IS ZERO CR
      1 CNE.', / )
      ITTEST = 2
      LAST = 2
      RETURN
      1101 PRINT 1101
      1101 FORMAT ( ' 30H THIS PLCT WILL NOT BE OUTPUT. , / )
      LAST = 1
      RETURN
      1009 IF(MCCUR - 2)1010,1008,1010
      1010 IF(MCCUR - 3)1007,1011,1007
      1011 ITTEST = 3
      GO TO 1008
      CHECK LEGALITY OF INPUT ARGUMENTS.
      1000 IF(NUMPTS - 2)1,2,2
      1001 PRINT 100
      1001 FORMAT ( /, 32H NUMPTS MUST NOT BE LESS THAN 2. )
      GO TO 1005
      9000 IF(IPCINT)9000,9004,9001
      9100 PRINT 9100
      9100 FORMAT ( /, 15H ILLEGAL ITYPE. )
      GO TO 1005
      9001 GO TO 1005
      9002 IF(IPCINT - 5)9002,9002,9000
      9003 IF(NUMPTS - 30)3,3,9003
      9101 PRINT 9101
      9101 FORMAT ( /, 46H NUMPTS MUST NOT EXCEED 30 FOR POINT PLOTTING. )

```

```

9004 GO TC 1005 - 900)3,3,5005
9005 IF (NLMPTS - 28H NLMPTS MUST NOT EXCEED 900. )
9102 FORMAT (/)
9102 GO TO 1005
3 IX=ICATA(1)
  IY=ICATA(2)
  AMAXX=X(1)
  AMAXY=Y(1)
  AMINX=X(1)
  AMINY=Y(1)
  CG 1020 IF=2,NLMPTS
  AMAXX=AMAXX(1,X(I),AMAXX)
  AMAXY=AMAXY(1,Y(I),AMAXY)
  AMINX=AMINX(1,X(I),AMINX)
  AMINY=AMINY(1,Y(I),AMINY)
1020 IF (AMAXX-AMINX) 1025,1025,1025
1022 IF (AMAXY-AMINY) 1025,1025,1025
1024 PRINT 1103
1103 FORMAT (/) 38H ALL FCINTS HAVE THE SAME COORDINATES. )
1025 GO TO 1005
4 IF (ITEST) 4,7,4
5 IF (MCCUR-2) 5,2240,5
6 IF (MCCUR-3) 6,2240,6
101 PRINT 101 17H ILLEGAL MCCURV. )
7 GO TO 1005
8 IF (MCCUR) 6,9,8
9 IF (MCCUR-1) 6,9,6
10 IF (IWIDE) 10,11,12
101 ITIT=ICAT8(1)
102 PRINT 102, ITIT, ITIT
  FORMAT (/) 9H ILLEGAL ,A5,29H. GRAPH WILL BE PLOTTED WITH ,A5,
  5H = 8. ,/)
11 JWIDE = 3
12 GC TC 14
13 IF (IWIDE-5) 13,13,10
14 JWIDE = IWIDE
15 IF (IHIGH) 15,16,17
16 ITIT=ICAT8(2)
16 PRINT 102, ITIT, ITIT
  JHIGH = 2
2240 GO TO 19
  CCNT INCL = 45
  BACKSPACE 45
17 GO TO 24
18 IF (IHIGH-15) 18,18,15
  JHIGH = HIGH

```



```

      ISIZE = JFICH
      AMAX = AMAXY
      AMIN = AMINY
      IYX = IY
      IYX = IX
      CHECK SCALE AND GO TO FIXED OR AUTC SCALE ROUTINES.
52 IF (SCALE) 53, 59, 58
53 PRINT 114, IYX, IYX
114 FORMAT (//, 9H, ILLEGAL, A1, 3SHSCALE. GRAPH WILL BE PLOTTED WITH AL
      1 TO, A1, 7H-SCALE. //)
      GO TO 59
      EXPRESS FIXED SCALE IN E FORMAT WITH ONE FIGURE SIGNIFICANCE.
      CALL SCALIT(SCALE, ISCLIO, FACTOR, 1)
      SCALE = FACTOR*10.*ISCLIC
      CHECK AND COMPUTE AXIS LOCATION IF NECESSARY. FIXED SCALE
      CASE. ITAG = 0 IF ORIGIN ON GRAPH CR 1 IF IT IS SUPPRESSED.
      CASE - 1) 1032, 1031, 1030
1030 IF (ICDE = C
      ITAG = C
      GO TO 59
1031 PRINT 1104, IYX, IYX, IYX
1104 FORMAT (//, 5H, MODE, A1, 24HAX MUST NOT BE 1 UNLESS, A1, 57HSCALE IS, C
      1 (AUTO-SCALE). GRAPH WILL BE PLOTTED WITH AUTC, A1, 7H-SCALE. //)
      GO TO 59
1032 IF (AMAX - AMIN) 1038, 1035, 1038
1039 IF (AMAX) 1036, 1034, 1037
1034 IAXIS = ISIZE/2
      GO TO 1030
1036 IAXIS = ISIZE
      GO TO 1030
1037 IAXIS = 1030
      GO TO 1030
1038 IF (SIGN(1., AMIN)) 1040, 1039, 1040
1040 ASIZE = ISIZE
      IAXIS = -AMIN/(AMAX - AMIN)*ASIZE + 0.5
      GO TO 1030
      SCALE ROUTINE.
55 IF (MCDE - 1) 60, 64, 69
60 AMAX = AMAX1(0., AMAX)
      AMIN = AMIN1(0., AMIN)
64 IF (AMAX - AMIN) 68, 65, 68
65 PRINT 116, IYX, IYX, IYX
116 FORMAT (//, 5H, ALL, A1, 47H VALUES EQUAL. AUTC SCALE POSSIBLE ONLY
      1 IF THE 1005
      GO TO 1035
68 ASIZE = ISIZE
      SCALE = (AMAX - AMIN)/ASIZE
      GO TO 33
69 IF (AMAX - AMIN) 74, 70, 74

```

```

70 IF (AMAX) 74,71,74
71 PRINT 118, IXY
118 FORMAT (/, 5H ALL ,A1,3EH VALUES ZERC. AUTC SCALE NOT POSSIBLE. )
GO TO 1005
74 IF (AMAX) 76,76,75
75 IF (ISIZE) - IAXIS) 77,76,77
76 SCALE1 = C.
GO TO 118
77 AXIS = IAXIS
ASIZE = ISIZE
SCALE1 = AMAX/(ASIZE - AXIS)
78 IF (AMIN) 79,79,80
79 IF (IAXIS) 81,8C,81
80 SCALE2 = C.
GO TO 82
81 AXIS = IAXIS
SCALE2 = -AMIN/AXIS
82 IF (SCALE1 + SCALE2) 1984,1982,1984
1982 PRINT 1982, IYX, IYX
1983 FORMAT (/, 56H NONE OF THE PLOT LIES ON THE GRAPH WITH THIS SPECIF
1IED ,A1,47H-AXIS LOCATION. GRAPH WILL BE PLOTTED WITH MODE,A1,
2 7HAX = C. ,/)
MODE = C
GO TO 60
1984 SCALE = AMAX1(SCALE1,SCALE2)
83 CALL SCALIT(SCALE,ISCL10,FACOR,3)
84 IF (FACOR = 5.05) 85,85,84
FACOR = ISCL10+1
GO TO 80
85 IF (FACOR = 2.02) 87,87,86
86 IF (FACOR = 5
FACOR = SC
GO TO 80
87 IF (FACOR = 1.01) 89,89,89
88 IF (FACOR = 1
FACOR = SC
GO TO 80
89 SCALE = FACOR*10.*#ISCL10
90 COMPUTE AXIS LOCATION IF NECESSARY. AUTC SCALE CASE.
IF (ACUE = 1) 92,91,93
91 IF (SIGN(1.,AMAX)-SIGN(1.,AMIN)) 92,94,92
92 IAXIS = -AMIN/SCALE + 0.5
93 ITAG = C
GO TO 203
94 IF (AMAX) 95,95,200
95 IAXIS = ISIZE
BETA = -AMAX/SCALE
IF (BETA - 1.E+12) 99,99,96

```

C











```

ICURV(I+2)=IC3
ICURV(I+3)=IC4
CGNT INDE WRITE RECORDS.
C 9010 IF (MODCUR-1)26C,26C,5015
260 CALL FLCTS (0,0,0)
XAXIS=C.
YAXIS=C.
CALL SYMBCL(XAXIS,YAXIS,.14,JXTIT,0.,72)
261 YAXIS=-.24
CALL SYMBCL(XAXIS,YAXIS,.14,JYIT,0.,72)
926E YAXIS=-.31
CALL SYMBCL(XAXIS,YAXIS,.21,ITITLE,0.,48)
YAXIS=-.31
CALL SYMBCL(XAXIS,YAXIS,.21,ITITLE(13),C.,48)
927C
9271 XAXIS=FLQAT(IH)/10C.
YAXIS=FLQAT(JH)/10C.
CALL FLCT(XAXIS,YAXIS,3)
XAXIS=FLQAT(IH+LV)/10C.
CALL FLCT(XAXIS,YAXIS,2)
CALL SPECNO(IH,IVH2,NH,XAXIS,YAXIS,1)
XAXIS=FLQAT(IV)/10C.
YAXIS=FLQAT(JV)/10C.
CALL PLCT(XAXIS,YAXIS,3)
YAXIS=FLQAT(JV+LV)/10C.
CALL PLCT(XAXIS,YAXIS,2)
CALL SPECNC(IV,IVV2,INV,XAXIS,YAXIS,2)
9015 IF (IFCIN)9020,270,9020
270 CALL SUB1(ICURV,INLM)
CALL WFERE(XAXIS,YAXIS)
9020 IF (MODCUR-1)272,272,9025
272 IF (IGENE RATE GRID IF CALLED FOR.
C 273 IX10C = ISIZEX*100
IY10C = ISIZEY*100
NEXT1 = IFTMGN + IX10C
NEXT2 = IFTMGN + IY10C
DO 1274 J=1,80,8
JGRID(J)=LEFTMGN
JGRID(J+1)=NEXT1
JGRID(J+2)=NEXT2
JGRID(J+3)=NEXT1
IF (NEXT1 - IFTMGN - IY10C)1273,1275,1275
NEXT1 = NEXT1 + 10C
JGRID(J+4)=NEXT2
JGRID(J+5)=NEXT1
JGRID(J+6)=LEFTMGN
1273

```

```

1274 JGRID(J+7)=NEXT1 - IY10C) 1274, 1276, 1276
1275 IF(NEXT1 - NEXT1 + 100
JGRID(J+4)=NEXT12
JGRID(J+5)=NEXT11
JGRID(J+6)=NEXT12
JGRID(J+7)=NEXT1
CONTINUE
1276 NUMGRD=J+7
CALL SUB1(JGRID, NUMGRD)
1277 NEXT1 = LEFTMGN + IY10C
NEXT12 = LEFTMGN + IY10C
DO 1279 J=1, 48, 8
JGRID(J)=NEXT1
JGRID(J+1)=LEFTMGN
JGRID(J+2)=NEXT11
JGRID(J+3)=NEXT12
JGRID(J+4)=NEXT12
JGRID(J+5)=NEXT11
JGRID(J+6)=NEXT11
JGRID(J+7)=LEFTMGN - IY10C) 1278, 1280, 1280
1278 NEXT1 = NEXT1 + ICC
JGRID(J+4)=NEXT1
JGRID(J+5)=NEXT12
JGRID(J+6)=NEXT11
JGRID(J+7)=LEFTMGN - IY10C) 1279, 1281, 1281
1279 NEXT1 = NEXT1 + ICC
JGRID(J+4)=NEXT1
JGRID(J+5)=NEXT12
JGRID(J+6)=NEXT11
JGRID(J+7)=NEXT12
CONTINUE
1281 NUMGRD=J+7
CALL SUB1(JGRID, NUMGRD)
9025 IF(1) PCINERATE PCINT PLOT RECDRC IF CALLED FCR.
9030 IOUT = C
DO 9050 I=1, NUMPTS
C1 = X(I)*SCX + SHIFIX
C2 = Y(I)*SCY + SHIFIX
IF(C1 - EXSIZE) 9031, 9031, 9034
IF(C2 - YSIZE) 9032, 9032, 9034
IF(C1 - EXSIZE) 9033, 9033, 9035
IF(C2 - YSIZE) 9034, 9034, 9035
IOUT = IOUT + 1
GO TO 9050
9031 IOUT = C1
9032 IOUT = C2
9033 IOUT = C1
9034 IOUT = C2
9035 IOUT = C1
GO TO 9036, 9037, 9038, 9039, 9040, 9041, 9042
C GENERATE CROSS.

```

9036

ICURV(1)=IC1-5  
ICURV(2)=IC2-5  
ICURV(3)=IC1+5  
ICURV(4)=IC2+5  
ICURV(5)=IC1  
ICURV(6)=IC2  
ICURV(7)=IC1-5  
ICURV(8)=IC2+5  
ICURV(9)=IC1+5  
ICURV(10)=IC2-5  
ICURV(11)=IC1+5  
ICURV(12)=IC2-5  
INUT=12  
GO TO 5041  
C 9037

1  
TE PLUS.  
ICURV(1)=IC1-5  
ICURV(2)=IC1  
ICURV(3)=IC1+5  
ICURV(4)=IC2+5  
ICURV(5)=IC1  
ICURV(6)=IC2  
ICURV(7)=IC1-5  
ICURV(8)=IC2+5  
ICURV(9)=IC1+5  
ICURV(10)=IC2  
ICURV(11)=IC1+5  
ICURV(12)=IC2  
INUT=12  
GO TO 5041  
C 9038

1  
TE SQUARE.  
ICURV(1)=IC1+4  
ICURV(2)=IC2-4  
ICURV(3)=IC1+4  
ICURV(4)=IC2+4  
ICURV(5)=IC1-4  
ICURV(6)=IC2+4  
ICURV(7)=IC1-4  
ICURV(8)=IC2-4  
ICURV(9)=IC1+4  
ICURV(10)=IC2-4  
ICURV(11)=IC1+4  
ICURV(12)=IC2-4  
INUT=12  
GO TO 5041  
C 9039

1  
TE CIAMCND.  
ICURV(1)=IC1+5  
ICURV(2)=IC2  
ICURV(3)=IC1

```

ICURV(4)=IC2+5
ICURV(5)=IC1-5
ICURV(6)=IC2
ICURV(7)=IC1
ICURV(8)=IC2-5
ICURV(9)=IC1+5
ICURV(10)=IC2
ICURV(11)=IC1+5
ICURV(12)=IC2
INUM=12
GO TO SC41
C 9040 GENERATE TRIANGLE.
ICURV(1)=IC1+5
ICURV(2)=IC2-3
ICURV(3)=IC1
ICURV(4)=IC2+6
ICURV(5)=IC1-5
ICURV(6)=IC2-3
ICURV(7)=IC1+5
ICURV(8)=IC2-3
INUM=8
CALL SUB1(ICURV, INUM)
9041 IF(I-POINTS)9043,SC42,9043
9042 CALL WFERE(XAXIS,YAXIS)
CALL WFERE(XAXIS,YAXIS,.C7,LABEL(2),0.,4)
GO TO SC46
9043 IF(I-SC45,SC44,SC45)
9044 CALL WFERE(XAXIS,YAXIS)
CALL WFERE(XAXIS,YAXIS,.C7,LABEL(1),0.,4)
GO TO SC46
9045 CONTINUE
9046 CALL INDE1(ICURV, INUM)
9050 CALL INDE1(SC45,276,SC48)
IF(OUT)9104,OUT
9048 PRINT(//,IX,I2,29H POINT(S) WERE OFF THE GRAPH.,/)
9104 FORMAT(//,LP,RETURN.
C 276 IF(MCOCUR)277,278,277
277 IF(MCOCUR-3)275,278,275
278 ITES=0
YAXIS=HIGH+4
CALL PLCT(0.,0,YAXIS,-3)
CALL PLCT(0.,0,955)
WRITE(6,130) TITLE
9130 H GRAPH TITLED/2(5X,12A4/),18H HAS BEEN PLOTTED.)
FORMAT(//,ITYP2(IDUMMY)
IDUMMY=28C
GO TO 28C
130

```





```

2 CALL SCALIT(BNUMBER,ISCLIC,FACTOR,3)
  ISGN=ISIGN(1,ISCLIC)
  ISCLIC=IABS(ISCLIC)
  IFACT=FACTOR*100.CC1
  II(8)=MCC (ISCLIC,10)
  II(7)=ISCLIC/10
  IF(ISGNSC) 4,3,3
  II(6)=IFLLS
3 GO TO 5
4 II(6)=MINDS
5 II(5)=IE
  II(4)=MCC(IFACT,10)
  II(3)=MCC(IFACT,100)/10
  II(2)=IFER
  II(1)=IFACT/100
  CALL ENCCCE(8,ICGDE,II)
  RETURN
END
FUNCTION IYYP2 (IDUMY)
  TYPE WORD GRAPH.
  RETURN
END
SUBROUTINE SUB1(IA,N)
  DIMENSION IA(2)
  IPEN=3
  DO 100 I=1,N,2
    X=IA(I)
    X=X/100.
    Y=IA(I+1)
    Y=Y/100.
    CALL PLCT(X,Y,IPEN)
    IPEN=2
  CONTINUE
  RETURN
END
SUBROUTINE SPECNO(IVF,IVF2,NH,XAXIS,YAXIS,IA)
  DATA MINDS/4H000-/
  DIMENSION II(4)
  MINDS=-252645280
  GO TO (100,200),IA
100 TH=0.
  GO TO 300
200 TH=90.
  STH=SIGN (IH*.0174533)
  CTH=COS (TH*.0174533)
  X=XAXIS-1.*CTH-1.*STH
  Y=YAXIS-1.*CTH-1.*STH
  INCLAS=IVF

```

```

DO 700 K=1,NH
I=0
INUM=INUMS
IF(INUM) 400,500,500
400 I=1
II(1)=MINUS
INUM=-INUM
500 I=I+1
II(I)=INUM/100
INUM=INUM-II(I)*100
I=I+1
II(I)=INUM/10
INUM=INUM-II(I)*10
I=I+1
II(I)=INUM
CALL ENCCDE(I,IS,II)
CALL SYMBOL(X,Y,.C7,IS,IF,I)
INUMS=INUMS+IVH2
X=X-1.*CTH
Y=Y-1.*STH
700 RETURN
END

```

## LIST OF REFERENCES

- Allen, J. S., "Models of wind-driven currents on the continental shelf", Annual Review of Fluid Mechanics, v. 12, pp. 389-433, 1980.
- Bakun, A., "Coastal upwelling indices, west coast of North America, 1946-71, U.S. Department of Commerce", NOAA Technical Report NMFS SSRF-671, pp. 103.
- Bakun, A., Personal communication, 1981.
- Coddington, K., "Measurement of the California Countercurrent", M.S. Thesis, Naval Postgraduate School, Monterey, June 1979.
- Dreves, D. A., "Sea levels and metered currents off central California", M.S. Thesis, Naval Postgraduate School, Monterey, September 1980.
- Ekman, V. W., "On the influence of the earth's rotation on ocean currents", Arkiv for Matematik, Astronomi, och Fysik, 2(11), pp. 1-52, 1905.
- Halpern, D., et al., "Oceanographic observations of the 1982 warming of the Tropical Eastern Pacific", Science, v. 221, pp. 1173-1175 16 September 1983.
- Hamilton, P. and M. Rattray, "A numerical model of the depth dependent wind-driven upwelling circulation on a continental shelf", Journal of Physical Oceanography, v. 8, pp. 437-457, May 1978.
- Hickey, B. M. and P. Hamilton, "A spin-up model as a diagnostic tool for interpretation of current and density measurements on the continental shelf of the Pacific Northwest", Journal of Physical Oceanography, v. 10, pp. 12-24, 1980.
- Hickey, B. M., "The California Current System - Hypothesis and Facts", Contribution Number 1038 of the Department of Oceanography, University of Washington, 24 April 1978.
- Hickey, B. M., A. Huyer and R. L. Smith, "The alongshore coherence and generation of fluctuations in currents and sea level on the Pacific Northwest continental shelf, winter and spring 1975", Journal of Physical Oceanography, v.11, pp. 822-835, June 1981.

- Huyer, A., E. J. C. Sobey and R. L. Smith, "The spring transition in currents over the Oregon continental shelf", Journal of Geophysical Research, v. 84, pp. 6995-7011, 20 November 1979.
- Janowitz, G. S., "A model and observations of time-dependent upwelling over the mid-shelf and slope", Journal of Physical Oceanography, v. 10, pp. 1574-1583, July 1980.
- Munk, W. H., "On the wind driven ocean circulation", Journal of Meteorology, v. 7, pp. 79-93, 1950.
- O'Brien, J. J. and H. E. Hurlburt, "A numerical model of coastal upwelling", Journal of Physical Oceanography, v. 2, pp. 14-26, January 1972.
- O'Brien, J. J., "Upwelling in the ocean: Two and three dimensional models of upper ocean dynamics and variability", Modeling and Prediction of the Upper Layers of the Ocean, Pergamon Press, 1977.
- Reid, J. L., G. I. Roden and J. G. Wyllie, "Studies of the California Current System", Progress Report of the California Cooperative Oceanic Fisheries Investigations, 1 July 1956 to 1 January 1958, pp. 28-56, Scripps Institution of Oceanography, La Jolla, California, 1958.
- Reid, J. L., Jr. and R. A. Schwatzlose, "Direct measurements of the Davidson Current off central California", Journal of Geophysical Research, v. 67, pp. 559-565, June 1962.
- Reid, J. L., Jr., "Measurements of the California Countercurrent at a depth of 250 meters", Journal of Marine Research, v. 20, pp. 134-137, 15 July 1962.
- Ryther, J. H., "Photosynthesis and fish production in the sea", Science, v. 166, pp. 72-76, 30 October 1969.
- Smith, R. L., "Peru coastal currents during El Nino: 1976 and 1982", Science, v. 221, pp. 1397-1399, 30 September 1983.
- Stewart, R. W., "The influence of friction on inertial models of oceanic circulation", Studies on Oceanography, University of Washington Press, 1965.
- Suginohara, N., "Coastal upwelling: onshore - offshore circulation, equatorward coastal jet and poleward undercurrent over a continental shelf slope", Journal of Physical Oceanography, v. 12, pp. 272-284, March 1982.

Sverdrup, H. U., M. W. Johnson and R. H. Fleming, The Ocean, their Physics, Chemistry, and general Biology, Prentice-Hall, Inc., Englewood Cliffs, N. J., 1942.

Sverdrup, H. U. and R. H. Fleming, "The waters off the coast of Southern California", Scripps Institute of Oceanography Bulletin, v. 4, pp. 261-375, 9 October 1941.

Wickham, J. B., "Observations of the California Undercurrent", Journal of Marine Research, v. 33, pp. 325-340, September 1975.

# INITIAL DISTRIBUTION LIST

	No. Copies
1. Chairman Code 68 Department of Oceanography Naval Postgraduate School Monterey, CA 93943	2
2. Director Naval Oceanography Division (OP952) Navy Department Washington, DC 20350	1
3. Office of Naval Research Code 480 Naval Ocean Research and Development Activity NSTL Station, MSD 39529	1
4. Dr. Robert E. Stevenson Scientific Liaison Office, ONR Scripps Institution of Oceanography La Jolla, CA 92037	1
5. SIO Library University of California, San Diego P.O. Box 2367 La Jolla, CA 92037	1
6. Department of Oceanography Library University of Washington Seattle, WA 98105	1
7. Department of Oceanograpny Library Oregon State University Corvallis, OR 97331	1
8. Commanding Officer Fleet Numerical Weather Central Monterey, CA 93940	1
9. Commanding Officer Naval Environmental Prediction Research Facility Monterey, CA 93940	1
10. Commander Oceanographic Systems Pacific Box 1390 Pearl Harbor, Hawaii 96860	1

- |     |   |   |
|-----|---|---|
| 11. | Defense Technical Information Center<br>Cameron Station<br>Alexandria, VA 22314                                     | 2 |
| 12. | Library Code 0142<br>Naval Postgraduate School<br>Monterey, CA 93943  | 2 |
| 13. | Commanding Officer<br>Naval Ocean Research and Development Activity<br>NSTL Station, MS 39529                       | 1 |
| 14. | Commander<br>Naval Oceanography Command<br>NSTL Station, MS 39529   | 1 |
| 15. | Commanding Officer<br>Naval Oceanographic Office<br>NSTL Station, MS 39529  | 1 |
| 16. | Dr. S. P. Tucker, Code 68Tx<br>Department of Oceanography<br>Naval Postgraduate School<br>Monterey, CA 93943        | 3 |
| 17. | Professor J. B. Wickham, Code 68Wk<br>Department of Oceanography<br>Naval Postgraduate School<br>Monterey, CA 93943 | 3 |
| 18. | Lt. K. Coddington<br>Department of Ocean Sciences<br>U.S. Coast Guard Academy<br>New London, Ct 06320               | 1 |
| 19. | LCDR R. L. Harrod<br>IAGS, Bldg. 144<br>Ft. Sam Houston, TX 78234   | 3 |















210236

Thesis

H29347 Harrod

c.1 Observations of the  
California Counter-  
current.

210236

Thesis

H29347 Harrod

c.1 Observations of the  
California Counter-  
current.



thesH29347

Observations of the California Countercu



3 2768 002 08257 0

DUDLEY KNOX LIBRARY